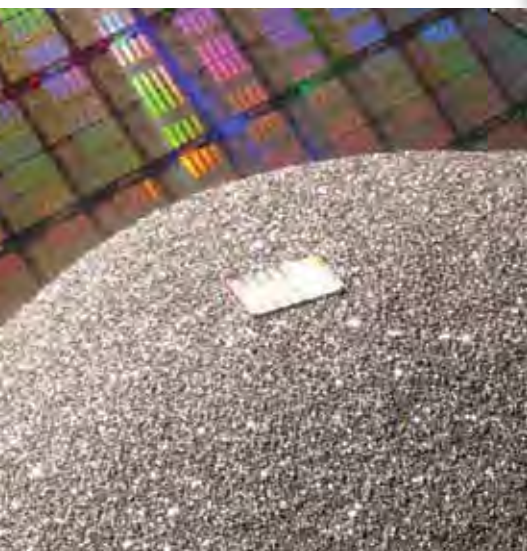
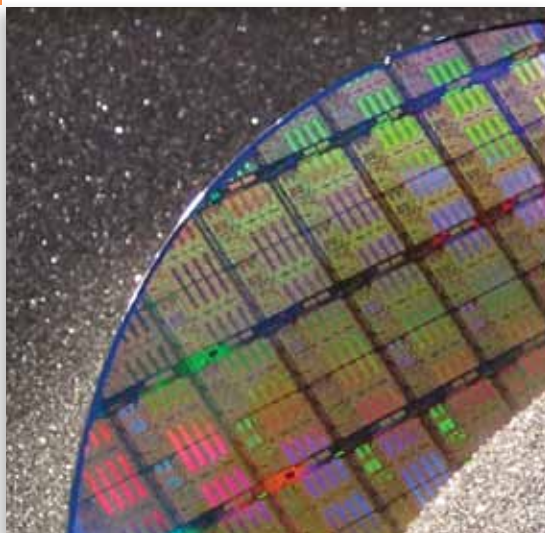


DoubleTree by Hilton Orlando
at Sea World® Orlando, FL
January 18-20, 2012

Electronic Materials and Applications 2012



MEETING GUIDE

Organized by
The American Ceramic Society and
The American Ceramic Society's Electronics Division and Basic Science Division



www.ceramics.org/ema2012

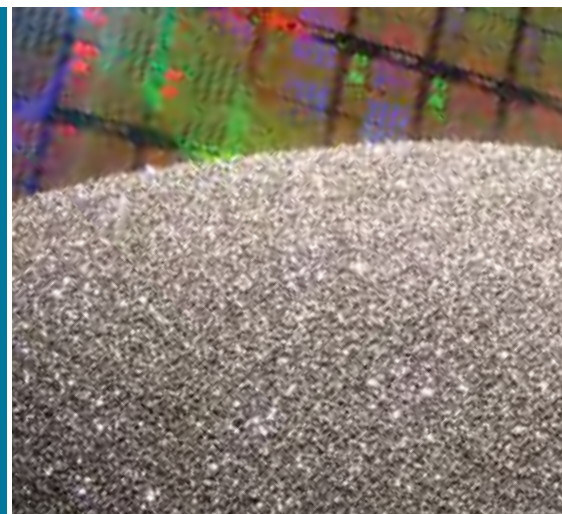


Table of Contents

Schedule At A Glance	3
Highlights of Student Research in Basic Science and Electronic Ceramics	
Student Symposium	4
Sponsors	4
Plenary Speakers	5
Hotel Floorplan	6
Symposia	7
Presenting Author List	9–10

Final Program

Wednesday Morning	11
Wednesday Afternoon	12–14
Thursday Morning	14–15
Thursday Afternoon	15–17
Friday Morning	17–18
Friday Afternoon	18–19
Abstracts	21
Author Index	54

Technical Programming Committee

Paul Clem, Sandia National Labs
Amit Goyal, Oak Ridge National Lab
Jacob Jones, University of Florida
Jian Luo, Clemson University
Wolfgang M. Sigmund, University of Florida
Clive Randall, Pennsylvania State University
Susan Troiler-Mckinstry, Pennsylvania State University
Ed Sabolsky, West Virginia University
Juan Nino, University of Florida
Qi Tan, General Electric
Victoria Blair, Alfred University
Nian Sun, Northeastern University
Steven Tidrow, University of Texas Pan American
Kristen Brosnan, General Electric
Alp Sehirlioglu, NASA-Glenn
Jeff Zhand, APC International
Thomas Daue, Smart Material Inc.
Michelle Bell, Radiant Technologies
Ahmad Safari, Rutgers University
Takaaki Tsurumi, Tokyo Institute of Technology

Endorsing Societies

UFFC
IEEE

International Scientific Advisory Committee (ISAC)

Jurgen Roedel, Darmstadt University of Technology
Michael Glazer, Clarendon Laboratory
Haosu Luo, Shanghai Institute of Ceramics,
Chinese Academy of Sciences
Sahn Nahm, Korea University
Junggho Ryu, Functional Ceramics Group, Korea
Institute of Materials Science (KIMS)

Basic Science Division Officers

Chair: Scott Misture
Chair-Elect: Kevin Trumble
Vice Chair: Jian Luo
Secretary: Wayne Kaplan
Programming Chair: Brian Huey, Adam Scotch

Electronics Division Officers

Trustee: Dwight Viehland
Chair: Amit Goyal
Chair-Elect: Quanxi Jia
Vice-chair: Steven C. Tidrow
Secretary: Tim J. Haugan
Secretary-Elect: Haiyan Wang
Programming Chairs: Quanxi Jia, Haiyan Wang

MEETING REGULATIONS

The American Ceramic Society is a nonprofit scientific organization that facilitates the exchange of knowledge meetings and publication of papers for future reference. The Society owns and retains full right to control its publications and its meetings. The Society has an obligation to protect its members and meetings from intrusion by others who may wish to use the meetings for their own private promotion purpose. Literature found not to be in agreement with the Society's goals, in competition with Society services or of an offensive nature will not be displayed anywhere in the vicinity of the meeting. Promotional literature of any kind may not be displayed without the Society's permission and unless the Society provides tables for this purpose. Literature not conforming to this policy or displayed in other than designated areas will be disposed. The Society will not permit unauthorized scheduling of activities during its meeting by any person or group when those activities are conducted at its meeting place in interference with its programs and scheduled activities. The Society does not object to appropriate activities by others during its meetings if it is consulted with regard to time, place, and suitability. Any person or group wishing to conduct any activity at the time and location of the Society meeting must obtain permission from the Executive Director or Director of Meetings, giving full details regarding desired time, place and nature of activity.

During oral sessions conducted during Society meetings, unauthorized photography, videotaping and audio recording is prohibited. Failure to comply may result in the removal of the offender from the session or from the remainder of the meeting.

Registration Requirements: Attendance at any meeting of the Society shall be limited to duly registered persons.

Disclaimer: Statements of fact and opinion are the responsibility of the authors alone and do not imply an opinion on the part of the officers, staff or members of The American Ceramic Society. The American Ceramic Society assumes no responsibility for the statements and opinions advanced by the contributors to its publications or by the speakers at its programs; nor does The American Ceramic Society assume any liability for losses or injuries suffered by attendees at its meetings. Registered names and trademarks, etc. used in its publications, even without specific indications thereof, are not to be considered unprotected by the law. Mention of trade names of commercial products does not constitute endorsement or recommendations for use by the publishers, editors or authors.

Final determination of the suitability of any information, procedure or products for use contemplated by any user, and the manner of that use, is the sole responsibility of the user. Expert advice should be obtained at all times when implementation is being considered, particularly where hazardous materials or processes are encountered.

Copyright© 2012. The American Ceramic Society (www.ceramics.org). All rights reserved.

Schedule At A Glance

Wednesday – January 18, 2012

Registration	7 a.m. – 6 p.m.	Oceans Ballroom Foyer
Opening Comments	8:45 a.m. – 9 a.m.	Indian
Plenary Session I	9 a.m. – 10 a.m.	Indian
Coffee Break	10 a.m. – 10:30 a.m.	Oceans Ballroom Foyer
Concurrent Technical Sessions	10:30 a.m. – 12 p.m.	Indian, Pacific, Coral B
Highlights of Student Research in Basic Science and Electronic Ceramics	12:15 p.m. – 1 p.m.	Pacific
Lunch On Own	12 p.m. – 1:15 p.m.	
Poster Session Set-Up	12 p.m. – 5 p.m.	Atlantic/Arctic
Concurrent Technical Sessions	1:30 p.m. – 5 p.m.	Indian, Pacific, Coral B
Coffee Break	2:45 p.m. – 3:15 p.m.	Oceans Ballroom Foyer
Poster Session & Reception	5 p.m. – 7 p.m.	Atlantic/Arctic

Thursday – January 19, 2012

Registration	7 a.m. – 6 p.m.	Oceans Ballroom Foyer
Plenary Session II	8 a.m. – 9 a.m.	Indian
Coffee Break	9 a.m. – 9:30 a.m.	Oceans Ballroom Foyer
Concurrent Technical Sessions	9:30 a.m. – 12 p.m.	Indian, Pacific, Coral B
Highlights of Student Research in Basic Science and Electronic Ceramics	12:15 p.m. – 1 p.m.	Pacific
Lunch On Own	12 p.m. – 1:15 p.m.	
Concurrent Technical Sessions	1:30 p.m. – 5 p.m.	Indian, Pacific, Coral B
Coffee Break	2:45 p.m. – 3:15 p.m.	Oceans Ballroom Foyer
Conference Dinner	7 p.m. – 9 p.m.	Atlantic/Arctic

Friday – January 20, 2012

Registration	7 a.m. – 5 p.m.	Oceans Ballroom Foyer
Plenary Session III	8 a.m. – 9 a.m.	Indian
Coffee Break	9 a.m. – 9:30 a.m.	Oceans Ballroom Foyer
Concurrent Technical Sessions	9:30 a.m. – 12 p.m.	Indian, Pacific, Coral B
Lunch On Own	12 p.m. – 1:30 p.m.	
Concurrent Technical Sessions	1:30 p.m. – 5 p.m.	Indian, Pacific, Coral B
Coffee Break	2:45 p.m. – 3:15 p.m.	Oceans Ballroom Foyer

Highlights of Student Research in Basic Science and Electronic Ceramics – Student Symposium

Student research is being conducted at all universities throughout the United States and the international community. However, there are few conferences or workshops where such research activities are highlighted. This symposium will showcase undergraduate as well as graduate research to encourage innovation and involvement of students throughout the ceramics community.

Wednesday, January 18, 2012 – 12:15 p.m. – 1 p.m.

Thursday, January 19, 2012 – 12:15 p.m. – 1 p.m.

Special Thanks to Our Sponsors For Their Generosity



Endorsing Societies:



2012 EMA Plenary Speakers

Indian Room

Wednesday, January 18th

8:45 a.m. – 9 a.m. Opening Remarks



Wednesday, January 18th, 9 a.m. – 10 a.m.

Dr. Bart Riley, Co-founder, CTO and VP of R&D, A123 Systems

Title: Advances in Li-ion Technology for Automotive and Grid Application

Dr. Riley is currently responsible for R&D at A123Systems and sits on the board of directors. Prior to co-founding A123 Systems in 2001, Dr. Riley held a number of key technical and management positions at American Superconductor. Dr. Riley holds more than 45 patents and has published over 85 papers in the fields of advanced materials and energy generation, storage & distribution systems. Dr. Riley holds Ph.D. and M.S. degrees in Materials Science and Engineering from Cornell University and a B.A. in Physics and Geology from Middlebury College.



Thursday, January 19th, 8 a.m. – 9 a.m.

Dr. Harriet Kung, Associate Director of Science for Basic Energy Sciences, United States Department of Energy

Title: Science to Energy

Dr. Kung has served as the Associate Director of Science for Basic Energy Sciences (BES) since 2008 and has worked for the Department of Energy since 2002. Under her leadership, BES has pursued new funding modalities in advancing the science for the energy research agenda, including the establishment of 46 Energy Frontier Research Centers and the Fuels from Sunlight Energy Innovation Hub. In 2010, BES also successfully completed the world's first x-ray free electron laser user facility-the Linac Coherent Light Source.



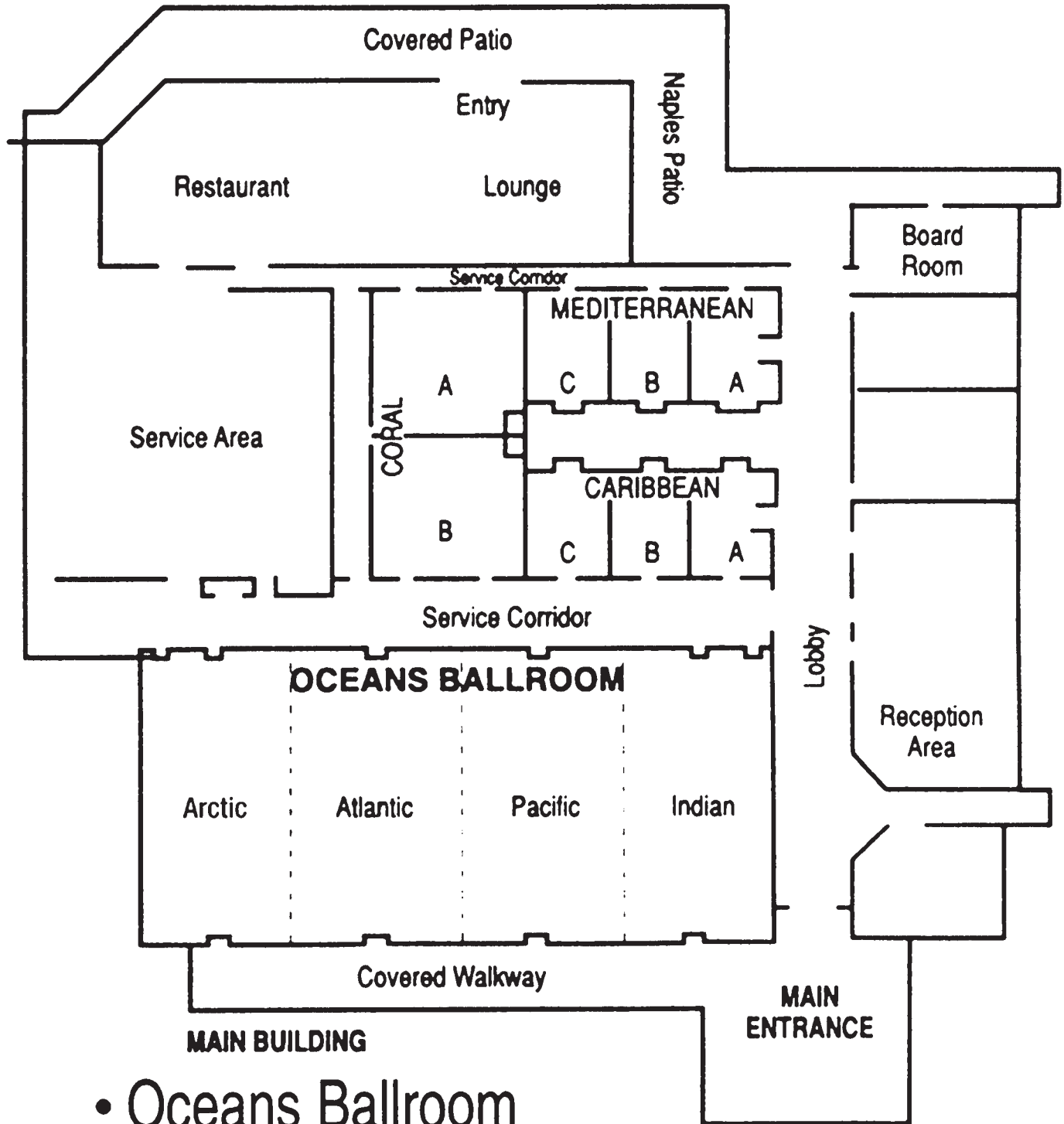
Friday, January 20th, 8 a.m. – 9 a.m.

Dr. John T. Prater, Materials Science Division, U.S. Army Research Office

Title: Future Opportunities in Materials Design

Since joining ARO in 1978, Dr. Prater has been a program manager in the Materials Sciences Division at the Army Research Office where he was responsible for overseeing the research portfolio under the Physical Properties of Materials Subfield and most recently under the Materials by Design Subfield. Dr. Prater was the head of the Materials Sciences Division at the ARO from 1998-2004. In addition, Dr. Prater has been an Adjunct Professor at North Carolina State University since 1989 where he has been conducting research on wide band-gap semiconductors. His research at NCSU has focused on the synthesis of high thermal conductivity diamond films and more recently on the development of dilute magnetic semiconducting ZnO. For 10 years prior to arriving at ARO Dr. Prater was in the Coatings and Advanced Materials Section of the Materials Department at the Pacific Northwest Laboratories where he was primarily involved in the high-rate sputter deposition and testing of magnetic films and protective coatings. Dr. Prater received his Ph.D. in Metallurgy and Materials Science from the University of Pennsylvania in 1978. Dr. Prater has over 70 journal publications.

Doubletree by Hilton Floor Plan



- Oceans Ballroom

Symposia

The 2012 Organizing Committee:

Amit Goyal, Electronics Division

Edward M. Sabolsky, Electronics Division

Steven C. Tidrow, Electronics Division

S1: New Frontiers in Electronic Ceramic Structures, Advanced Electronic Material Devices and Circuit Integration

Organizers: Vojislav V. Mitic, Serbian Academy of Science and Arts and University of Nis; Amar Bhalla, University of Texas at San Antonio; J. J. (Jack) Mecholsky, University of Florida; Martha L. Mecartney, University of California, Irvine; Ljubisa Kocic, University of Nis; Hirokazu Chazono, Taiyo Yuden Co.; Eugene Medvedovski, Umicore Thin Film Products; Vladimir Pavlovic, Serbian Academy of Science and Arts; Guorong Li, Shanghai Institute of Ceramics; Linan An, University of Central Florida

S2: Advanced Dielectric, Piezoelectric and Ferroic Materials, and Emerging Materials in Electronics

Organizers: Sahn Nahm, Korea University; Jurgen Rödel, Technische Universität Darmstadt; Shashank Priya, Virginia Polytechnic Institute and State University; Pam A. Thomas, University of Warwick; Steven C. Tidrow, University of Texas Pan American

S3: Symposium on Thin Film Integration and Processing Science

Organizers: Jon Ihlefeld, Sandia National Laboratories; Brady Gibbons, Oregon State University; Jon-Paul Maria, North Carolina State University

S4: Advanced Energy Storage Materials and Systems: Lithium and Beyond

Organizers: Jagjit Nanda, Oak Ridge National Laboratory; Yue Qi, General Motors R&D; Sergey Lopatin, Applied Materials; Amit Goyal, Oak Ridge National Laboratory

S5: Unconventional Thermoelectrics: Defect Chemistry, Doping and Nanoscale Effects

Organizers: Alp Sehirliglu, Case Western Reserve University; Jon Ihlefeld, Sandia National Laboratories; Anke Weidenkaff, EMPA

S6: Technologies for Sustainability and Green Materials Processing

Organizers: Paul Clem, Sandia National Laboratories; Edward M. Sabolsky, West Virginia University

S7: Metamaterials and Microwave Materials

Organizers: Paul Clem, Sandia National Laboratory

S8: Highlights of Student Research in Basic Science and Electronic Ceramics

Organizers: David Shahin, PCSA Council Chair; Jaime George, PCSA Programming Chair; Geoff Brenneka, Sandia National Laboratories

4th International Congress on Ceramics

Shaping the Future of Ceramics

ICC4 will bring more than 600 international leaders in business and research to discuss emerging opportunities as well as what's in store for the future of ceramics and glass. This meeting features invited presentations in these tracks :

- Energy, Environment, and Transportation
- Biology and Medicine
- Aerospace
- Nanostructured Ceramics
- Infrastructure
- Security
- Electro-, Optical- and Magnetic Ceramics and Devices
- Manufacturing and Business
- Entrepreneurship and Technology Transfer
- Workforce Development

Present your research and technology during the **Interactive Technology Forum**. This highly-publicized, groundbreaking event allows you to give an interactive technology presentation to ceramic professionals using your laptop, iPad, or other electronic device. You may also choose to simply present a traditional poster or supplement your poster by bringing a hands-on demonstration. **Submit your abstract by January 31, 2012.**

Interactive Technology Forum presentation options:

1. Interactive Technology Presentation – Make a presentation using your laptop, iPad or other electronic tablet device.*
2. Poster Plus Demonstration – In addition to your 4ft. by 4ft. poster display, bring a hands-on demonstration of your material, process, application, etc. to display on a tabletop in front of the poster board.
3. Poster Plus Electronic Device* - In addition to your 4ft. by 4ft. poster display, use your laptop, iPad, or other electronic tablet device to present additional material.
4. Traditional Poster – Present your research via a 4ft. by 4 ft. poster display.

* A limited number of 32" LCD monitors will be provided. Indicate your interest in using one when you submit. **Abstracts due January 31, 2012.**

The American Ceramic Society is pleased to host and organize the 4th International Congress on Ceramics. The International Ceramic Federation convenes the ICC every two years in cooperation with ACerS, the European Ceramic Society, the Ceramic Society of Japan, and other ICF Member Societies.

www.ceramics.org/icc4

July 15-19, 2012 | Sheraton Chicago Hotel & Towers | Chicago, IL, USA



Oral Presenters

Name	Date	Time	Room	Page Number	Name	Date	Time	Room	Page Number
					A				
Amani, M.	18-Jan	4:00PM	Pacific	13	Jee, S.	20-Jan	10:45AM	Coral B	18
Ansell, T.	19-Jan	2:30PM	Indian	16	Jeon, Y.	19-Jan	9:30AM	Indian	14
					B				
Banavara Seshadri, S.	20-Jan	2:15PM	Indian	18	Jones, J.L.	18-Jan	11:30AM	Indian	11
Bassiri-Gharb, N.	20-Jan	11:15AM	Indian	17	Jow, T.R.	18-Jan	10:30AM	Coral B	11
Bastani, Y.	20-Jan	3:45PM	Pacific	19	Jur, J.S.	20-Jan	10:45AM	Pacific	18
Bhattacharya, S.	19-Jan	4:00PM	Coral B	17	K				
Biegalski, M.D.	19-Jan	4:00PM	Pacific	16	Kakimoto, K.	18-Jan	2:30PM	Indian	12
Bilheux, H.	19-Jan	2:00PM	Coral B	16	Kang, K.	19-Jan	10:45AM	Coral B	15
Bugga, R.	19-Jan	1:30PM	Coral B	16	Karbasi, A.	18-Jan	12:45PM	Pacific	12
Burch, M.J.	20-Jan	2:15PM	Pacific	19	Kawai, A.	18-Jan	4:30PM	Indian	12
Bux, S.	18-Jan	3:15PM	Pacific	13	Kim, B.	19-Jan	11:30AM	Indian	14
					C				
Cahill, D.	18-Jan	10:30AM	Pacific	11	Kim, E.	19-Jan	9:45AM	Pacific	15
Caillat, T.	18-Jan	2:00PM	Pacific	13	Kobayashi, K.	18-Jan	2:15PM	Indian	12
Chen, A.	19-Jan	10:30AM	Indian	14	Kohler, C.	20-Jan	9:45AM	Indian	17
Clem, P.	19-Jan	11:00AM	Pacific	15	Kumar, B.	20-Jan	10:00AM	Coral B	18
Coker, E.N.	20-Jan	3:15PM	Coral B	19	Kumar, S.	18-Jan	1:45PM	Indian	12
					D				
Dai, S.	19-Jan	1:45PM	Indian	15	Kundaliya, D.	19-Jan	4:30PM	Pacific	16
Depla, D.	19-Jan	1:30PM	Pacific	16	Kung, H.	19-Jan	8:00AM	Indian	14
Dhanjal, D.K.	20-Jan	10:30AM	Indian	17	Kutnjak, Z.	19-Jan	3:45PM	Indian	16
Dias, A.	20-Jan	2:00PM	Coral B	19	L				
Dudis, D.	18-Jan	1:30PM	Pacific	13	Lam, P.	20-Jan	10:00AM	Indian	17
Dudney, N.J.	18-Jan	11:30AM	Coral B	11	Lestriez, B.	19-Jan	3:15PM	Coral B	17
Dunn, B.	19-Jan	9:30AM	Coral B	14	Llano, C.	19-Jan	12:15PM	Pacific	15
Dwivedi, A.	19-Jan	5:15PM	Indian	16	Lopatin, S.	19-Jan	11:45AM	Coral B	15
					E				
Ehara, Y.	20-Jan	11:30AM	Indian	17	Lu, N.	20-Jan	9:30AM	Pacific	17
Ehmke, M.	18-Jan	2:00PM	Indian	12	Lucht, B.	18-Jan	11:00AM	Coral B	11
					F				
Fancher, C.	18-Jan	3:45PM	Indian	12	M				
Finkel, P.	18-Jan	10:30AM	Indian	11	Mackey, J.	18-Jan	2:30PM	Pacific	13
Freer, R.	20-Jan	10:15AM	Indian	17	Mahajan, S.K.	20-Jan	3:45PM	Indian	18
Fukata, K.	20-Jan	2:00PM	Indian	18	Maignan, A.	18-Jan	3:30PM	Pacific	13
Funakubo, H.	20-Jan	11:30AM	Pacific	18	Maiti, T.	19-Jan	11:45AM	Indian	14
					G				
Ghosh, D.	19-Jan	11:00AM	Indian	14	Martha, S.K.	19-Jan	11:15AM	Coral B	15
Gibbons, B.J.	20-Jan	2:30PM	Pacific	19	Masumdar, E.U.	20-Jan	10:00AM	Pacific	17
Gorman, B.P.	20-Jan	4:00PM	Coral B	19	Matias, V.	19-Jan	2:15PM	Pacific	16
Gorman, B.P.	20-Jan	3:15PM	Indian	18	Mion, T.	19-Jan	10:30AM	Pacific	15
Gorzowski, E.	18-Jan	11:00AM	Indian	11	Mion, T.	19-Jan	10:45AM	Pacific	15
Guduru, P.R.	18-Jan	1:30PM	Coral B	12	Mion, T.	20-Jan	10:45AM	Indian	17
					H				
HaiBo, X.	20-Jan	11:00AM	Indian	17	Mitic, V.	20-Jan	2:30PM	Indian	18
Hamad, E.K.	19-Jan	11:15AM	Pacific	15	Mitic, V.	20-Jan	3:30PM	Indian	18
Harris, D.T.	19-Jan	4:15PM	Indian	16	Morales, J.	19-Jan	10:15AM	Pacific	15
Haugan, T.J.	19-Jan	2:00PM	Pacific	16	Muchenik, T.I.	18-Jan	11:15AM	Indian	11
Hoke, B.	18-Jan	12:15PM	Pacific	12	N				
Hopkins, P.	18-Jan	11:00AM	Pacific	11	Nahm, S.	19-Jan	2:00PM	Indian	15
Hotza, D.	20-Jan	3:45PM	Coral B	19	Nazri, G.	20-Jan	11:00AM	Coral B	18
Huey, B.D.	19-Jan	10:00AM	Indian	14	Nittala, K.	20-Jan	4:00PM	Pacific	19
					I				
Idrobo, J.C.	18-Jan	3:30PM	Coral B	12	O				
Ihlefeld, J.	20-Jan	4:15PM	Pacific	19	Oder, T.	20-Jan	1:45PM	Indian	18
Ito, D.	20-Jan	2:30PM	Coral B	19	P				
					J				
					Q				
					R				

Presenting Author List

Oral Presenters

Name	Date	Time	Room	Page Number	Name	Date	Time	Room	Page Number
R					T				
Raengthon, N.	19-Jan	1:30PM	Indian	15	Tabei, S.	19-Jan	10:45AM	Indian	14
Riley, B.	18-Jan	9:00AM	Indian	11	Tan, X.	18-Jan	4:00PM	Indian	12
Riman, R.	20-Jan	1:30PM	Coral B	19	Tasaki, K.	19-Jan	4:30PM	Coral B	17
Rivas, M.	18-Jan	12:30PM	Pacific	12	Thomas, P.A.	18-Jan	3:15PM	Indian	12
Rogers, M.	19-Jan	9:45AM	Indian	14	Tidrow, S.	20-Jan	12:00PM	Indian	17
Rossetti, G.A.	19-Jan	5:00PM	Indian	16	Trolrier-McKinstry, S.	20-Jan	3:15PM	Pacific	19
S					U				
Sabolsky, E.M.	20-Jan	1:30PM	Indian	18	Usher, T.	18-Jan	4:15PM	Indian	12
Sakamoto, J.	20-Jan	10:15AM	Coral B	18	V				
Samuelis, D.	18-Jan	2:00PM	Coral B	12	Van der Ven, A.	18-Jan	4:00PM	Coral B	13
Sanchez, L.M.	20-Jan	2:00PM	Pacific	19	Veber, A.	20-Jan	11:15AM	Pacific	18
Schneller, T.	20-Jan	1:30PM	Pacific	19	W				
Sebastian, M.	19-Jan	12:30PM	Pacific	15	Wang, S.	20-Jan	4:00PM	Indian	18
Sehirlioglu, A.	18-Jan	4:15PM	Pacific	13	West, A.R.	19-Jan	2:15PM	Indian	15
Sehirlioglu, A.	19-Jan	3:45PM	Pacific	16	Wong-Ng, W.	18-Jan	11:30AM	Pacific	11
Shahbazian Yassar, R.	18-Jan	3:45PM	Coral B	13	Wong-Ng, W.	20-Jan	2:15PM	Coral B	19
Sheldon, B.W.	19-Jan	2:30PM	Coral B	16	X				
Shelton, C.T.	19-Jan	4:45PM	Pacific	16	Xu, K.	18-Jan	4:30PM	Coral B	13
Shen, W.	19-Jan	10:15AM	Indian	14	Y				
Shenoy, V.B.	18-Jan	3:15PM	Coral B	12	Yadav, K.	19-Jan	11:15AM	Indian	14
Shi, S.	19-Jan	3:45PM	Coral B	17	Yoon, S.	19-Jan	3:15PM	Indian	16
Shukla, A.K.	19-Jan	10:15AM	Coral B	14	Yushin, G.	19-Jan	10:00AM	Coral B	14
Siegel, D.	20-Jan	11:30AM	Coral B	18	Z				
Singh, G.	20-Jan	11:45AM	Indian	17	Zawodzinski, T.	20-Jan	9:30AM	Coral B	18
Small, L.J.	19-Jan	4:30PM	Indian	16	Zhang, H.G.	19-Jan	11:30AM	Coral B	15
Spoerke, E.	20-Jan	10:15AM	Pacific	17	Zhu, J.	19-Jan	4:00PM	Indian	16
Stemme, F.	20-Jan	9:30AM	Indian	17					
Sun, C.	19-Jan	4:15PM	Coral B	17					
Suvorov, D.	19-Jan	9:30AM	Pacific	15					

Poster Presenters

Name	Date	Time	Room	Page Number	Name	Date	Time	Room	Page Number
Aksel, E.	18-Jan	5:00PM	Atlantic/Arctic	13	Park, K.	18-Jan	5:00PM	Atlantic/Arctic	13, 14
Araujo, E.B.	18-Jan	5:00PM	Atlantic/Arctic	13	Pierce, B.	18-Jan	5:00PM	Atlantic/Arctic	14
Cho, J.	18-Jan	5:00PM	Atlantic/Arctic	13	Rhee, K.	18-Jan	5:00PM	Atlantic/Arctic	13
Forrester, J.S.	18-Jan	5:00PM	Atlantic/Arctic	13	Salame, P.H.	18-Jan	5:00PM	Atlantic/Arctic	13
Ghosh, D.	18-Jan	5:00PM	Atlantic/Arctic	13	Singh, J.	18-Jan	5:00PM	Atlantic/Arctic	14
Goswami, A.	18-Jan	5:00PM	Atlantic/Arctic	14	Teng, H.	18-Jan	5:00PM	Atlantic/Arctic	13
Hotza, D.	18-Jan	5:00PM	Atlantic/Arctic	14	Tutuncu, G.	18-Jan	5:00PM	Atlantic/Arctic	13
Jahantigh, F.	18-Jan	5:00PM	Atlantic/Arctic	14	Wang, Z.	18-Jan	5:00PM	Atlantic/Arctic	14
Jung, J.	18-Jan	5:00PM	Atlantic/Arctic	13	Yang, C.	18-Jan	5:00PM	Atlantic/Arctic	13
Kim, E.	18-Jan	5:00PM	Atlantic/Arctic	13, 14	Zeng, J.	18-Jan	5:00PM	Atlantic/Arctic	13
Kowalski, B.	18-Jan	5:00PM	Atlantic/Arctic	14	Zhou, W.	18-Jan	5:00PM	Atlantic/Arctic	14
Lee, S.	18-Jan	5:00PM	Atlantic/Arctic	13	Zhu, J.	18-Jan	5:00PM	Atlantic/Arctic	13
Mitic, V.	18-Jan	5:00PM	Atlantic/Arctic	13					

Wednesday, January 18, 2012

Plenary I

Room: Indian

8:45 AM

Opening Remarks

Amit Goyal, Edward M. Sabolsky, Steven C. Tidrow

9:00 AM

(EMA-PL-001-2012) Advances in Li-ion Technology for Automotive and Grid Application (Invited)

B. Riley*, A123 Systems, USA

S2: Advanced Dielectric, Piezoelectric and Ferroic Materials, and Emerging Materials in Electronics

Electromechanical Phenomena of Piezoelectric Composites, Actuators, Sensors and Motors

Room: Indian

Session Chair: Jacob Jones, University of Florida

10:30 AM

(EMA-S2-001-2012) Giant Broadband Electro-Mechanical Energy Conversion in [011] Relaxor Ferroelectric Single Crystals (Invited)

P. Finkel*, Naval Undersea Warfare Center Newport, USA; W. Dong, University of California, Los Angeles, USA; A. Amin, Naval Undersea Warfare Center Newport, USA; C. S. Lynch, University of California, Los Angeles, USA

11:00 AM

(EMA-S2-002-2012) Dielectric Composites Produced via Directional Freezing of Non-aqueous Solutions

E. Gorzkowski*, M. Pan, Naval Research Lab, USA

11:15 AM

(EMA-S2-003-2012) Development of Micro-Magnetometers by Sol Gel Deposition of PZT-Spinel Composites

T. I. Muichenik*, K. Sabolsky, E. M. Sabolsky, West Virginia University, USA

11:30 AM

(EMA-S2-004-2012) Origin of high piezoelectric coefficient in $x\text{BiScO}_3-(1-x)\text{PbTiO}_3$ ceramics near the morphotropic phase boundary

J. L. Jones*, G. Tutuncu, University of Florida, USA; J. Chen, University of Science and Technology, China; D. Damjanovic, Swiss Federal Institute of Technology (EPFL), Switzerland

11:45 AM

(EMA-S2-005-2012) Harnessing PZT Thin Films to Create Mobile MEMS Platforms

R. G. Polcawich*, J. Pulskamp, G. Smith, L. Sanchez, R. Rudy, D. Potrepka, US Army Research Laboratory, USA

S4: Advanced Energy Storage Materials and Systems: Lithium and Beyond

Next Generation Advanced Energy Storage Devices: Lithium-air, Lithium-sulfur and All Solid State Batteries I

Room: Coral B

Session Chairs: Bruce Dunn, UCLA; Gholam-Abbas Nazri, Wayne State University

10:30 AM

(EMA-S4-001-2012) Electrolytes for Lithium-ion Batteries (Invited)

T. R. Jow*, O. A. Borodin, Army Research Laboratory, USA; L. Xing, University of Utah, USA

11:00 AM

(EMA-S4-002-2012) New developments in high voltage electrodes, electrolytes and alternative red-ox chemistries (Invited)

B. Lucht*, University of Rhode Island, USA

11:30 AM

(EMA-S4-003-2012) Solid Electrolytes for Li Battery Applications (Invited)

N. J. Dudney*, W. E. Tenhaeff, Oak Ridge National Laboratory, USA; E. G. Herbert, University of Tennessee, USA; K. Hong, S. Kalnaus, A. S. Sabau, Oak Ridge National Laboratory, USA

S5: Unconventional Thermoelectrics: Defect Chemistry, Doping and Nanoscale Effects

Thermal Science and Theory I

Room: Pacific

Session Chair: Alp Sehirlioglu, Case Western Reserve University

10:30 AM

(EMA-S5-001-2012) Nanostructures and the control of thermal conductivity (Invited)

D. Cahill*, U. Illinois, USA

11:00 AM

(EMA-S5-002-2012) Controlling thermal transport with nanoscale composites (Invited)

P. Hopkins*, University of Virginia, USA

11:30 AM

(EMA-S5-003-2012) Phases Diagrams, Crystal Chemistry and Thermoelectric Properties of the Ca-M-Co-O (M=Sr, Zn, and La) Systems

W. Wong-Ng*, NIST, USA; G. Liu, Chinese Academy of Sciences, China; S. Gutierrez, NIST, USA; T. Luo, University of Maryland, USA; Q. Huang, J. Martin, Y. Yan, NIST, USA; J. A. Kaduk, Illinois Institute of Technology, USA

S8 Highlights of Student Research in Basic Science and Electronic Ceramics

Future of Ceramics I

Room: Pacific

Session Chair: Harlan Brown-Shaklee, Sandia National Laboratories

12:10 PM

Opening Remarks

12:15 PM

(EMA-S8-001-2012) Electrical and Structural Properties of Ba(Ho,Ta)_{0.05}Ti_{0.90}O₃, a Dipole-like B-Site Substituted Material, Characterized as Functions of Temperature and Frequency

B. Hoke*, T. Mion, University of Texas - Pan American, USA; D. Potrepka, F. Crowne, U.S. Army Research Laboratory, USA; A. Tauber, Geo-Centers, Inc. (retired), USA; S. Tidrow, University of Texas - Pan American, USA

12:30 PM

(EMA-S8-002-2012) Electrical and Structural Properties of Ba(Ga,Ta)_{0.05}Ti_{0.90}O₃, a Dipole-like B-Site Substituted Material, Characterized as Functions of Temperature and Frequency

M. Rivas*, T. Mion, University of Texas - Pan American, USA; D. Potrepka, F. Crowne, U.S. Army Research Laboratory, USA; A. Tauber, Geo-Centers, Inc. (retired), USA; S. Tidrow, University of Texas - Pan American, USA

12:45 PM

(EMA-S8-003-2012) Study of Platinum/Alumina Interaction for Implantable Neurostimulator Applications

A. Karbasi*, A. Hadjikhani, A. Durygin, W. Jones, Florida International University, USA

S2: Advanced Dielectric, Piezoelectric and Ferroic Materials, and Emerging Materials in Electronics

Lead Free Piezoelectrics

Room: Indian

Session Chairs: Ken-ichi Kakimoto, Nagoya Institute of Technology; Xiaoli Tan, Iowa State Univ

1:30 PM

(EMA-S2-006-2012) Piezoelectric Fatigue of Bi(Zn_{0.5}Ti_{0.5})O₃-(Bi_{0.5}K_{0.5})TiO₃-(Bi_{0.5}Na_{0.5})TiO₃ Ceramics

E. Patterson*, D. Cann, Oregon State University, USA

1:45 PM

(EMA-S2-007-2012) Phase Transitional Behavior and Electrical Properties of Ba_{1-x}Ca_xBi₄Ti₄O₁₅ Lead-Free Ceramics

S. Kumar*, Indian Institute of Science, India; D. A. Ochoa, J. E. Garcia, Universitat Politècnica de Catalunya, Spain; K. Varma, Indian Institute of Science, India

2:00 PM

(EMA-S2-008-2012) The Effect of Composition, Poling, and Texture on the Performance of Ba(Zr_{0.2}Ti_{0.8})O₃-x(Ba_{0.7}Ca_{0.3})TiO₃ (BZT-BCT) Piezoelectric Materials

M. Ehmke*, B. Li, J. E. Blendell, K. J. Bowman, Purdue University, USA

2:15 PM

(EMA-S2-009-2012) A New Opportunity in Non-Lead Piezoelectrics with Ni Co-fired Electrodes

K. Kobayashi*, Y. Doshida, Y. Mizuno, The Pennsylvania State University, USA; C. A. Randall, TAIYO YUDEN Co., Ltd., Japan

2:30 PM

(EMA-S2-010-2012) Particle-size-related Crystal Structure in (Na,K)NbO₃ Ceramics

K. Kakimoto*, Y. Shinkai, R. Kaneko, Nagoya Institute of Technology, Japan

2:45 PM

Break

3:15 PM

(EMA-S2-011-2012) The intriguing ternary lead-free piezoelectric system Na_{1/2}Bi_{1/2}TiO₃ - BaTiO₃ - K_{1/2}Na_{1/2}NbO₃: reconciliation of structure and properties across the phase diagram (Invited)

P. A. Thomas*, D. Walker, D. I. Woodward, J. Davies, L. Collins-MacIntyre, D. Wood, University of Warwick, United Kingdom; R. Dittmer, W. Jo, J. Roedel, Technische Universität Darmstadt, Germany

3:45 PM

(EMA-S2-012-2012) Texture Enhanced Properties in the Lead-Free Piezoelectric Na_{0.5}Bi_{0.5}TiO₃ System

C. Fancher*, Purdue University, USA; K. J. Bowman, Illinois Institute of Technology, USA; J. E. Blendell, Purdue University, USA

4:00 PM

(EMA-S2-013-2012) In situ TEM Study on the Phase Transitions in (Bi_{1/2}Na_{1/2})TiO₃-BaTiO₃ Ceramics

C. Ma, X. Tan*, Iowa State Univ, USA

4:15 PM

(EMA-S2-014-2012) In situ Neutron Diffraction Study of Ferroelasticity in NBT-xBT in the Region of the Morphotropic Phase Boundary

T. Usher*, J. S. Forrester, C. Llano, University of Florida, USA; J. Neufeind, M. Hagen, A. Pramanick, K. An, H. Skorpenske, Oak Ridge National Laboratory, USA; J. L. Jones, University of Florida, USA

4:30 PM

(EMA-S2-015-2012) Advantage of SPS for Dense (Na,K)NbO₃ with Enhanced Piezoelectric Properties

A. Kawai*, K. Kakimoto, Nagoya Institute of Technology, Japan; K. Hatano, Y. Doshida, TAIYO YUDEN CO.,LTD., Japan

S4: Advanced Energy Storage Materials and Systems: Lithium and Beyond

Interfacial Processes and In Situ Methods for Energy Storage Materials and Devices I

Room: Coral B

Session Chairs: Brian Sheldon, Brown University; Vivek Shenoy, Brown University

1:30 PM

(EMA-S4-004-2012) Why Mechanics Phenomena are Essential in Designing Lithium Ion Battery Electrodes (Invited)

P. R. Guduru*, V. Sethuraman, M. Chon, N. Van Winkle, S. Nadimpalli, Brown University, USA

2:00 PM

(EMA-S4-005-2012) Ionic / electronic wiring of lithium ion battery electrodes (Invited)

D. Samulidis*, J. Shin, Y. Yu, C. Zhu, L. Fu, J. Maier, Max Planck Institute for Solid State Research, Germany

2:30 PM

(EMA-S4-006-2012) A micro-macroscopic volume-averaged model for batteries

S. Pannala*, S. Allu, P. Mukherjee, J. Nanda, N. Dudney, S. Martha, J. Turner, Oak Ridge National Laboratory, USA

2:45 PM

Break

3:15 PM

(EMA-S4-007-2012) Location- and Orientation-Dependent Progressive Crack Propagation in Cylindrical Graphite Electrode Particles

R. Grantab, V. B. Shenoy*, Brown University, USA

3:30 PM

(EMA-S4-008-2012) Vacancy-Driven Anisotropic Defect Distribution in the Battery-Cathode Material LiFePO₄ (Invited)

J. Lee, W. Zhou, Vanderbilt University, USA; J. C. Idrobo*, S. J. Pennycook, Oak Ridge National Laboratory, USA; S. T. Pantelides, Vanderbilt University, USA

3:45 PM**(EMA-S4-009-2012) Lithium Intercalation in Low Dimensional Materials as Anodes for Li-ion Batteries**

R. Shahbazian Yassar*, H. Ghassemi, Michigan Technological University, USA; M. Au, Savannah River National Laboratory, USA

4:00 PM**(EMA-S4-010-2012) Elucidating the kinetics of complex Li-insertion reactions in Li batteries (Invited)**

A. Van der Ven*, University of Michigan, USA

4:30 PM**(EMA-S4-011-2012) Interphasial Chemistry and Processes in Li Ion Batteries (Invited)**

A. Cresce, J. Ho, K. Xu*, Army Research Lab, USA

S5: Unconventional Thermoelectrics: Defect Chemistry, Doping and Nanoscale Effects

Thermal Science and Theory II

Room: Pacific

Session Chair: Patrick Hopkins, University of Virginia

1:30 PM**(EMA-S5-004-2012) Unconventional Approaches to Thermoelectric Materials Using Soft Matter (Invited)**

D. Dudis*, M. Check, D. Turner, C. Cheng, J. Shumaker, N. Gothard, E. Kemp, P. Borton, US Air Force, USA

2:00 PM**(EMA-S5-005-2012) Advanced High-Temperature Thermoelectric Materials and Components (Invited)**

T. Caillat*, Jet Propulsion Laboratory/California Institute of Technology, USA

2:30 PM**(EMA-S5-006-2012) High Temperature Thermoelectric Silicides**

J. Mackey*, University of Akron, USA; A. Sehirlioglu, Case Western Reserve, USA; F. Dynys, NASA Glenn Research Center, USA

2:45 PM**Break****3:15 PM****(EMA-S5-007-2012) Magnesium Silicide-Based Nanocomposites for Improved Thermoelectric Efficiency**

S. Bux*, G. Hakimeh, J. Fleurial, Jet Propulsion Laboratory/California Institute of Technology, USA

3:30 PM**(EMA-S5-008-2012) MX₂ layers to generate thermoelectrics: from oxides to selenides (Invited)**

A. Maignan*, S. Hébert, F. Gascoin, E. Guilmeau, Laboratoire CRISMAT, France

4:00 PM**(EMA-S5-009-2012) Thermoelectric Figure of Merit of In₂O₃:Pd Nanocomposites for Energy Harvesting Applications**

M. Amani*, O. J. Gregory, Department of Chemical Engineering, USA; G. C. Fralick, NASA Glenn Research Center, USA

4:15 PM**(EMA-S5-010-2012) Thermoelectric Properties of Undoped and Doped (Ti_{0.75}Sn_{0.25})O₂**

F. Dynys, NASA Glenn Research Center, USA; M. Berger, MINES-ParisTech, France; A. Sehirlioglu*, Case Western Reserve University, USA

Posters

Room: Atlantic/Arctic

5:00 PM**(EMA-S1-P001-2012) Microstructure and Ferroelectric Characteristics of Doped BaTiO₃-ceramics**

V. Mitic*, V. Paunovic, J. Purenovic, J. Nedin, Faculty of Electronic Engineering, Serbia

(EMA-S1-P002-2012) Enhancement of mechanical properties of clay reinforced epoxy nanocomposites with clay modification

K. Rhee*, J. Lee, S. Ha, Kyunghee university, Republic of Korea

(EMA-S2-P003-2012) Synthesis of BaSr_{1-x}TiO₃ films by a low temperature hydrothermal-galvanic couple technique

H. Teng*, P. Chan, F. Lu, National Chung Hsing University, Taiwan

(EMA-S2-P004-2012) Synthesis of barium titanate films on TiN-coated substrates by plasma electrolytic oxidation

J. Zeng*, H. Teng, F. Lu, National Chung Hsing University, Taiwan

(EMA-S2-P005-2012) Synthesis of BaTiO₃ thin film on TiN-coated substrates by a hydrothermal-galvanic couple technique

C. Yang*, D. Tsai, P. Chan, F. Lu, National Chung Hsing University, Taiwan

(EMA-S2-P006-2012) Tailored Processing of Na_{0.5}Bi_{0.5}TiO₃-xBaTiO₃: Role of Barium Content in Phase Formation during Solid State Synthesis

J. S. Forrester*, B. Lettman, T. Usher, J. L. Jones, University of Florida, USA

(EMA-S2-P007-2012) Effect of grain size on domain dynamics and macroscopic dielectric and piezoelectric properties of BaTiO₃ ceramics

D. Ghosh*, A. Sakata, H. Han, J. C. Nino, J. L. Jones, University of Florida, USA

(EMA-S2-P008-2012) Crystal Structure and Phase Transitions in Chemically Modified Sodium Bismuth Titanate

E. Aksel*, J. S. Forrester, J. L. Jones, University of Florida, USA

(EMA-S2-P009-2012) In situ X-ray scattering of Na_{0.5}K_{0.5}NbO₃ based piezoelectric ceramics during reactive templated grain growth

G. Tutuncu*, J. L. Jones, University of Florida, USA; G. L. Messing, Y. Chang, Penn State University, USA

(EMA-S2-P010-2012) Nature of self-polarization effect in the PZT thin film

E. B. Araujo*, E. C. Lima, Sao Paulo State University, Brazil; I. Bdkin, A. L. Kholkin, University of Aveiro, Portugal

(EMA-S2-P011-2012) Dependence of Piezoelectric Properties on Structural Characteristics of (K, Na)NbO₃-based Ceramics

E. Kim*, J. Lee, Kyonggi University, Republic of Korea; J. Cho, B. Kim, Korea Institute of Ceramic Engineering and Technology, Republic of Korea

(EMA-S2-P012-2012) Dielectric and AC electrical conductivity studies of Ln₂CuO₄ (Ln=Nd, Gd) ceramics

P. H. Salame*, O. Prakash, A. Kulkarni, IIT Bombay, India

(EMA-S2-P013-2012) Integrated Humidity Sensor System Using Carbon Nitride Film Based on Analog Mixed CMOS Technology

S. Lee, J. Jung*, Kyungnam University, Republic of Korea

(EMA-S3-P014-2012) Effect of different layer thickness on the Properties of 0.7BiFeO₃-0.3PbTiO₃-Based Multilayer Thin Films Prepared by Sol-gel Process

W. Zhang, Z. Xu, H. Liu, D. Xiao, J. Zhu*, Sichuan University, China

(EMA-S4-P015-2012) Tunable Thermal Transport in Lithium-ion Battery Cathodes as Measured by Time-domain Thermal-reflectance

J. Cho*, M. Losego, D. Cahill, P. Braun, University of Illinois at Urbana Champaign, USA

(EMA-S4-P016-2012) Characteristic of NiO/Li-La-Zr-O solid-state electrolyte by laser annealing for thin film battery

S. Lee*, S. Jee, Yonsei university, Republic of Korea; T. Kim, Korea Institute of Industrial Technology, Republic of Korea; Y. Yoon, Yonsei university, Republic of Korea

(EMA-S5-P017-2012) Improvement in thermoelectric properties by adding P₂O₅ in Fe₂O₃ ceramics

H. K. Hwang, G. W. Lee, K. Park*, Sejong Univ., Republic of Korea

(EMA-S6-P018-2012) Conceptual Design of a No-chamber, Bioethanol-fueled Solid Oxide Fuel Cell

J. L. Aguilar, Universidad Nacional de Colombia, Colombia; A. A. Oliveira, D. Hotza*, Universidade Federal de Santa Catarina, Brazil

(EMA-S6-P019-2012) A novel route for the synthesis of nano-sized high-quality (Y_{0.5}Gd_{0.5})PO₄:Eu³⁺ red phosphors

K. Park*, K. Y. Kim, M. H. Heo, Sejong Univ., Republic of Korea

(EMA-S7-P020-2012) Dielectric Properties of MgNb₂O₆ / Polypropylene Composites at Microwave Frequencies

E. Kim*, C. Jeon, D. Im, Kyonggi University, Republic of Korea

(EMA-S7-P021-2012) New theory to study metamaterials

Z. Wang*, Zhejiang Agriculture & Forestry University, China

(EMA-S8-P022-2012) Synthesis of cordierite dense glass-ceramic and its Structural Optimization using back-scattering Raman Spectroscopy

F. Jahantigh*, Tarbiat Modares University, Islamic Republic of Iran

(EMA-S8-P023-2012) A diffusionless transformation path relating Th₃P₄ and spinel structure: opportunities to synthesize ceramic materials at high pressures

A. Goswami*, UT Arlington, Texas, USA

(EMA-S8-P024-2012) Necessity of the Hanai method to evaluate concentrated dielectric slurries consisting of ceramic powders with high permittivity

W. Zhou*, J. Nino, University of Florida, USA

(EMA-S8-P025-2012) High Temperature Piezoelectrics for Thermoacoustic Engines

B. Kowalski*, A. Sehrioglu, Case Western Reserve University, USA

(EMA-S8-P026-2012) Synthesis, characterization and magnetic properties of Li-Ca-Zn nanoferrite system

J. Singh*, B. S. Randhawa, Guru Nanak Dev University, India

(EMA-S8-P028-2012) Liquid Hydrogen for Cryogenic Cooling and Aviation Fuel Additive

B. Pierce*, T. Haugan, WPAFB, USA

Thursday, January 19, 2012

Plenary II

Room: Indian

8:00 AM

(EMA-PL-002-2012) Science to Energy (Invited)

H. Kung*, U.S. Dept. of Energy, USA

S2: Advanced Dielectric, Piezoelectric and Ferroic Materials, and Emerging Materials in Electronics**Multiferroic Oxides, Heterostructures, and Thin Films**

Room: Indian

Session Chair: Aiping Chen, Texas A&M University

9:30 AM

(EMA-S2-016-2012) Bi-based Piezoelectric Thin Films via Chemical Solution Deposition

Y. Jeon*, Oregon State Univ, USA; J. F. Ihlefeld, G. L. Brennecke, Sandia National Laboratories, USA; B. J. Gibbons, Oregon State Univ, USA

9:45 AM

(EMA-S2-017-2012) Localized Domain Structure in Ferroelectric Thin Films

M. Rogers*, Y. Jing, S. Leech, R. García, J. E. Blendell, Purdue Univ, USA

10:00 AM

(EMA-S2-018-2012) Mapping and Statistics of Ferroelectric Domain Boundary Angles and Types

L. Ye, J. Desmarais, University of Connecticut, USA; J. F. Ihlefeld, Sandia National Laboratories, USA; T. Heeg, Cornell University, USA; J. Schubert, Research Centre Jülich, Germany; D. G. Schlom, Cornell, USA; B. D. Huey*, University of Connecticut, USA

10:15 AM

(EMA-S2-019-2012) Nd-doped BiFeO₃ thin films prepared by Pulsed Laser Deposition

W. Shen*, University of Sheffield, United Kingdom; A. Bell, University of Leeds, United Kingdom; S. Karimi, I. Sterianou, I. Reaney, University of Sheffield, United Kingdom

10:30 AM

(EMA-S2-020-2012) Tunable Physical Properties of Self-assembled Manganite-Based Vertical Aligned Nanocomposite Thin Films

A. Chen*, Z. Bi, X. Zhang, Texas A&M University, USA; Q. Jia, Los Alamos National Laboratory, USA; J. L. MacManus-Driscoll, University of Cambridge, United Kingdom; H. Wang, Texas A&M University, USA

10:45 AM

(EMA-S2-021-2012) Optimization of Magnetic and Ferroelectric Properties of MFe₂O₄(M=Ni, Co) / Pb(Zr_{0.52}Ti_{0.48})O₃ Multilayer Composites

S. Taber*, Georgia Institute of Technology, USA; S. Seifkar, F. Hunte, J. Schwartz, North Carolina State University, USA; N. Bassiri-Gharb, Georgia Institute of Technology, USA

11:00 AM

(EMA-S2-022-2012) Spark plasma sintering (SPS) of nanostructured BaTiO₃-CoFe₂O₄ multiferroic composites

D. Ghosh*, H. Han, A. Sakata, J. C. Nino, J. L. Jones, University of Florida, USA

11:15 AM

(EMA-S2-023-2012) Synthesis and characterization of xCo_{0.7}Zn_{0.3}Fe₂O₄- Bi_{0.9}La_{0.1}FeO₃ multiferroic nanocomposites

K. Yadav*, Indian Institute of Technology Roorkee, India

11:30 AM

(EMA-S2-024-2012) Effect of annealing atmosphere on the structural and electrical properties of the (Na_{0.5}K_{0.5})NbO₃ thin film

B. Kim*, T. Seong, I. Seo, M. Jang, S. Nahm, Korea University, Republic of Korea

11:45 AM

(EMA-S2-025-2012) BaZrxTi1-xO₃ relaxors: self-assembled nanocomposite

T. Maiti*, Indian Institute of Technology Kanpur, India; R. Guo, A. S. Bhalla, The University of Texas at San Antonio, USA

S4: Advanced Energy Storage Materials and Systems: Lithium and Beyond**Novel Electrode Architecture, Assembly and Design for Advanced Batteries**

Room: Coral B

Session Chairs: Nancy Dudney, Oak Ridge National Laboratory; Jeff Sakamoto, Michigan State University

9:30 AM

(EMA-S4-012-2012) Design and Fabrication of 3D Electrodes and Battery Architectures (Invited)

N. Cirigliano, E. Perre, B. Dunn*, UCLA, USA

10:00 AM

(EMA-S4-013-2012) Carbon-Containing Nanocomposite Materials for Energy Storage (Invited)

G. Yushin*, Georgia Institute of Technology, USA

10:15 AM

(EMA-S4-014-2012) Lead-Carbon Hybrid Ultracapacitors and their Applications (Invited)

A. K. Shukla*, Indian Institute of Science, India

10:45 AM

(EMA-S4-015-2012) Fe based fluoride nanocomposite cathode for lithium rechargeable batteries (Invited)

K. Kang*, Seoul National University, Republic of Korea

11:15 AM

(EMA-S4-016-2012) Metal Free, Binder Free Silicon- Carbon Fiber Composite Anode Architecture

S. K. Martha*, J. Nanda, R. R. Unocic, W. D. Porter, N. J. Dudney, Oak Ridge National Laboratory, USA

11:30 AM

(EMA-S4-017-2012) Three-dimensional Bicontinuous Composite Electrodes for High Power and Energy Density Batteries

H. G. Zhang*, P. V. Braun, University of Illinois at Urbana-Champaign, USA

11:45 AM

(EMA-S4-018-2012) High Capacity Prismatic Li-Ion Cell Alloy Anodes for Electric Vehicle Applications (Invited)

S. Lopatin*, R. Bachrach, D. Brevnov, S. Thirupapuliur, K. Chen, L. Chen, Applied Materials, USA

S7: Metamaterials and Microwave Materials

Microwave Composites and Metamaterials

Room: Pacific

Session Chair: Paul Clem, Sandia National Laboratories

9:30 AM

(EMA-S7-001-2012) Engineering of High-K, High-Q Microwave Dielectrics

D. Suvorov*, B. Jančar, Jozef Stefan Institute, Slovenia

9:45 AM

(EMA-S7-002-2012) Dependence of Microwave Dielectric Properties on Structural Characteristics of AB_2O_6 (A = Ni, Mg, Zn, and B = Nb, Ta) Ceramics

E. Kim*, C. Jeon, Kyonggi University, Republic of Korea

10:00 AM

(EMA-S7-003-2012) Flexible Polymer/Ferrite Composites for High Frequency Applications

L. Qin*, K. Shqau, H. Verweij, Ohio State University, USA

10:15 AM

(EMA-S7-004-2012) Electrical and Structural Properties of $Ba(Y,Sb)_{0.05}Ti_{0.90}O_3$, a Dipole-like B-Site Substituted Material, Characterized as Functions of Temperature and Frequency

J. Morales*, T. Mion, University of Texas - Pan American, USA; D. Potrepka, F. Crowne, U.S. Army Research Laboratory, USA; A. Tauber, Geo-Centers, Inc. (retired), USA; S. Tidrow, University of Texas - Pan American, USA

10:30 AM

(EMA-S7-005-2012) Dielectric and X-Ray Diffraction Analysis of $Ba(Lu,Ta)_{0.05}Ti_{0.90}O_3$

T. Mion*, M. Rivas, University of Texas - Pan American, USA; D. Potrepka, F. Crowne, U.S. Army Research Laboratory, USA; A. Tauber, Geo-Centers, Inc. (retired), USA; S. Tidrow, University of Texas - Pan American, USA

10:45 AM

(EMA-S7-006-2012) Structural Investigation of $Ba(Yb,Ta)_{0.05}Ti_{0.90}O_3$ Grain Size Using SEM, XRD

T. Mion*, M. Rivas, University of Texas - Pan American, USA; D. Potrepka, F. Crowne, U.S. Army Research Laboratory, USA; A. Tauber, Geo-Centers, Inc. (retired), USA; S. Tidrow, University of Texas - Pan American, USA

11:00 AM

(EMA-S7-007-2012) Microwave dielectric metamaterials: influence of dielectric loss and permittivity variation on metamaterial performance

P. Clem*, M. P. Rye, Sandia National Laboratories, USA; E. Kim, C. Jeon, Kyonggi University, Republic of Korea

11:15 AM

(EMA-S7-008-2012) Design and Comprehensive Study of Compact LH Metamaterials CSRR and CSSR-Based BPWG Filter

E. K. Hamad*, H. A. Atallah, Faculty of Engineering, Egypt

S8 Highlights of Student Research in Basic Science and Electronic Ceramics

Future of Ceramics II

Room: Pacific

Session Chair: Elena Aksel, University of Florida

12:10 PM

Opening Remarks

12:15 PM

(EMA-S8-004-2012) Development and Implementation of a Polarization and Strain Measurement System

C. Llano*, E. Aksel, S. Banavara Seshadri, J. Forrester, J. Jones, University of Florida, USA

12:30 PM

(EMA-S8-005-2012) Optimizing Flux Pinning of YBCO Superconductor with Mixed Phase Nanoparticle Additions

M. Sebastian*, J. N. Reichart, M. M. Ratcliff, AFRL, USA; J. Burke, University of Dayton Research Institute, USA; T. Haugan, AFRL, USA

12:45 PM

(EMA-S8-006-2012) Effects of Surface Step on Oxygen Distribution and Silicon Oxidation State Transformation on Si (001)

M. A. Pamungkas*, B. Kim, K. Lee, Korea Institute of Science and Technology, Republic of Korea

S2: Advanced Dielectric, Piezoelectric and Ferroic Materials, and Emerging Materials in Electronics

Pervoskite Dielectric, Mott Insulators, Ferroelectric and Piezoelectric Materials

Room: Indian

Session Chairs: Steve Dai, Sandia National Labs; Akansha Dwivedi, IIT-Mandi

1:30 PM

(EMA-S2-026-2012) Temperature Stability in High Temperature Capacitor $BaTiO_3 - Bi(Zn_{1/2}Ti_{1/2})O_3$ Based Solid Solutions

N. Raengthon*, D. P. Cann, Oregon State University, USA

1:45 PM

(EMA-S2-027-2012) $Ca(Zr,Ti)O_3$ Ceramics for Energy Storage Applications

S. Dai*, B. A. Hernandez-Sanchez, T. Garino, P. Lu, N. Bell, J. Wheller, D. L. Moore, B. A. Tuttle, Sandia National Labs, USA

2:00 PM

(EMA-S2-028-2012) High energy density $(0.65+y)Pb(Zr_{0.47}Ti_{0.53})O_3 - (0.35-y)Pb[(Ni_{1-x}Zn_x)_{1/3}Nb_{2/3}]O_3$ ceramics for energy harvesting devices

S. Nahm*, I. Seo, Y. Cha, I. Kang, J. Choi, Korea University, Republic of Korea

2:15 PM

(EMA-S2-029-2012) Electrical Properties of Bismuth Zinc Niobate Pyrochlore Relaxor

R. Osman, University Malaysia Perlis, Malaysia; N. Masó, A. R. West*, University of Sheffield, United Kingdom

2:30 PM**(EMA-S2-030-2012) Piezoelectric Properties of High Temperature Ternary Perovskite Ceramics**

T. Ansell*, J. Nikkel, D. Cann, Oregon State University, USA

2:45 PM**Break****3:15 PM****(EMA-S2-031-2012) Flexible Energy Harvesters Based on Laser Transferred Piezoelectric Micro-Ribbons (Invited)**

S. Yoon*, H. Song, Y. Do, C. Kang, Korea Institute of Science & Technology, Republic of Korea

3:45 PM**(EMA-S2-032-2012) Enhancement of the Electromechanical and Electrocaloric Effects Near the Critical Point in Relaxor Ceramics**

Z. Kutnjak*, B. Rozic, Jozef Stefan Institute, Slovenia; B. Malič, H. Uršič, J. Holc, M. Kosec, Jozef Stefan Institute, Slovenia; R. Pirc, Jozef Stefan Institute, Slovenia; Q. M. Zhang, The Pennsylvania State University, USA

4:00 PM**(EMA-S2-033-2012) Influence of Magnesium and Yttrium codoping on the intrinsic pyroelectric property of BST ceramics**

J. Zhu*, Z. Xu, W. Zhang, G. Liu, D. Xiao, P. Yu, Sichuan University, China

4:15 PM**(EMA-S2-034-2012) Flux-assisted growth of BaTiO₃ thin films**

D. T. Harris*, M. Burch, P. G. Lam, E. C. Dickey, J. Maria, North Carolina State University, USA

4:30 PM**(EMA-S2-035-2012) Electrochemical Response of Pb(Zr,Ti)O₃ Thin Films**

L. J. Small*, Rensselaer Polytechnic Institute, USA; C. Apblett, J. Ihlefeld, Sandia National Laboratories, USA; D. Duquette, Rensselaer Polytechnic Institute, USA

4:45 PM**(EMA-S2-036-2012) Electric-field-induced structural changes in 111-oriented domain-engineered tetragonal BaTiO₃**

A. Pramanick*, K. An, A. D. Stoica, L. G. Clonts, A. A. Parizzi, D. Maierhafer, Oak Ridge National Laboratory, USA; D. Damjanovic, Swiss Federal Institute of Technology, Switzerland; J. L. Jones, University of Florida, USA; X. Wang, Oak Ridge National Laboratory, USA

5:00 PM**(EMA-S2-037-2012) Thermodynamic Theory of Inter-Ferroelectric Transitions in Binary and Ternary Ferroelectric Solid Solutions**

G. A. Rossetti*, A. A. Heilmann, University of Connecticut, USA

5:15 PM**(EMA-S2-038-2012) Unusual Phase Transition Behavior in Rhombohedral xBi(Mg_{1/2}Ti_{1/2})O₃-yBi(Zn_{1/2}Ti_{1/2})O₃-zPbTiO₃ Ternary Ferroelectric System**

A. Dwivedi*, W. Qu, C. A. Randall, The Pennsylvania State University, USA

S3: Symposium on Thin Film Integration and Processing Science

Physical Vapor Deposition and Strain Engineering

Room: Pacific

Session Chair: Yu Hong Jeon, Oregon State Univ

1:30 PM**(EMA-S3-001-2012) Magnetron sputter deposition of biaxial aligned thin films (Invited)**

D. Depla*, M. Saraiva, J. Lamas, Ghent University, Belgium

2:00 PM**(EMA-S3-002-2012) Optimizing Nanophase Additions to YBCO Superconductor to Enhance Low Temperature Flux Pinning**

T. J. Haugan*, M. A. Sebastian, J. N. Reichart, M. M. Ratcliff, B. T. Pierce, J. L. Burke, E. L. Brewster, The Air Force Research Laboratory, USA

2:15 PM**(EMA-S3-003-2012) Ion-Beam Assisted Nano-Texturing of MgO Films (Invited)**

V. Matias*, Los Alamos National Laboratory, USA

2:45 PM**Break****3:15 PM****(EMA-S3-004-2012) Surfactant Assisted Growth of Smooth Epitaxial Oxides on GaN (Invited)**

E. Paisley*, North Carolina State University, USA; M. Biegalski, Oak Ridge National Laboratory, USA; J. Lebeau, B. Gaddy, S. Mita, R. Collazo, Z. Sitar, D. Irving, J. Maria, North Carolina State University, USA

3:45 PM**(EMA-S3-005-2012) Strain Analysis of LaAlO₃/SrTiO₃ Hetero-interfaces**

W. Wei, A. Sehirirlioglu*, Case Western Reserve University, USA

4:00 PM**(EMA-S3-006-2012) Control of the Octahedral Tilts in Lanthanum Cobaltite and the Impact on Magnetic Properties (Invited)**

M. D. Biegalski*, W. Siemons, Z. Gai, A. Hallermark, V. Lutter, Oak Ridge National Lab, USA; A. Mehta, Stanford Synchrotron Radiation Lightsource, USA; Y. Kim, A. Borisevich, Oak Ridge National Lab, USA; Y. Takamura, University of California, USA; H. M. Christen, Oak Ridge National Lab, USA

4:30 PM**(EMA-S3-007-2012) Luminescent, structural and compositional properties of thin garnet phosphor layer for light emitting diodes**

D. Kundaliya*, M. Raukas, A. Scotch, D. Hamby, M. Stough, K. Mishra, OSRAM SYLVANIA, USA

4:45 PM**(EMA-S3-008-2012) Control of ZnO thin film polarity through interface chemistry**

C. T. Shelton*, J. Maria, NCSU, USA

S4: Advanced Energy Storage Materials and Systems: Lithium and Beyond

Interfacial Processes and In Situ Methods for Energy Storage Materials and Devices II

Room: Coral B

Session Chairs: Sreekanth Pannala, Oak Ridge National Laboratory; Kang Xu, Army Research Lab; Don Siegel, University of Michigan

1:30 PM**(EMA-S4-019-2012) Transitioning From LiCoO₂ to Layered-Layered Composite Li₂MnO₃-LiMO₂ (M=Mn, Ni, Co) Li-ion Cathodes: Benefits and Challenges (Invited)**

R. Bugga*, W. West, M. Smart, J. Soler, Jet Propulsion Laboratory, USA; R. Staniewicz, C. Ma, J. Robak, SAFT America Inc., USA

2:00 PM**(EMA-S4-020-2012) Neutron Computed Tomography of Lithium Distribution in Porous Carbon Foams and Discharged Li-Air Cathodes (Invited)**

H. Bilheux*, J. Nanda, S. Voisin, G. Veith, L. Walker, S. Allu, S. Pannala, P. Mukherjee, N. Dudney, Oak Ridge National Laboratory, USA

2:30 PM**(EMA-S4-021-2012) Using in situ thin film stress measurements to understand fundamental lithiation mechanisms in battery electrode materials**

B. W. Sheldon*, A. Mukhopadhyay, S. K. Soni, A. Tokranov, D. Liu, Brown University, USA

2:45 PM**Break**

3:15 PM**(EMA-S4-022-2012) Multiscale electronic transport mechanism and true conductivities in amorphous carbon-LiFePO₄ nanocomposites (Invited)**

K. Seid, Université de Nantes, CNRS, France; J. Badot, Chimie ParisTech (ENSCP), CNRS, UPMC Univ Paris 06, France; O. Dubrunfaut, SUPELEC, UPMC Univ Paris 06, Univ Paris-Sud, CNRS, France; D. Guyomard, Université de Nantes, CNRS, France; S. Levasseur, UMI-CORE Cobalt & Specialty Materials, Belgium; B. Lestriez*, Université de Nantes, CNRS, France

3:45 PM**(EMA-S4-023-2012) Knock-off Mechanism of Li-ion Diffusion in Solid Electrolyte Interphase**

S. Shi*, Brown University, USA; P. Lu, L. G. Hector, S. J. Harris, Y. Qi, General Motors R&D Center, USA

4:00 PM**(EMA-S4-024-2012) Surface and Subsurface Damage Characterization of Graphite Anodes Electrochemically Cycled in Lithium-ion Cells**

S. Bhattacharya*, A. Riahi, A. Alpas, University of Windsor, Canada

4:15 PM**(EMA-S4-025-2012) Study of the ions and ion pair transport and component interactions in PPG-LiTFSI complexes**

C. Sun*, Y. Wang, T. Zawodzinski, A. Sokolov, Oak Ridge National Laboratory, USA

4:30 PM**(EMA-S4-026-2012) Computational Modeling for Cycling Characteristics of Various Electrolytes in Lithium-Ion Battery Cells (Invited)**

K. Tasaki*, Mitsubishi Chemical America, USA

Friday, January 20, 2012**Plenary III**

Room: Indian

8:00 AM**(EMA-PL-003-2012) Future Opportunities in Materials Design (Invited)**

J. T. Prater*, U.S. Army Research Office, USA

S2: Advanced Dielectric, Piezoelectric and Ferroic Materials, and Emerging Materials in Electronics**Microwave Dielectrics, Metamaterials and Frequency Tunable Devices and Nanoscale Phenomena in Dielectric, Ferroelectric and Piezoelectric Materials**

Room: Indian

Session Chairs: Nazanin Bassiri-Gharb, Georgia Institute of Technology; Robert Freer, University of Manchester

9:30 AM**(EMA-S2-039-2012) Dielectric and Structural Characterization of Co-doped Ba_{0.6}Sr_{0.4}TiO₃ Thin Films for Tunable Passive Microwave Applications**

F. Stemme*, H. Gesswein, C. Azucena, Karlsruhe Institute of Technology, Germany; M. Sazegar, Darmstadt University of Technology, Germany; J. R. Binder, M. Bruns, Karlsruhe Institute of Technology, Germany

9:45 AM**(EMA-S2-040-2012) The effect of ZnO-B₂O₃ addition on the dielectric properties of screen-printed low-sintering Barium Strontium Titanate (BST) thick-films**

C. Kohler*, X. Zhou, Karlsruhe Institute of Technology (KIT), Germany; M. Sazegar, R. Jakoby, Technische Universität Darmstadt, Germany; F. Stemme, J. Hausselt, J. R. Binder, Karlsruhe Institute of Technology (KIT), Germany

10:00 AM**(EMA-S2-041-2012) Integration of Fluxed-Barium Strontium Titanate Thin Films in Bandpass Tunable Filter**

P. Lam*, V. Haridasan, M. B. Steer, J. Maria, North Carolina State University, USA

10:15 AM**(EMA-S2-042-2012) Atomic-Resolution Transmission Electron Microscopy (HAADF-STEM) Z-Contrast Imaging and EELS of Microwave Dielectrics**

R. Freer*, F. Azough, B. Schaffer, University of Manchester, United Kingdom

10:30 AM**(EMA-S2-043-2012) Dielectric Properties of Complex Barium Neodymium Titanates in Microwave Regime**

D. K. Dhanjal*, Punjab Technical University, India

10:45 AM**(EMA-S2-044-2012) Analysis of Ba(Sc,Ta)_{0.05}Ti_{0.90}O₃ as a Frequency Agile Microwave Material**

T. Mion*, M. Rivas, University of Texas - Pan American, USA; D. Potrepka, F. Crowne, U.S. Army Research Laboratory, USA; A. Tauber, Geo-Centers, Inc., USA; S. Tidrow, University of Texas - Pan American, USA

11:00 AM**(EMA-S2-045-2012) Synthesis of the Na_xK_{1-x}NbO₃ nanowires using hydrothermal method**

X. HaiBo*, J. Mi-Ri, S. In-Tae, N. Sahn, Korea university, Republic of Korea

11:15 AM**(EMA-S2-046-2012) Piezoelectric response of lead zirconate titanate nanotubes processed via soft template infiltration**

N. Bassiri-Gharb*, A. Bernal, Georgia Inst. of Technology, USA

11:30 AM**(EMA-S2-047-2012) Crystal Structure and Ferroelectric property of Epitaxial Rhombohedral Pb(Zr,Ti)O₃ Films**

Y. Ehara*, S. Yasui, T. Oikawa, M. Nakajima, Tokyo Institute of Technology, Japan; T. Yamada, Nagoya University, Japan; T. Iijima, Advanced Industrial Science and Technology, Japan; H. Funakubo, Tokyo Institute of Technology, Japan

11:45 AM**(EMA-S2-048-2012) Solar air conditioning using ceramic composite and nano-structured materials**

G. Singh*, P. Singh, P. Vyas, G. Sharma, College of Engineering & Technology, Bikaner, India

12:00 PM**(EMA-S2-049-2012) Another Look at Goldschmidt's Tolerance Factor for Design of Advanced Material**

S. Tidrow*, University of Texas - Pan American, USA

S3: Symposium on Thin Film Integration and Processing Science**Low Temperature Processing**

Room: Pacific

Session Chair: Elizabeth Paisley, North Carolina State University

9:30 AM**(EMA-S3-009-2012) Bio-Integrated Soft Electronics (Invited)**

N. Lu*, University of Texas at Austin, USA

10:00 AM**(EMA-S3-010-2012) Optical and Electrical Transport Properties of Chemically Deposited Antimony - Cadmium Selenide Thin Film Structures**

E. U. Masumdar*, Rajarshi hahu College, Latur, India

10:15 AM**(EMA-S3-011-2012) Templating Nanostructured Cadmium Sulfide Thin Films (Invited)**

E. Spoecker*, Sandia National Laboratories, USA

10:45 AM**(EMA-S3-012-2012) Nanoscale ceramic thin film integration on fibrous materials (Invited)**

J. S. Jur*, C. J. Oldham, W. J. Sweet, G. N. Parsons, North Carolina State University, USA

11:15 AM**(EMA-S3-013-2012) The influence of a Bi-precursor on the formation of β -Bi₂O₃ thin films**

A. Veber*, Institut "Jožef Stefan", Slovenia, Institut "Jožef Stefan", Slovenia, Jozef Stefan Institute, Slovenia; S. Kunej, Institut "Jožef Stefan", Slovenia, Institut "Jožef Stefan", Slovenia, Jozef Stefan Institute, Slovenia; D. Suvorov, Institut "Jožef Stefan", Slovenia, Institut "Jožef Stefan", Slovenia, Jozef Stefan Institute, Slovenia

11:30 AM**(EMA-S3-014-2012) Low temperature synthesis of epitaxial KNbO₃ thick films grown by hydrothermal Method (Invited)**

H. Funakubo*, T. Shiraishi, H. Einishi, T. Hasegawa, M. Ishikawa, Tokyo Institute of Technology, Japan; T. Morita, The University of Tokyo, Japan; M. Kurosawa, Tokyo Institute of Technology, Japan

S4: Advanced Energy Storage Materials and Systems: Lithium and Beyond

Next Generation Advanced Energy Storage Devices: Lithium-air, Lithium-sulfur and All Solid State Batteries II

Room: Coral B

Session Chairs: Anton Van der Ven, University of Michigan; Jagjit Nanda, Oak Ridge National Lab; Jack Wells, Oak Ridge National Lab

9:30 AM**(EMA-S4-027-2012) Improving Performance in Vanadium Flow Batteries (Invited)**

T. Zawodzinski*, Z. Tang, D. Aaron, J. Lawton, R. Counce, M. Moore, J. Watson, M. Mench, A. Papandrew, U. Tennessee-Knoxville, USA

10:00 AM**(EMA-S4-028-2012) A Practical, Rechargeable Lithium-Oxygen Battery (Invited)**

B. Kumar*, UDRI, USA

10:15 AM**(EMA-S4-029-2012) Fast ion conducting ceramic electrolyte based on Li₇La₃Zr₂O₁₂ garnet (Invited)**

J. Sakamoto*, Michigan State University, USA

10:45 AM**(EMA-S4-030-2012) Investigation on solid electrolyte materials for micro electronic devices**

S. Jee*, Y. Yoon, Yonsei Univ, Republic of Korea; D. Kim, Auburn University, USA

11:00 AM**(EMA-S4-031-2012) All Silicon Based Lithium Battery (Invited)**

G. Nazri*, Wayne State University, USA

11:30 AM**(EMA-S4-032-2012) Identifying Performance-Limiting Phenomena in Li-air Batteries via First-Principles Simulation (Invited)**

D. Siegel*, M. Radin, F. Tian, J. Rodriguez, University of Michigan, USA

S1: New Frontiers in Electronic Ceramic Structures, Advanced Electronic Material Devices and Circuit Integration

Electronic Ceramic Structures

Room: Indian

Session Chairs: Vojislav Mitic, Faculty of Electronic Engineering; Amar Bhalla, University of Texas, San Antonio

1:30 PM**(EMA-S1-001-2012) High-Temperature Nanomaterials for Electrochemical Micro-Sensors**

E. M. Sabolsky*, C. Wildfire, E. Ciftiyurek, K. Sabolsky, West Virginia University, USA

1:45 PM**(EMA-S1-002-2012) Optimum Conditions For Deposition of ZnO Semiconductor Films By RF Sputtering**

T. Oder*, A. Smith, M. McMaster, N. Velpukonda, Youngstown State University, USA; M. L. Nakarmi, Brooklyn College, USA

2:00 PM**(EMA-S1-003-2012) Fibrous BaTiO₃ Filler / PVDF Composite Sheet for Transducer Application**

K. Fukata*, K. Kakimoto, Nagoya Institute of Technology, Japan; H. Ogawa, Otsuka Chemical Co., Ltd, Japan

2:15 PM**(EMA-S1-004-2012) Contribution of non-180° domain wall motion and lattice strain to the frequency dependence of the piezoelectric coefficient in ferroelectric ceramics**

S. Banavara Seshadri*, A. D. Prewitt, University of Florida, USA; D. Damjanovic, Swiss Federal Institute of Technology - EPFL, Switzerland; A. J. Studer, ANSTO, Australia; J. L. Jones, University of Florida, USA

2:30 PM**(EMA-S1-005-2012) Microstructure Fractal Analysis of Er Doped BaTiO₃-ceramics**

V. Mitic*, V. Paunovic, J. Purenovic, L. Kocic, Faculty of Electronic Engineering, Serbia; S. Jankovic, Faculty of Mathematics, Serbia; V. Pavlovic, Faculty of Agriculture, Serbia

2:45 PM**Break****3:15 PM****(EMA-S1-006-2012) Atom Probe Tomography of Oxide Ceramics**

R. Kirchhofer, D. R. Diercks, B. P. Gorman*, Colorado School of Mines, USA

3:30 PM**(EMA-S1-007-2012) Mechanically Activated BaTiO₃ Microstructure Fractal Nature**

V. Mitic*, Faculty of Electronic Engineering, Serbia; V. Pavlovic, Faculty of Mechanical Engineering, Serbia; L. Kocic, V. Paunovic, J. Purenovic, J. Nedin, Faculty of Electronic Engineering, Serbia; V. Pavlovic, Faculty of Agriculture, Serbia

3:45 PM**(EMA-S1-008-2012) Intense cooperative upconversion emission in Yb/Er : TeO₂-Li₂O-WO₃ oxyfluoride glass ceramics**

G. F. Ansari, All Saints' College of Technology, Bhopal (M.P.) 462036 India, India; S. K. Mahajan*, Samrat Ashok Technological Institute, Vidisha (M.P.) 464001 India, India

4:00 PM**(EMA-S1-009-2012) Analytical model for ion-implanted 4H silicon carbide metal-semiconductor field-effect transistors**

S. Wang*, Northwest University, China

S3: Symposium on Thin Film Integration and Processing Science

Complex Oxide Thin Film Synthesis

Room: Pacific

Session Chair: Christopher Shelton, NCSU

1:30 PM

(EMA-S3-015-2012) Advanced chemical solution deposition methods of complex electronic oxide films (Invited)

T. Schneller*, RWTH Aachen, Germany

2:00 PM

(EMA-S3-016-2012) Orientation Control in Pb(Zr_{0.52}Ti_{0.48})O₃ Thin Films for Use in Multilayer Actuators

L. M. Sanchez*, D. Potrepka, Army Research Laboratory, USA; G. Fox, Fox Materials Consulting LLC, USA; I. Takeuchi, University of Maryland, USA; R. G. Polcawich, Army Research Laboratory, USA

2:15 PM

(EMA-S3-017-2012) Microstructural Evolution of Flux-Grown Barium Titanate Thin Films

M. J. Burch*, A. Moballegh, D. T. Harris, J. Maria, E. C. Dickey, North Carolina State University, USA

2:30 PM

(EMA-S3-018-2012) Synthesis and Characterization of Pb(Zr_xTi_{1-x})O₃ Thin Films on Copper Foils by RF Magnetron Sputtering

J. Walenza-Slabe, A. D. Mason, B. J. Gibbons*, Oregon State University, USA

2:45 PM

Break

3:15 PM

(EMA-S3-019-2012) Piezoelectric MEMS on Alternative Substrates (Invited)

D. Wilke, S. Bharadwaja, S. Trolier-McKinstry*, Penn State, USA; P. Reid, D. Schwartz, Harvard Smithsonian, USA

3:45 PM

(EMA-S3-020-2012) Epitaxial-Like Polycrystalline PZT Superlattices Processed by Chemical Solution Deposition

Y. Bastani*, N. Bassiri-Gharb, Georgia Institute of Technology, USA

4:00 PM

(EMA-S3-021-2012) Effect of pre-crystallization aging on microstructure and properties of solution derived PZT thin films

K. Nittala*, University of Florida, USA; K. E. Meyer, Sandia National Laboratories, USA; S. Mhin, University of Florida, USA; J. F. Ihlefeld, G. L. Brennecke, Sandia National Laboratories, USA; J. L. Jones, University of Florida, USA

4:15 PM

(EMA-S3-022-2012) Chemically homogeneous ferroelectric thin films with enhanced electromechanical responses

J. Ihlefeld*, Sandia National Laboratories, USA; C. T. Shelton, North Carolina State University, USA; G. L. Brennecke, Sandia National Laboratories, USA; P. G. Lam, North Carolina State University, USA; P. G. Kotula, B. B. McKenzie, M. J. Rye, J. A. Ohlhausen, K. E. Meyer, Sandia National Laboratories, USA; B. J. Gibbons, Oregon State University, USA; J. Maria, North Carolina State University, USA

S6: Technologies for Sustainability and Green Materials Processing

Technologies for Sustainability and Green Materials Processing

Room: Coral B

Session Chair: Paul Clem, Sandia National Laboratories

1:30 PM

(EMA-S6-001-2012) Carbonate Ceramics: A Disruptive Technology for CO₂ Utilization (Invited)

R. Riman*, Q. Li, S. Gupta, M. A. Bitteto, Rutgers University, USA; V. Atakan, Solidia Technologies, USA

2:00 PM

(EMA-S6-002-2012) Microwave processing of soapstone under supercritical carbon dioxide atmosphere

A. Dias*, UFOP, Brazil

2:15 PM

(EMA-S6-003-2012) NaY-Zeolite for CO₂ Capture Applications

W. Wong-Ng*, NIST, USA; J. A. Kaduk, Illinois Institute of Technology, USA; J. Bures, Q. Huang, L. Espinal, T. Yildirim, NIST, USA

2:30 PM

(EMA-S6-004-2012) Greener Synthesis of Functional Oxide Nanoparticle Inks

D. Ito*, S. Yokoyama, B. A. Weintraub, K. Masuko, J. E. Hutchison, University of Oregon, USA

2:45 PM

Break

3:15 PM

(EMA-S6-005-2012) Sunshine to petrol: a metal oxide-based thermochemical route to solar fuels (Invited)

E. N. Coker*, J. E. Miller, Sandia National Laboratories, USA

3:45 PM

(EMA-S6-006-2012) Food additives in ceramic processing: a review

C. M. Costa, B. Walber, M. B. Quadri, D. Hotza*, UFSC, Brazil

4:00 PM

(EMA-S6-007-2012) Tape Casting with Non-VOC Solvents and Food Grade Additives

B. Wendt, B. P. Gorman*, Colorado School of Mines, USA

MS&T'12[®]

Materials Science & Technology
2012 Conference & Exhibition

OCTOBER 7–11, 2012
DAVID L. LAWRENCE CONVENTION CENTER
PITTSBURGH, PENNSYLVANIA, USA

Call for Papers

Abstract Deadline:
March 15, 2012

www.matscitech.org

*The leading forum
addressing structure,
properties, processing
and performance
across the materials
community.*

Organized by:



Sponsored by:



Wednesday, January 18, 2012

Plenary I

Room: Indian

9:00 AM

(EMA-PL-001-2012) Advances in Li-ion Technology for Automotive and Grid Application (Invited)

B. Riley*, A123 Systems, USA

not available

S2: Advanced Dielectric, Piezoelectric and Ferroic Materials, and Emerging Materials in Electronics

Electromechanical Phenomena of Piezoelectric Composites, Actuators, Sensors and Motors

Room: Indian

Session Chair: Jacob Jones, University of Florida

10:30 AM

(EMA-S2-001-2012) Giant Broadband Electro-Mechanical Energy Conversion in [011] Relaxor Ferroelectric Single Crystals (Invited)

P. Finkel*, Naval Undersea Warfare Center Newport, USA; W. Dong, University of California, Los Angeles, USA; A. Amin, Naval Undersea Warfare Center Newport, USA; C. S. Lynch, University of California, Los Angeles, USA

Giant broadband electro-mechanical energy conversion is demonstrated under ferroelectric/ferroelectric phase transformation in [011] cut and poled $\text{Pb}(\text{In}_{1/2}\text{Nb}_{1/2})\text{O}_3\text{-Pb}(\text{Mg}_{1/3}\text{Nb}_{2/3})\text{O}_3\text{-PbTiO}_3$ (PIN-PMN-PT). The reversible effect is observed with the sharp high strain and polarization jumps accompanying the stress-induced FR-FO transition. The phase-transitioning in ferroelectric material results in an output electrical energy density of $\sim 750 \mu\text{J cm}^{-3}$ per cycle which is more than an order of magnitude larger than that reported for linear piezoelectric materials. The upper bound of the energy density of the phase transitioning material under the ideal thermodynamic cycle is far greater than demonstrated in the experiments performed using resistive load. This effect can be utilized to harvest electrical energy from mechanical work done during FR-FO-FR transition. The efficiency of the phase transition energy harvesting and its potential technical realizations will be discussed.

11:00 AM

(EMA-S2-002-2012) Dielectric Composites Produced via Directional Freezing of Non-aqueous Solutions

E. Gorzkowski*, M. Pan, Naval Research Lab, USA

In previous research freeze casting was used to construct ceramic-polymer composites in which the two phases are arranged in an electrically parallel configuration. By doing so, the composites exhibit dielectric constant (K) up to two orders of magnitude higher than that of composites with ceramic particles randomly dispersed in a polymer matrix. This technique has been successful with both an aqueous and camphene based ceramic slurry that is frozen uni-directionally to form ice platelets and ceramic aggregates that are aligned in the temperature gradient direction. In this paper an update will be given on non-aqueous solutions such as camphene, dimethyl sulfone, and tertiary butanol based samples in order to process the slurry at room temperature. Dielectric properties will be discussed in light of slurry choice, ceramic particle size, and polymer composition.

11:15 AM

(EMA-S2-003-2012) Development of Micro-Magnetometers by Sol Gel Deposition of PZT-Spinel Composites

T. I. Muchenik*, K. Sabolsky, E. M. Sabolsky, West Virginia University, USA

There are many available systems to measure magnetic fields with high precision, but these current technologies cannot combine high

sensitivity, reduced size, low power consumption and low cost. Therefore, there exists a need to develop a magnetometer that addresses all of these characteristics especially for wireless sensor operations. This work focuses on the development of composite magnetolectric structures based on ferroelectric (PZT) and ferromagnetic spinel compositions, and the processes developed will provide the path for direct integration of the composite into micro-scale devices. Research has been completed to deposit laminate and particulate composites of the PZT/spinel materials through sol gel routes. In this work, process parameters were optimized in order to obtain dense thin films with low defect formation due to co-sintering and clamping issues. Current work focuses on the addition of spinel nanoparticulates synthesized through hydrothermal processes into PZT matrix to produce 0-3 composites. The impact of all of this work will foster the inexpensive implementation of multiferroic magnetometers to a host of applications where efficient long distance and high sensitivity metal detection is required.

11:30 AM

(EMA-S2-004-2012) Origin of high piezoelectric coefficient in $\text{xBiScO}_3\text{-(1-x)PbTiO}_3$ ceramics near the morphotropic phase boundary

J. L. Jones*, G. Tutuncu, University of Florida, USA; J. Chen, University of Science and Technology, China; D. Damjanovic, Swiss Federal Institute of Technology (EPFL), Switzerland

The solid solution between BiScO_3 (BS) and PbTiO_3 (PT) ceramics exhibits a morphotropic phase boundary at approximately 0.36BS-0.64PT. Compositions within this region exhibit both a high piezoelectric coefficient (460 pC/N) and a high Curie temperature ($\sim 450^\circ\text{C}$). Prior measurements of the piezoelectric and dielectric coefficients have suggested some degree of extrinsic contributions to this coefficient, possibly related to domain wall motion. In this work, we use time-resolved X-ray and neutron diffraction to determine the contribution of extrinsic and intrinsic mechanisms to the piezoelectric coefficient at various subcoercive electric field amplitudes and frequencies. While the synthesized composition is a mixture of rhombohedral and tetragonal perovskite phases, during subcoercive electric field cycling, domain switching of the tetragonal phase is very small at low fields and increases with field amplitude; this mechanism can explain the field-amplitude dependence of the piezoelectric coefficient. At low fields, the rhombohedral phase exhibits large electric-field-induced lattice strain coefficients, which decrease with increasing frequency, indicating they do not originate from the intrinsic piezoelectric effect. A complete description of the contributions to the piezoelectric coefficient will be summarized.

11:45 AM

(EMA-S2-005-2012) Harnessing PZT Thin Films to Create Mobile MEMS Platforms

R. G. Polcawich*, J. Pulskamp, G. Smith, L. Sanchez, R. Rudy, D. Potrepka, US Army Research Laboratory, USA

This presentation will discuss several key aspects necessary to create mobility in mm to cm-scale devices. Specifically, the roles of thin film process control, residual stress as a function of thin film texture, and processing induced damage in device design and performance. These issues will be related to chemical solution processing of lead zirconate titanate (PZT) thin films, to surface and bulk micromachining of MEMS devices, and to thin film actuators for insect-inspired microflight and ultrasonic traveling wave motors. As an example, fine tuning the (001) texture in PZT can have tremendous benefit in piezoelectric response of thin film PZT. However, it can also result in substantial changes in the residual stress gradients within a thin film actuator that could result in a non-functioning device. A certain degree of processing induced damage can be tolerated and still yield functioning actuators. However, the long term device reliability can be affected and will be

highlighted in this presentation. In the final component of the presentation, fabrication process flow integration strategies will be discussed so that multiple capabilities can be achieved in a single fabrication process.

S4: Advanced Energy Storage Materials and Systems: Lithium and Beyond

Next Generation Advanced Energy Storage Devices: Lithium-air, Lithium-sulfur and All Solid State Batteries I

Room: Coral B

Session Chairs: Bruce Dunn, UCLA; Gholam-Abbas Nazri, Wayne State University

10:30 AM

(EMA-S4-001-2012) Electrolytes for Lithium-ion Batteries (Invited)

T. R. Jow*, O. A. Borodin, Army Research Laboratory, USA; L. Xing, University of Utah, USA

High energy density Li-ion batteries are widely used in today's portable electronic devices. The electrolyte plays a critical role in ensuring proper operation of the state-of-the-art Li-ion batteries. The fact that the electrolyte components including LiPF₆ in ethylene carbonate and ethylmethyl carbonate form a protective solid-electrolyte interface (SEI) on the carbonaceous anode makes the operation of Li-ion batteries possible. The applications of Li-ion batteries for hybrid electric vehicles require more powerful batteries that could operate in a wider temperature range. To further improve the energy density, the approach of using higher voltage cathodes also needs compatible high voltage electrolytes to operate. In this talk, the limitation of the state-of-the-art electrolytes will be reviewed. Intrinsic oxidative stability of electrolytes from quantum chemistry calculations and influence of the anion on the oxidation reactions of electrolyte solvents will be presented. The lithium cation desolvation free energy and the associated interfacial resistance for EC/LiPF₆ and EC:DMC(3:7)/LiPF₆ electrolytes at graphite electrode extracted from molecular dynamics simulations will be compared with experimental data. The challenges and recent progress of the low temperature and high voltage electrolytes including the effort using modeling for guiding the electrolyte development will be reviewed and discussed.

11:00 AM

(EMA-S4-002-2012) New developments in high voltage electrodes, electrolytes and alternative red-ox chemistries (Invited)

B. Lucht*, University of Rhode Island, USA

The development of Lithium Ion Battery (LIB) electrolytes with improved thermal and electrochemical stability for Electric Vehicle (EV) applications will be presented. The most extensively used LIB electrolytes are composed of LiPF₆ dissolved in organic carbonates. However, LiPF₆ electrolytes have poor thermal stability and the required use of EC limits low temperature performance. Significant energy fading occurs after several years at room temperature and over only a few months at moderately elevated temperatures (>60 °C). While there are several different factors that limit the thermal stability of LIBs, the reactions of the electrolyte with the surface of the electrode materials is frequently reported to be the most important. We will discuss a thorough analysis of the reactions of common electrolytes with and without additives as solutions in the absence of electrode materials and on the surface of the electrode materials after initial formation cycling and upon accelerated aging.

11:30 AM

(EMA-S4-003-2012) Solid Electrolytes for Li Battery Applications (Invited)

N. J. Dudney*, W. E. Tenhaeff, Oak Ridge National Laboratory, USA; E. G. Herbert, University of Tennessee, USA; K. Hong, S. Kalnaus, A. S. Sabau, Oak Ridge National Laboratory, USA

Solid electrolyte materials are investigated for lithium and lithium-ion batteries with both planar and 3D architectures. In many cases it may be desirable to use multiple electrolytes either as layers or in an alternative composite structure in order to provide adequate ion transport and robust mechanical and electrochemical properties. Results of studies of both bulk and interfacial properties will be reported for several inorganic and polymeric electrolytes. Simulations provide a means to extrapolate to other architectures and compositions. Compatibility with metallic lithium anodes is an important application that is under investigation. Acknowledgement: Research has been supported by the Laboratory Directed Research and Development Program of Oak Ridge National Laboratory, and by the Assistant Secretary for Energy Efficiency and Renewable Energy, Office of Vehicle Technologies of the U.S. Department of Energy.

S5: Unconventional Thermoelectrics: Defect Chemistry, Doping and Nanoscale Effects

Thermal Science and Theory I

Room: Pacific

Session Chair: Alp Sehirlioglu, Case Western Reserve University

10:30 AM

(EMA-S5-001-2012) Nanostructures and the control of thermal conductivity (Invited)

D. Cahill*, U. Illinois, USA

In recent years, the thermal properties of nanostructured materials have been intensely studied with the hope of providing improved materials for the conversion of heat to electrical power. I will discuss two examples of this research; i) "nanodot" superlattices of PbTe thermoelectrics; and ii) ultralow thermal conductivity in disordered layered crystals. Time-domain thermoreflectance (TDTR) enables routine measurements of nanostructured thin film materials and is also applicable to materials under extreme conditions of high temperature, high pressure, and high magnetic fields. Nanostructuring of thermoelectrics is intended to scatter the long-wavelength acoustic phonons that carry a significant fraction of heat in semiconductor alloys. In contradiction with previous reports, our work shows that the lattice thermal conductivity of PbTe/PbSe nanodots superlattices does not fall significantly below 1 W/m-K and therefore the figure of merit of merit of these materials is $ZT < 1$. Solids that combine order and disorder in the random stacking of two-dimensional crystalline sheets, so-called "disordered layered crystals" such as WSe₂ display the lowest thermal conductivity ever observed in a fully dense material. The cause of this low thermal conductivity may be explained by the large anisotropy in elastic constants that suppresses the density of phonon modes that propagate along the soft direction

11:00 AM

(EMA-S5-002-2012) Controlling thermal transport with nanoscale composites (Invited)

P. Hopkins*, University of Virginia, USA

Thermal management has assumed a critical role in the design and development of electronic devices, power generation modules, and waste energy harvesting techniques. In these applications, performance depends on the thermal conductivity of the component nanomaterials. In this work, I will discuss two studies in which the material structure is used to manipulate the thermal transport in nanosystems. In both of these studies, the thermal transport properties in the

various nanosystems were measured with Time Domain Thermoreflectance (TDTR), a ultrashort pulsed pump-probe technique that is ideal for measuring the thermal conductivity and thermal boundary conductance (TBC) in nanoscale materials and composites. In the first study, we examine the heat transfer across silicon interfaces that have been patterned with GeSi(1-x) quantum dots (QDs). The functional dependence of TBC with RMS surface roughness reveals a trend that suggests that both vibrational mismatch and localized phonon scattering near the interface contribute to the reduction in TBC. In the second study, we examine the thermal conductivity of nanograined strontium titanate (STO). We grow a series of STO films with different grain sizes, ranging from ~700 nm to ~1 micron. The thermal conductivity shows a clear dependence on grain size, indicating a very strong relationship between grain structure and thermal transport.

11:30 AM

(EMA-S5-003-2012) Phases Diagrams, Crystal Chemistry and Thermoelectric Properties of the Ca-M-Co-O (M= Sr, Zn, and La) Systems

W. Wong-Ng*, NIST, USA; G. Liu, Chinese Academy of Sciences, China; S. Gutierrez, NIST, USA; T. Luo, University of Maryland, USA; Q. Huang, J. Martin, Y. Yan, NIST, USA; J. A. Kaduk, Illinois Institute of Technology, USA

Thermoelectric research is of increasing importance in the development of technologies for improving vehicular fuel economy and for mitigating green house gas emissions. There is a well-defined need for efficient energy conversion materials and environmentally friendly technologies. For waste heat energy conversion applications, oxide materials which have high temperature stability are potential candidates. In addition to the well-known $\text{Ca}_3\text{Co}_4\text{O}_9$ phase that exhibits excellent thermoelectric properties in the Ca-M-Co-O (M= Sr, Zn, and La) systems, there exists other interesting phases including members of the low-dimensional homologous series, $\text{A}_{n+2}\text{Co}_n\text{Co}'\text{O}_{3n+3}$ (where A= Sr, Ca, (Ca,Sr) or (Sr,Ca)). However, while the members of the $\text{A}_{n+2}\text{Co}_n\text{Co}'\text{O}_{3n+3}$ series have reasonably high Seebeck coefficients and relatively low thermal conductivity, the electrical conductivity needs to be increased in order to achieve higher ZT values. This paper discusses our phase equilibria/structural/property studies of selected cobaltites, including those in the SrO-CaO-CoO_x , CaO-ZnO-CoO_x , and $\text{CaO-La}_2\text{O}_3\text{-CoO}_x$ systems.

S8 Highlights of Student Research in Basic Science and Electronic Ceramics

Future of Ceramics I

Room: Pacific

Session Chair: Harlan Brown-Shaklee, Sandia National Laboratories

12:15 PM

(EMA-S8-001-2012) Electrical and Structural Properties of $\text{Ba}(\text{Ho,Ta})_{0.05}\text{Ti}_{0.90}\text{O}_3$, a Dipole-like B-Site Substituted Material, Characterized as Functions of Temperature and Frequency

B. Hoke*, T. Mion, University of Texas - Pan American, USA; D. Potrepka, F. Crowne, U.S. Army Research Laboratory, USA; A. Tauber, Geo-Centers, Inc. (retired), USA; S. Tidrow, University of Texas - Pan American, USA

An investigation into the electric properties including dielectric constant, tunability, dissipation factor and figure of merit of the material as a function of temperature, -50 °C to 125 °C, and frequency, 10 Hz to 2 MHz, is presented for $\text{Ba}(\text{Ho,Ta})_{0.05}\text{Ti}_{0.90}\text{O}_3$, a B-site dipole-like substituted material. In addition to electrical data, structure phase transitions as determined using x-ray diffraction for $\text{Ba}(\text{Ho,Ta})_{0.05}\text{Ti}_{0.90}\text{O}_3$ will be discussed. *This material is based upon work supported by, or in part by, the U.S. Army Research Laboratory and the U.S. Army Research Office under contract/grant number W911NF-08-1-0353.*

12:30 PM

(EMA-S8-002-2012) Electrical and Structural Properties of $\text{Ba}(\text{Ga,Ta})_{0.05}\text{Ti}_{0.90}\text{O}_3$, a Dipole-like B-Site Substituted Material, Characterized as Functions of Temperature and Frequency

M. Rivas*, T. Mion, University of Texas - Pan American, USA; D. Potrepka, F. Crowne, U.S. Army Research Laboratory, USA; A. Tauber, Geo-Centers, Inc. (retired), USA; S. Tidrow, University of Texas - Pan American, USA

The dielectric constant, tunability, dissipation factor and material figure of merit for the B-site dipole-like substituted material, $\text{Ba}(\text{Ga,Ta})_{0.05}\text{Ti}_{0.90}\text{O}_3$, are reported as functions of temperature, -50°C to 125°C, and frequency, 10 Hz to 2 MHz. The properties: dielectric constant; tunability; dissipation factor; and, material figure of merit; are discussed in terms of temperature dependent structural changes as identified using x-ray diffraction. *This material is based upon work supported by, or in part by, the U.S. Army Research Laboratory and the U.S. Army Research Office under contract/grant number W911NF-08-1-0353.*

12:45 PM

(EMA-S8-003-2012) Study of Platinum/Alumina Interaction for Implantable Neurostimulator Applications

A. Karbasi*, A. Hadjikhani, A. Durygin, W. Jones, Florida International University, USA

There is increasing demand for hermetic metal/ceramic bonds for application in biomedical engineering, in particular for use in neurostimulating prosthetic devices such as cochlear implants, muscular stimulators and retinal prosthesis, where required high input/output hermetic structure. Platinum/Alumina bonds are particularly interesting because of the proven biocompatibility of the two materials and their strong bonding. Yet, the true nature of their bonding is not clear. Pt/Al₂O₃ interactions in different atmosphere (i.e. air and hydrogen) and different temperatures were studied by means of X-ray diffraction, SEM and EDS analyses, to better understand the interfacial reactions and bonding mechanism.

S2: Advanced Dielectric, Piezoelectric and Ferroic Materials, and Emerging Materials in Electronics

Lead Free Piezoelectrics

Room: Indian

Session Chairs: Ken-ichi Kakimoto, Nagoya Institute of Technology; Xiaoli Tan, Iowa State Univ

1:30 PM

(EMA-S2-006-2012) Piezoelectric Fatigue of $\text{Bi}(\text{Zn}_{0.5}\text{Ti}_{0.5})\text{O}_3\text{-(Bi}_{0.5}\text{K}_{0.5})\text{TiO}_3\text{-(Bi}_{0.5}\text{Na}_{0.5})\text{TiO}_3$ Ceramics

E. Patterson*, D. Cann, Oregon State University, USA

Lead-free piezoelectric ceramic compositions of $\text{Bi}(\text{Zn}_{0.5}\text{Ti}_{0.5})\text{O}_3\text{-(Bi}_{0.5}\text{K}_{0.5})\text{TiO}_3\text{-(Bi}_{0.5}\text{Na}_{0.5})\text{TiO}_3$ (BZT-BKT-BNT) solid solutions were investigated. Based on previous optimization studies, xBZT-(0.4)BKT-(0.6-x)BNT for x=0.025, 0.05 and 0.1 were produced. Maximum strain of 0.32% with little negative strain was observed at x=0.05 with high saturation polarizations (~30.2 $\mu\text{C}/\text{cm}^2$) but with limited remanent polarization (10.5 $\mu\text{C}/\text{cm}^2$). A well-saturated, normal ferroelectric hysteretic response was found at 0.025 BZT ($P_{\text{MAX}}=33.5$ and $P_r=20.6\mu\text{C}/\text{cm}^2$). Bipolar fatigue measurements at 50 kV/cm and 10 Hz were performed for 1 million cycles for all compositions. The fatigued 0.025BZT composition exhibits excellent fatigue resistance with an increase of 1.4% of maximum polarization and a loss of 5.1% of P_r after 1 million cycles. A corresponding decrease in S_{MAX} of 14% was also observed. The largest reduction in polarization values was for the 0.1BZT composition, where P_{MAX} and P_r were reduced by 0.96% and 20.5%, respectively.

Overall the decreases in polarization were shown to be much less severe than those of the lead zirconate titanate system.

1:45 PM

(EMA-S2-007-2012) Phase Transitional Behavior and Electrical Properties of $Ba_{1-x}Ca_xBi_4Ti_4O_{15}$ Lead-Free Ceramics

S. Kumar*, Indian Institute of Science, India; D. A. Ochoa, J. E. Garcia, Universitat Politècnica de Catalunya, Spain; K. Varma, Indian Institute of Science, India

Bismuth layer-structured ferroelectrics have received increasing interest owing to their high Curie temperature, high resistance to polarization fatigue and lead-free nature making them attractive candidates for high temperature piezoelectric and nonvolatile memory applications. In the present work, ceramics with nominal compositions of $Ba_{1-x}Ca_xBi_4Ti_4O_{15}$ (where $x=0, 0.25, 0.50, 0.75$ and 1) were fabricated. X-ray diffraction (XRD) and Raman scattering techniques have been employed to probe into the structural changes on changing x . XRD analyses showed an increase in orthorhombic distortion with increase in x . Raman spectra revealed a redshift in A_{1g} peak and an increase in the B_{2g}/B_{3g} splitting with increasing Ca content. The average grain size was found to increase with increasing x . The temperature of phase transition (T_m) increased linearly with increasing Ca-content whereas the diffuseness was found to decrease with the end member $CaBi_4Ti_4O_{15}$ showing a frequency independent sharp phase transition around 1048 K. Ca doping resulted in a decrease in the remnant polarization and an increase in the coercive field. Ceramics with $x=0.75$ showed an enhanced piezoelectric coefficient d_{33} of 15 pC/N at room temperature. Our results also demonstrate the tunability of temperature coefficient of dielectric constant (τ_ϵ) in the present solid-solution over a wide range of temperature.

2:00 PM

(EMA-S2-008-2012) The Effect of Composition, Poling, and Texture on the Performance of $Ba(Zr_{0.2}Ti_{0.8})O_3-x(Ba_{0.7}Ca_{0.3})TiO_3$ (BZT-BCT) Piezoelectric Materials

M. Ehmke*, B. Li, J. E. Blendell, K. J. Bowman, Purdue University, USA

The lead-free $Ba(Zr_{0.2}Ti_{0.8})O_3-x(Ba_{0.7}Ca_{0.3})TiO_3$ (BZT-BCT) system that has been shown to exhibit extraordinarily high piezoelectric performance has been investigated to understand and further improve the properties. The proposed morphotropic phase boundary (MPB) region was investigated using both dielectric permittivity measurements and in-situ temperature-dependent X-ray diffraction. A region of phase coexistence between rhombohedral and tetragonal phases can be identified over a considerable compositional as well as temperature range. Piezoelectric constants determined from strain measurements are on the order of 1000-1300 pm/V for these compositions. In addition, an electric poling method is found to be effective in further improving the ratio between strain and electric field of up to 40%. The underlying mechanism is discussed in terms of ferroelastic texture and the development of an internal bias field. Further improvement in piezoelectric properties can be achieved by inducing a crystallographic texture through tape-casting.

2:15 PM

(EMA-S2-009-2012) A New Opportunity in Non-Lead Piezoelectrics with Ni Cofired Electrodes

K. Kobayashi*, Y. Doshida, Y. Mizuno, The Pennsylvania State University, USA; C. A. Randall, TAIYO YUDEN Co., Ltd., Japan

$(Na,K)NbO_3$ ceramics (NKN) has been considered as a good candidate for lead-free piezoelectrics. To develop new applications of lead-free materials, base metal cofired multilayer structures should be promising. However there is limited success because of the difficulty in designing the piezoelectric properties of low-pO₂ fired ceramics. In this study, the point defects and domain structures in Li-doped NKN (Li-NKN) ceramics fired in various pO₂ atmospheres were investigated by a variety of techniques including thermally stimulated depolarization current (TSDC), impedance spectroscopy and

Rayleigh analysis. Li-NKN ceramics fired in reduced atmospheres exhibited high resistivity sufficient for practical use. The domain motion was found not sensitive to firing atmosphere as inferred by Rayleigh analysis. TSDC results implied that the alkali vacancies were suppressed at low pO₂ firing, which resulted in the lower space charge. Consequently, reduced firing materials had comparable or superior properties to air-fired Li-NKN. Ni-cofired multilayer Li-NKN prototypes were fabricated to clarify the influence of the Ni electrode on the piezoelectric properties and reliability. Despite inferior piezoelectric properties of the NKN to the PZT, the actuation characteristics are comparable at the device level on these preliminary assessments because of the ability to integrate these materials in thinner layers.

2:30 PM

(EMA-S2-010-2012) Particle-size-related Crystal Structure in (Na,K)NbO₃ Ceramics

K. Kakimoto*, Y. Shinkai, R. Kaneko, Nagoya Institute of Technology, Japan

The critical size for inducing a high dielectric constant and enhancing piezoelectric properties is of great interest in the fundamental discussion involved with the domain structure of ferroelectrics. The authors have recently recognized that enhanced piezoelectric properties, $k_p=0.44$, $Q_m=280$, and $d_{33}=161$ pC/N, can be obtained, even by atmospheric sintering, in pure (Na,K)NbO₃ ceramics consisting of uniform fine grains around 3 μ m in size. However, grain-size-related crystal structure and property have never discussed for (Na,K)NbO₃, in spite of its importance in lead-free piezoelectric ceramics, whereas the size-effect has been well reported for BaTiO₃. In this study, therefore, a model experiment regarding the size effect was carried out to find relations to the above-mentioned excellent properties. The size classification of (Na,K)NbO₃ particles was achieved by a wet-type centrifugal separation technique using an elaborate sample source. The selected rotational speeds corresponding to centrifugal forces provided a beneficial effect in the narrow size classification of 6 kinds of (Na,K)NbO₃ powders with different mean particle sizes from 0.3 to around 40 μ m. The refined crystal structures confirmed that a considerable change occurred for the samples in their lattice parameters, Nb-O bond distance and the bond angle, indicating that grain-size-related properties was certainly predicted for (Na,K)NbO₃ ceramics.

3:15 PM

(EMA-S2-011-2012) The intriguing ternary lead-free piezoelectric system $Na_{1/2}Bi_{1/2}TiO_3 - BaTiO_3 - K_{1/2}Na_{1/2}NbO_3$: reconciliation of structure and properties across the phase diagram (Invited)

P. A. Thomas*, D. Walker, D. I. Woodward, J. Davies, L. Collins-MacIntyre, D. Wood, University of Warwick, United Kingdom; R. Dittmer, W. Jo, J. Roedel, Technische Universität Darmstadt, Germany

The $Na_{1/2}Bi_{1/2}TiO_3 - BaTiO_3 - K_{1/2}Na_{1/2}NbO_3$ (NBT-BT-KNN) system is of interest as a Pb-free ferroelectric material, with particular interest in the materials with compositions 92NBT-6BT-2KNN and 94NBT-5BT-1KNN as they exhibit high field-induced strain [1] and enhanced piezoelectric properties, respectively [2]. Recent structural investigations have shown that the former phase is predominantly tetragonal, while the latter comprises a mixture of rhombohedral and tetragonal phases.[3] Compositions in the $(96-2x)NBT - (x+4)BT - xKNN$ solid solution series have been made by a solid-state route and high-resolution powder X-ray diffraction used as the primary method of structural investigation. Rietveld refinements at room temperature favour a monoclinic (Cc) structure at $x = 0$ and a mixture of both monoclinic (Cc) and tetragonal (P4bm) phases at $x = 1$, while the best fit at $x = 2$ was obtained with an untilted tetragonal (P4mm) structure. Compositions at $x \geq 3$ refine as rhombohedral, untilted structures, indicating a complex sequence of different transition types.

3:45 PM

(EMA-S2-012-2012) Texture Enhanced Properties in the Lead-Free Piezoelectric $\text{Na}_{0.5}\text{Bi}_{0.5}\text{TiO}_3$ System

C. Fancher*, Purdue University, USA; K. J. Bowman, Illinois Institute of Technology, USA; J. E. Blendell, Purdue University, USA

$\text{Na}_{0.5}\text{Bi}_{0.5}\text{TiO}_3$ (NBT) is a promising piezoelectric material being investigated as a replacement for PZT in a variety of consumer electronics and actuator applications. NBT materials processed using conventional powder processing techniques do not achieve the performance of PZT; however inducing a preferred orientation (texture) is one route that may enable enhanced piezoelectric performance of NBT. In this investigation, pure phase NBT templates were used to texture NBT-xBT-yKNN. NBT platelets were synthesized using a two-step molten salt process; first $\text{Na}_{0.5}\text{Bi}_{4.5}\text{Ti}_4\text{O}_{15}$ (NBiT) platelets were synthesized then converted into pure phase NBT. Conversion from NBiT to NBT forms both plate-like and microcube particles. Template particles were oriented by tape casting slurries with 5wt% NBT templates using a beveled doctor blade at a rate of 30 cm/min. Crystallographic texture was investigated by 2 dimensional X-Ray Diffraction (2DXRD) using both laboratory and synchrotron facilities. Templated sintered samples showed a strong $\langle 100 \rangle$ preferred orientation with MRD > 4 . The piezoelectric response of textured NBT based materials are compared to randomly oriented materials.

4:00 PM

(EMA-S2-013-2012) In situ TEM Study on the Phase Transitions in $(\text{Bi}1/2\text{Na}1/2)\text{TiO}_3\text{-BaTiO}_3$ Ceramics

C. Ma, X. Tan*, Iowa State Univ, USA

In the present work, the structure-property relationship in the unpoled $(1-x)(\text{Bi}1/2\text{Na}1/2)\text{TiO}_3\text{-xBaTiO}_3$ ceramics was studied using transmission electron microscopy (TEM) and dielectric characterization. In contrast to the reported phase diagrams determined using poled ceramics, an additional phase region exhibiting P4bm nanodomains was revealed at room temperature around the $x = 0.06$ morphotropic phase boundary, where optimal properties are obtained. The P4bm nanodomains are associated with the "relaxor anti-ferroelectric" behavior. In situ TEM experiments were performed to visualize the electric field-induced phase transition during the poling process in the composition $0.93(\text{Bi}1/2\text{Na}1/2)\text{TiO}_3\text{-}0.07\text{BaTiO}_3$. It was found that a P4bm to P4mm phase transition starts to occur from grain boundaries at an electric field lower than the bulk coercive field. As the P4bm/P4mm phase interface moves, coalescence of lamellar domains into large domains takes place in the induced ferroelectric P4mm phase. After the P4bm to P4mm phase transition is complete in the grain, coalescence of P4mm domains continues until the whole grain becomes almost a single-domain grain. When applied electric fields are removed, the induced P4mm phase remains and does not change back to the original P4bm phase.

4:15 PM

(EMA-S2-014-2012) In situ Neutron Diffraction Study of Ferroelasticity in NBT-xBT in the Region of the Morphotropic Phase Boundary

T. Usher*, J. S. Forrester, C. Llano, University of Florida, USA; J. Neuefeind, M. Hagen, A. Pramanick, K. An, H. Skorpenske, Oak Ridge National Laboratory, USA; J. L. Jones, University of Florida, USA

Polycrystalline $(1-x)\text{Na}_0.5\text{Bi}_0.5\text{TiO}_3\text{-xBaTiO}_3$ (NBT-xBT) materials are part of a new generation of Pb-free ceramics that may replace some of the Pb-rich piezoelectrics currently in widespread use. NBT and BT have a morphotropic phase boundary (MPB) at approximately 6-7%BT, and at these compositions, superior piezoelectric properties have been found relative to those compositions further from the MPB. Further research is required in order to fully characterize the response of different compositions of NBT-BT to applied mechanical loads and electric fields. The current work involves the application of mechanical stresses to polycrystalline samples of NBT-

xBT, with $x = 4, 6, 7, 9$ and 13%BT. Neutron diffraction patterns were measured during loading at 25 MPa incremental steps, from 0 MPa to sample failure, on the instrument VULCAN at the SNS, Oak Ridge National Laboratory. Using single peak fitting, the contributions to strain such as lattice strains, domain switching and stress-induced phase transitions were examined. It was found that the composition with the largest deformation behavior was NBT-6%BT, and the data suggests that a stress-induced phase transition occurred during the loading procedure. The compositions further from the MPB had higher Young's Moduli and lower strains. The origins of these differences will be discussed.

4:30 PM

(EMA-S2-015-2012) Advantage of SPS for Dense $(\text{Na,K})\text{NbO}_3$ with Enhanced Piezoelectric Properties

A. Kawai*, K. Kakimoto, Nagoya Institute of Technology, Japan; K. Hatano, Y. Doshida, TAIYO YUDEN CO.,LTD., Japan

Spark plasma sintering (SPS) technique facilitates very fast heating and cooling rates in contrast to the standard firing route, hence the densification can be finished within a few minutes and avoid coarsening grain size. The SPS applies a pulsed DC current and pressing pressure to the sample through the graphite die in a reduced atmosphere, but it has not been yet fully understood that how DC current (field), pressing pressure and atmosphere affect the densification process and the dielectric properties of non-conductive ceramics, while heat is generated internally in case of the powder compact of conductive ceramic and metals. In this study, pure $(\text{Na,K})\text{NbO}_3$ ceramics with excellent ferroelectric ($\text{Pr} = 29 \mu\text{C}/\text{cm}^2$) and piezoelectric ($d_{33} = 144 \text{ pC}/\text{N}$) properties were successfully obtained by a SPS technique under the controlled conditions. The SPS-derived specimens showed dense and uniform microstructure without abnormal grain growth. They also demonstrated a good mechanical property in higher sound velocity and Vickers hardness up to 5.1 GPa, since the SPS technique provided the specimen with a harder bonding strength between grain boundaries. In this talk, the relations between the role of the SPS parameters in $(\text{Na,K})\text{NbO}_3$ ceramics and the tuned properties are discussed, then it is experimentally verified that some key parameters can work well even by standard firing route.

S4: Advanced Energy Storage Materials and Systems: Lithium and Beyond**Interfacial Processes and In Situ Methods for Energy Storage Materials and Devices I**

Room: Coral B

Session Chairs: Brian Sheldon, Brown University; Vivek Shenoy, Brown University

1:30 PM

(EMA-S4-004-2012) Why Mechanics Phenomena are Essential in Designing Lithium Ion Battery Electrodes (Invited)

P. R. Guduru*, V. Sethuraman, M. Chon, N. Van Winkle, S. Nadimpalli, Brown University, USA

Increasing the energy density of lithium ion batteries has emerged as an important challenge in recent years, especially because of their critical need in enabling large scale use of electric vehicles. One of the main challenges in developing higher energy density battery systems is managing the large stresses and the consequent mechanical damage that accrues in the electrodes during charge-discharge cycling. We discuss the mechanics issues in designing electrode materials, and present selected results on silicon: (i) stress evolution and plastic deformation in silicon; (ii) coupling between stress and electrical potential; (iii) characterization of mechanical properties of lithiated silicon as a function of the state of charge; and (iv) mechanics of crystalline to amorphous phase transformation in silicon during initial lithium

insertion. We also discuss how knowledge of mechanical behavior and properties can help improve electrode design and durability.

2:00 PM

(EMA-S4-005-2012) Ionic / electronic wiring of lithium ion battery electrodes (Invited)

D. Samuelis*, J. Shin, Y. Yu, C. Zhu, L. Fu, J. Maier, Max Planck Institute for Solid State Research, Germany

The storage kinetics of electrode materials for lithium ion batteries critically depend on the chemical diffusivity of Li in these materials. The two major transport processes included in this chemical diffusivity are the transport of Li^+ ions and the electronic conductivity. Promising materials such as LiFePO_4 or TiO_2 suffer from intrinsically low electronic conductivities, rendering the pure materials unusable as electrodes. Here, superimposing networks of electronically conductive second phases can help improving the electron transport. This contribution presents some concepts to improve the Li transport in electrode materials, while keeping volume of secondary phases low. We report on novel electronic/ionic mixed conducting networks of anatase $\text{TiO}_{2-\delta}$ nanoparticles formed by thermal treatment in hydrogen. A major effect of this treatment is the reduction of stoichiometric TiO_2 nanoparticles, giving rise to the formation of additional n-type charge carriers. The treated anatase particles show almost triple capacities compared to stoichiometric anatase, with strongly enhanced rate capability. At the same time, there is no volume loss for a secondary phase. We compare to conductive network formation by second-phase mixed conducting oxides. Furthermore we also report on electrospinning techniques employed to create 1-d electrode structures with excellent electronic wiring and good access for the Li^+ ions.

2:30 PM

(EMA-S4-006-2012) A micro-macroscopic volume-averaged model for batteries

S. Pannala*, S. Allu, P. Mukherjee, J. Nanda, N. Dudney, S. Marthia, J. Turner, Oak Ridge National Laboratory, USA

The challenging aspect of modeling battery chemistry and materials (electrodes, electrolytes, and additives) is the wide-range of both temporal and spatial scales encountered in these systems where the chemicals/materials are produced, utilized, or consumed. The challenge is to accurately account and bridge (as seamlessly as possible) the length and time scales involved in the problem. First, this challenging problem is introduced using a lithium-ion battery with sample results covering a subset of scales. We will present the development of a unified macroscopic formulation across the electrode-electrolyte-electrode system. In this approach, a unified, single-domain approach is adopted where complex geometries are naturally incorporated so that one can account for different spatial arrangements of electrodes and separator. In addition, the formulation provides flexibility to include spatiotemporal variations of the different properties such as electrode/void volume fractions and anisotropic conductivities. The resulting governing equations at the macroscale are solved in a finite element framework for cell-performance of a prototypical Carbon/LiMn 2O_4 system to explore the effect of the various parameters that go into the model.

3:15 PM

(EMA-S4-007-2012) Location- and Orientation-Dependent Progressive Crack Propagation in Cylindrical Graphite Electrode Particles

R. Grantab, V. B. Shenoy*, Brown University, USA

Crack propagation in graphite electrodes has been discovered to facilitate the growth of solid electrolyte interphases (SEI) that greatly affect the long-term capacity of lithium-ion batteries. Using cohesive zone models in finite element calculations, we have studied crack propagation in cylindrical graphite anodes by considering the progressive growth of preexisting defects during cyclic charging. We have

found that for a defect to grow, it must be situated far from the center of the particle in order to be placed under high tensile stress, and it must also be closely aligned with the radial direction so the components of stress normal to the defect are high enough to cause crack propagation. Such defects begin to grow during the delithiation - not the lithiation - phase of the charging. Upon subsequent cycles, the cracks progressively grow further, until complete failure of the particle is observed. Our simulations show that for typical charging conditions, defects situated within 88% of the particle's radius from the center, and those mis-aligned from radial lines by more than 26 degrees, will not propagate. A failure diagram that demarcates safe and unsafe crack growth regimes is presented as a function of the location and orientation of defects. We also discuss the influence of particle size, crack microstructure, and charging rate on the failure map.

3:30 PM

(EMA-S4-008-2012) Vacancy-Driven Anisotropic Defect Distribution in the Battery-Cathode Material LiFePO_4 (Invited)

J. Lee, W. Zhou, Vanderbilt University, USA; J. C. Idrobo*, S. J. Pennycook, Oak Ridge National Laboratory, USA; S. T. Pantelides, Vanderbilt University, USA

Li-ion mobility in LiFePO_4 , a key property for energy applications, is impeded by Fe antisite defects (Fe_{Li}) that form in select b-axis channels. Here we combine first-principles calculations, statistical mechanics, and scanning transmission electron microscopy to identify the origin of the effect: Li vacancies (V_{Li}) are confined in one-dimensional b-axis channels, shuttling between neighboring Fe_{Li} . Segregation in select channels results in shorter $\text{Fe}_{\text{Li}}-\text{Fe}_{\text{Li}}$ spans, whereby the energy is lowered by the V_{Li} 's spending more time bound to endpoint Fe_{Li} 's. $\text{V}_{\text{Li}}-\text{Fe}_{\text{Li}}-\text{V}_{\text{Li}}$ complexes also form, accounting for observed electron energy loss spectroscopy features. This research was partially supported by the U.S. NSF under Grant No. DMR-0938330 (J. C. I. and W. Z.), by ORNL's Shared Research Equipment (SHaRE) User Facility, which is sponsored by the Office of Basic Energy Sciences, U.S. Department of Energy (J. C. I.) and the Office of Basic Energy Sciences, Materials Sciences and Engineering Division, U.S. Department of Energy (S.J.P., J.L., and S.T.P.), DOE Grant No. DE-FG02-09ER46554 (S.T.P.), and by the McMinn Endowment (S.T.P.) at Vanderbilt University. This research used resources of the National Energy Research Scientific Computing Center, which is supported by the Office of Science of the U.S. Department of Energy under Contract No. DE-AC02-05CH11231.

3:45 PM

(EMA-S4-009-2012) Lithium Intercalation in Low Dimensional Materials as Anodes for Li-ion Batteries

R. Shahbazian Yassar*, H. Ghassemi, Michigan Technological University, USA; M. Au, Savannah River National Laboratory, USA

Silicon nanowires and TiO_2 nanotubes are promising materials for Lithium-ion batteries. This report focuses on the in-situ observation of lithiation and delithiation in Si nanorods and TiO_2 nanotubes. The intercalation of Li ions in Si nanorods was monitored during charging and the fracture of nanorods was quantified in terms of size. The electrochemical testing of these low dimensional structures were conducted inside a transmission electron microscope equipped with a novel in-situ electrical probing holder. In addition, the intercalation of crystalline anatase and amorphous TiO_2 was studied and their fracture events were monitored in real time.

4:00 PM

(EMA-S4-010-2012) Elucidating the kinetics of complex Li-insertion reactions in Li batteries (Invited)

A. Van der Ven*, University of Michigan, USA

Current Li-ion battery technology relies on intercalation processes involving the insertion and removal of Li ions from the interstitial sites of a crystalline host material. However, this mechanism of energy storage is characterized by low capacities that are too low for automotive and large-scale energy storage applications. To overcome

these capacity limitations inherent to intercalation processes, new reaction mechanisms are being explored ranging from alloying reactions (e.g. Li+Si) to displacement and conversion reactions. In a displacement/conversion reaction, Li insertion forces a simultaneous extrusion of a valence shifting transition metal, which reduces to the metallic state, thereby leading to significant enhancements of capacity. The kinetics of these reactions remain poorly controlled and understood, leading to low charge and discharge rates, large hysteresis between charge and discharge and short life-times. The lack of understanding about displacement/conversion reactions is impeding our ability to rationally design and optimize this new energy storage approach. In this talk I will describe how first-principles statistical mechanical modeling tools can aid in the elucidation of complex reaction mechanisms in new electrode materials for Li battery applications.

4:30 PM

(EMA-S4-011-2012) Interphasial Chemistry and Processes in Li Ion Batteries (Invited)

A. Cresce, J. Ho, K. Xu*, Army Research Lab, USA

Since the birth of Li ion technology it has been recognized that interphases on both anode and cathode play the critical role in supporting the reversible intercalation/de-intercalation chemistry of Li+. 1, 2 The chemical composition and morphology of these interphases dictate not only the reversibility (cycle or calendar life), but also the kinetics of the cell chemistry (power density). However, due to the elusive manner in which these interphases are formed, they remain the least understood components despite extensive research efforts. Following the efforts by Winter and Besenhard, it was increasingly accepted that the formation of such interphases on anode is preceded by the co-intercalation of electrolyte solvents into the interstitial of graphene structure, leading to the intermediate ternary graphitic intercalation compound (GIC). 3 More recent work by Kyoto University and ARL further identified the role of Li+-solvation sheath in the formation of ternary GIC. 4, 5 Meanwhile such interphases on cathode remain little understood. This presentation summarizes our efforts in addressing the above issue. By designing additives, we attempt to alter the interphasial chemistries at both anode and cathode surfaces, on the purpose of either accelerate Li+-movement or stabilize the electrolyte at those extreme potentials.

S5: Unconventional Thermoelectrics: Defect Chemistry, Doping and Nanoscale Effects

Thermal Science and Theory II

Room: Pacific

Session Chair: Patrick Hopkins, University of Virginia

1:30 PM

(EMA-S5-004-2012) Unconventional Approaches to Thermoelectric Materials Using Soft Matter (Invited)

D. Dudis*, M. Check, D. Turner, C. Cheng, J. Shumaker, N. Gothard, E. Kemp, P. Borton, US Air Force, USA

Thermoelectric technologies are useful for localized cooling, small scale refrigeration, energy harvesting, power generation, heat pumping, and sensing. These rugged solid state devices are heat pumps in which charge carriers are the working fluid. The production of thermoelectric devices continue to grow dramatically, yet the underlying materials are based on discoveries 50 years old. New materials and new material approaches are needed to increase the overall efficiencies of thermoelectric. Some approaches, recent progress, and challenges using molecular conductors as well as superatom clusters will be presented.

2:00 PM

(EMA-S5-005-2012) Advanced High-Temperature Thermoelectric Materials and Components (Invited)

T. Caillat*, Jet Propulsion laboratory/California Institute of Technology, USA

Radioisotope Thermoelectric Generators have been successfully used to power spacecrafts for deep space missions as well as terrestrial applications where unattended operation in remote locations is required. They have consistently demonstrated their extraordinary reliability and longevity (more than 30 years of life). NASA's Radioisotope Power Systems Technology Advancement Program is pursuing the development of more efficient thermoelectric technologies that can increase performance by a factor of 2 to 4 times over state-of-practice systems that are limited to device-level efficiencies of 7.5% or less, and system-level specific power of 2.8 to 5 W/kg. Over the last few years, several advanced high-temperature thermoelectric materials including n-type La_{3-x}Te₄, p-type Yb₁₄MnSb₁₁, and n- and p-type filled skutterudites have been developed for integration into advanced power generation devices at the Jet Propulsion Laboratory for integration. JPL is now focusing on developing segmented couple technology using these high-temperature materials. Recent performance tests have demonstrated 11 to 15% conversion efficiencies with cold and hot side temperatures in the 150 - 200 C and 800 - 1000 C range, respectively. A summary of key accomplishments to date on materials, components and couples will be presented and discussed. Remaining technical challenges and future development work required will also be discussed.

2:30 PM

(EMA-S5-006-2012) High Temperature Thermoelectric Silicides

J. Mackey*, University of Akron, USA; A. Sehirlioglu, Case Western Reserve, USA; F. Dynys, NASA Glenn Research Center, USA

Thermoelectrics may be used as solid state devices capable of reliable energy harvesting from waste heat generated in harsh environments. The solid-state conversion of thermal energy into electrical energy makes thermoelectric devices simple and dependable power generation sources for sensors and larger systems alike. Si/Ge based radioisotope thermoelectric generators (RTGs) have provided select NASA satellites with over one billion combined service hours of power. Investigation into silicide systems reveals several potential candidate materials suitable for novel device fabrication. Critical characteristics achieved by silicides include the ability to operate in high temperature and oxidizing environments. Additionally, silicides such as Mg₂Si-Si/Ge and TiSi₂-Si/Ge, are composed of elements in relatively high abundance and low toxicity. Our work in a number of silicide systems has generated materials with high power factors (4,000 μW/m²K²). Nano-structuring by means of fast-processing techniques, such as spark plasma sintering, is believed to provide a method of minimizing thermal transport with the generation of interfaces introduced by nano-precipitates. Introduction of these coherent interfaces scatters phonons, minimizes total thermal conductivity and leads to materials with high figure of merit (ZT). To be presented are thermoelectric properties and microstructure investigation of several promising silicide systems.

3:15 PM

(EMA-S5-007-2012) Magnesium Silicide-Based Nanocomposites for Improved Thermoelectric Efficiency

S. Bux*, G. Hakimeh, J. Fleurial, Jet Propulsion Laboratory/California Institute of Technology, USA

Thermoelectric materials based upon magnesium and silicon are ideal materials for large scale waste heat recovery applications as they are lightweight, non-toxic and made up of abundant materials. Recently, we have developed a scalable mechanochemical approach to synthesize these materials. This process yields high quality n-type magnesium silicide with effective Bi doping with a ZT_{max} of 0.7 at 775 K. However, in order to be viable for large scale waste heat recovery applications, much larger performance increases are still needed

(factor of 2). A potential method of enhancing ZT is through the formation of nanostructured composites with nanoscale silicide inclusions. The inclusions are predicted to not only reduce the lattice thermal conductivity but also enhance the density of states, thus the Seebeck coefficient via carrier injection. Here we present the impact of silicon-based nanoparticle composites on ZT. The nanostructured composites were formed via mechanochemical approach and sintering at high pressure. The thermoelectric properties and microstructure of the silicon-based composites will be presented and discussed.

3:30 PM

(EMA-S5-008-2012) MX₂ layers to generate thermoelectrics: from oxides to selenides (Invited)

A. Maignan*, S. Hébert, F. Gascoin, E. Guilmeau, Laboratoire CRISMAT, France

Harvesting waste-heat by using thermoelectric generators (TE) requires to get high ZT materials for $T \gg 300\text{K}$. The phonon glass (low thermal conductivity) and electron crystal (high electrical conductivity) concept is providing a framework to search for such materials. In particular, the layer compounds made of the alternation of conducting and separating layers, are attracting much interest. This has been widely prospected in the case of the metal transition oxides in which the metal-oxygen conducting layer crystallizes in the CdI₂-type structure. Among them, the Ca₃Co₄O₉ oxide and the Bi-based relative cobaltites are the most studied. However, to go beyond their ZT values reaching only ≈ 0.2 at 1000K, the role of the anion (X^{2-}) has been investigated. Two interesting sulfide and selenide phases have been studied: Cu_xTiS₂ and AgCrSe₂. Going from oxygen to selenium through sulfur, it is found that the covalency increasing has a beneficial impact on ZT with values as high as 1 for the selenide. In this presentation, a comparison between these three types of layered materials will be made. A special care will be given to the important structural features governing the TE properties of the CdI₂-type layer materials.

4:00 PM

(EMA-S5-009-2012) Thermoelectric Figure of Merit of In₂O₃:Pd Nanocomposites for Energy Harvesting Applications

M. Amani*, O. J. Gregory, Department of Chemical Engineering, USA; G. C. Fralick, NASA Glenn Research Center, USA

Nanocomposites, capable of operating continuously at temperatures as high as 1100C in air, were prepared by imbedding palladium nanoparticles into an In₂O₃ matrix via co-sputtering, to achieve relatively large thermoelectric figures of merit (ZT). By employing combinatorial chemistry techniques to simultaneously optimize Seebeck coefficient and electrical conductivity as a function of palladium content, a number of promising candidate materials were identified. Based on these results, several compositions were down selected to further examine their electrical and thermal properties at high temperatures. By utilizing the 3- ω technique, the thermal conductivity of selected In₂O₃:Pd nanocomposites was characterized from room temperature to 500C. Since the 3- ω technique has been applied successfully to a number of thin film dielectrics as well as thermoelectric films in the past, the resulting thermal conductivity was used to estimate the figure of merit as a function of temperature, which in some instances, were comparable to those established from low temperature thermoelectrics based on skutterudites and SiGe alloys.

4:15 PM

(EMA-S5-010-2012) Thermoelectric Properties of Undoped and Doped (Ti_{0.75}Sn_{0.25})O₂

F. Dynys, NASA Glenn Research Center, USA; M. Berger, MINES-ParisTech, France; A. Schirlioglu*, Case Western Reserve University, USA

Thermoelectric properties of undoped and doped (Ti_{0.75}Sn_{0.25})O₂ were investigated for high-temperature thermoelectric conversion application. Nano-composites were formed by annealing above 1000 °C. Outside the spinodal dome, metastable ilmenite-type SnTiO₃ pre-

cipitated from the rutile structure. Thermoelectric properties were measured in the temperature range from room temperature to 1000 °C. (Ti_{0.75}Sn_{0.25})O₂ was doped with both acceptor and donor dopants. Both undoped and doped (Ti_{0.75}Sn_{0.25})O₂ exhibit n-type electrical behavior independent of the type of the dopant. The electrical conductivity was enhanced three orders of magnitude by donor doping with Nb₂O₅ or Ta₂O₅; achieving a maximum of 546 S/m at 850 °C. The increase in electrical conductivity was accompanied by reduction of the absolute Seebeck coefficient. Seebeck coefficient reduction of $-600 \mu\text{V/K}$ was observed between undoped and 4% Ta₂O₅ doped samples. The solid solution and doping reduced the thermal conductivity to $< 4 \text{ W/mK}$, far below the parent materials TiO₂ and SnO₂. Lattice thermal conductivity decreased with increasing temperature, achieving 1.9 W/mK at 900 °C for 4% Ta₂O₅ doping. No further reduction in thermal conductivity was observed in annealed samples containing nano-sized SnTiO₃ precipitates. Dimensionless figure of merit (ZT) attained was less than 0.1.

Poster Session

Room: Atlantic/Arctic

(EMA-S1-P001-2012) Microstructure and Ferroelectric Characteristics of Doped BaTiO₃-ceramics

V. Mitic*, V. Paunovic, J. Purenovic, J. Nedin, Faculty of Electronic Engineering, Serbia

In this article, Yb₂O₃ is used as doping materials for BaTiO₃-based multilayer devices. BaTiO₃-ceramics doped with 0.1 and 0.5 wt% of Yb₂O₃ was prepared by conventional solid state procedure and sintered in temperature interval from 1320°C to 1380°C for four hours. SEM/EDS analyses showed that with the higher dopant concentration the abnormal grain growth is inhibited and the grain size ranged between 2-10 μm . With prolonged sintering time the increase of grain size is observed. The measurements of capacitance and dielectric losses as a function of frequency and temperature have been done in order to correlate the microstructure and dielectric properties of doped BaTiO₃-ceramics. We applied the fractal method in microstructure analysis of sintered ceramics, especially as influence on dielectric properties of BaTiO₃-ceramics. These fractal effects have been used for better understanding of intergranular capacitors.

(EMA-S1-P002-2012) Enhancement of mechanical properties of clay reinforced epoxy nanocomposites with clay modification

K. Rhee*, J. Lee, S. Ha, Kyunghee university, Republic of Korea

In recent years, researches on the material properties of clay-reinforced polymer nanocomp(nanocomposites) have been extensively conducted because clay have very high strength and rich deposits. The use of clay is economical and environmentally friendly. This study investigated the method to improve material properties of C/E(clay/epoxy)nanocomp. For this purpose, virgin clay, Na+-montmorillonite, was S(surface)-treated using silane(3-aminopropyltriethoxysilane) and C/E nanocomp were fabricated by mixing the clay with a epoxy resin. The effect of surface-treatment of clay on the mechanical properties of C/E nanocomp was investigated as comparing S-treated sample with untreated sample using various mechanical methods. The results were as follows; D-spacing between the clay layers increased by more than 55% and the intercalation improved as a result of clay S-treatment with silane. The glass transition temperature of S-treated C/E nanocomp slightly increased due to the decrease of crosslink mobility of epoxy by clay S-treatment. With the clay S-treatment, the tensile properties of the S-treated C/E nanocomp were improved by 8% and 12% compared to untreated cases. This occurred due to the increase of intercalation and dispersion of clay and the improvement of interfacial bonding strength between the clay and the epoxy resin with S-treatment of the clay.

(EMA-S2-P003-2012) Synthesis of BaxSr1-xTiO₃ films by a low temperature hydrothermal-galvanic couple technique

H. Teng*, P. Chan, F. Lu, National Chung Hsing University, Taiwan

BaxSr1-xTiO₃ (BST) films were prepared by a hydrothermal-galvanic couple technique at temperature as low as 60oC for 2 h. Titanium ni-

tride films were first deposited on Si substrates prepared by physical vapor deposition. Subsequently, the TiN/Si specimens were immersed in Ba(CH₃COO)₂ and Sr(CH₃COO)₂ alkaline solutions with different Ba/(Ba+Sr) ratios. The growth rate of BST films by using the hydrothermal-galvanic couple technique is much faster than the conventional hydrothermal method. Internal currents could be observed even no external voltages and currents were applied during the hydrothermal-galvanic couple method. The obtained BST films possessed a strongly preferred orientation over the TiN underlayer. Moreover, BST films showed spherical-grained morphologies by field-emission scanning electron microscopy. Dielectric constants of the BST films decreased almost linearly with the Ba/(Ba+Sr) ratios in the solutions.

(EMA-S2-P004-2012) Synthesis of barium titanate films on TiN-coated substrates by plasma electrolytic oxidation

J. Zeng*, H. Teng, F. Lu, National Chung Hsing University, Taiwan

Barium titanate (BaTiO₃) films were synthesized by plasma electrolytic oxidation (PEO) on TiN/Si substrates in a mixed alkaline electrolytes of 0.5 M Ba(CH₃COO)₂ and 2 M NaOH. The films were synthesized using a potentiostatic mode with voltages ranging from 30 to 80 V for 1 min at 70°C. X-ray diffraction results confirmed that cubic BaTiO₃ films were successfully prepared over the investigated voltage range. Moreover, the morphology of obtained BaTiO₃ films was investigated by field-emission scanning electron microscopy. The BaTiO₃ films possessed uniformly distributed spherical-particulate surface morphology below 60 V due to electrochemical effect. As the voltage increased up to 66 V, the porous feature fulfills characteristic of PEO. The obtained BaTiO₃ films show a dielectric constant of around 20 to 30 and the leakage current density of about 10⁻⁷ A/cm².

(EMA-S2-P005-2012) Synthesis of BaTiO₃ thin film on TiN-coated substrates by a hydrothermal-galvanic couple technique

C. Yang*, D. Tsai, P. Chan, F. Lu, National Chung Hsing University, Taiwan

BaTiO₃ films were prepared on TiN-coated Si substrates by a low temperature (<100°C) hydrothermal-galvanic couple technique in barium ion contained alkaline solutions. Highly conductive TiN/Si was used as a working electrode and the counter electrode was the platinum foil while the two electrodes were directly connected without applying any external power sources. From the X-ray diffraction analysis and electron back-scattered diffraction results, the obtained BaTiO₃ thin films were directionally-oriented growth on the TiN/Si substrate. The surface morphologies reveal that the BaTiO₃ nucleated and grew over the TiN surface with a single layer. The coverage rate of BaTiO₃ increased with the reaction temperature ranging from 45°C to 70°C. From kinetic analysis results, the growth rate of BaTiO₃ films by using hydrothermal galvanic couple was faster than hydrothermal method.

(EMA-S2-P006-2012) Tailored Processing of Na_{0.5}Bi_{0.5}TiO₃-xBaTiO₃: Role of Barium Content in Phase Formation during Solid State Synthesis

J. S. Forrester*, B. Lettman, T. Usher, J. L. Jones, University of Florida, USA

(1-x)Na_{0.5}Bi_{0.5}TiO₃-xBaTiO₃ (NBT-xBT) is a materials system that has attracted recent attention due to promising piezoelectric properties. This work focused on developing a fundamental understanding of phase formation in NBT-xBT with compositions spanning the morphotropic phase boundary (x=4, 6, 7, 9 and 13%). Ex situ synchrotron and in situ high temperature laboratory X-ray diffraction data will be presented that show critical temperatures during the solid state synthesis of NBT-BT from the oxide reactants. These include the onset of the reaction temperature, the temperature range between which transient phases exist, and the temperature at which all reactants and transient phases have been consumed in the reaction to form the final single phase perovskite. For example, in NBT-7%BT, at ~500°C there is the first appearance of the NBT-BT phase. At this temperature much of the reactants remain, and a transient phase identified as Bi₁₂Ti₂₀ appears. At 900°C, only NBT-7%BT

remains. These results also show that increasing the Barium content necessitates an increased calcining temperature before all the Barium source is consumed in the reaction. Rietveld refinement of selected diffraction patterns will be used to establish the phase assemblage and other notable aspects of NBT-BT formation at selected temperatures of interest.

(EMA-S2-P007-2012) Effect of grain size on domain dynamics and macroscopic dielectric and piezoelectric properties of BaTiO₃ ceramics

D. Ghosh*, A. Sakata, H. Han, J. C. Nino, J. L. Jones, University of Florida, USA

Domain size in barium titanate ceramics (BaTiO₃) varies with grain size in a parabolic fashion and thus, dielectric and piezoelectric properties vary with grain size. However, parabolic relationship breaks down when the grain size is reduced to the nanometer range when the grains become mono-domain. Starting from nanocrystalline (50 nm) powder, BaTiO₃ ceramics in the grain size range of 200 nm to 10 μm were developed by spark plasma sintering (SPS) and pressureless sintering (PS) methods to study effect of grain size on dielectric and piezoelectric properties. XRD peaks from the starting BTO nanocrystalline powder were very broad and splitting of the pseudocubic {200} to (200) and (002) reflections was almost absent, suggesting a pseudocubic symmetry in the starting powder. Tetragonality (c/a) of the BaTiO₃ phase increased upon sintering, where tetragonality was significantly larger in the BaTiO₃ ceramics sintered by the PS than the BaTiO₃ ceramics sintered by SPS. The relative permittivity and piezoelectric coefficient (d₃₃) were found to be maximum in the grain size range of 1-2 μm and decreased below and above of this grain size range for the BaTiO₃ ceramics.

(EMA-S2-P008-2012) Crystal Structure and Phase Transitions in Chemically Modified Sodium Bismuth Titanate

E. Aksel*, J. S. Forrester, J. L. Jones, University of Florida, USA

The properties of piezoelectric materials are strongly influenced by their crystal structure; therefore, having a thorough structural understanding of a material is imperative. This work focuses on developing a comprehensive understanding of the lead-free material system – sodium bismuth titanate (NBT). NBT ceramics were prepared with the addition of Fe³⁺, Mn²⁺, or La³⁺ in concentrations ranging from 0.5-2 at%, along with unmodified samples. To examine these materials, high resolution synchrotron diffraction patterns were measured at the Advanced Photon Source. Diffraction patterns were also measured as a function of increasing temperature for various compositions. Rietveld refinement was then utilized to extract structural information such as space groups, lattice parameters, and atomic positions from the diffraction patterns. Also, a single peak fitting method was used to understand the phase evolution with temperature. The room temperature space group of NBT is found to be Cc (monoclinic). The addition of La³⁺ decreases the monoclinic distortion while that of Fe³⁺ and Mn²⁺ increases it. The presence of local disordered regions is also observed and their proportion increases with temperature up to ~300°C. This increase is the first report of a structural change seen in XRD across the same temperature range where depoling occurs in these materials.

(EMA-S2-P009-2012) In situ X-ray scattering of Na_{0.5}K_{0.5}NbO₃ based piezoelectric ceramics during reactive templated grain growth

G. Tutuncu*, J. L. Jones, University of Florida, USA; G. L. Messing, Y. Chang, Penn State University, USA

Due to their promising piezoelectric properties, (K,Na)NbO₃ (KNN)-based materials are currently under investigation as alternatives to Pb-containing ferroelectric ceramics. It has been shown that chemical modification (e.g. incorporation of Li⁺) and controlled microstructure (e.g. through templated grain growth (TGG) process) can achieve significant enhancements in the piezoelectric properties and electromechanical coupling factors. However, in order for these ceramics to approach the commercial ubiquity of Pb-based materials, they must be developed with high texture and single crystal-like

properties. For this, a better understanding of their high-temperature phase and texture evolution during fabrication is required. In this study, we present an in situ X-ray diffraction technique that allows phase and texture evolution to be monitored concurrently during the KNN sintering process, across the template-matrix interface. In situ changes in these two distinctive phases are tracked independently throughout the sintering process, and precursor NaNbO₃ particles are observed to template the crystallographic texture of a Li⁺-modified KNN matrix. The conversion of NaNbO₃ templates was completed at approximately 1150 °C. Above this, a homoepitaxial growth of the KNN matrix texture was observed through the increased orientation dependence of intensity.

(EMA-S2-P010-2012) Nature of self-polarization effect in the PZT thin film

E. B. Araujo*, E. C. Lima, Sao Paulo State University, Brazil; I. Bdkin, A. L. Kholkin, University of Aveiro, Portugal

Often, ferroelectric thin films prepared by different techniques exhibit a self-polarization effect of similar magnitude to those films subsequently polarized by an external electric field. Although several theoretical developments have been proposed to explain the mechanisms of the self-polarization in ferroelectric films, its real nature is still object of discussion and controversy. In the present work, the structural properties and domain structure of polycrystalline Pb(Zr_{0.50}Ti_{0.50})O₃ (PZT) thin films were studied by small-angle X-ray Diffraction (XRD) and Scanning Force Microscopy (SFM) techniques. The films were deposited by a chemical method on Pt/TiO₂/SiO₂/Si substrate at different thicknesses (200-710 nm). A pronounced (100) texture near the ferroelectric-electrode interface was observed and this texture increases considerably for thinnest films. The piezoresponse signal distribution of the films showed only one peak shifted to the negative d₃₃ values before poling. It was observed that the local d₃₃ coefficients increase as the film thickness decreases. This dependence corroborate the results observed by XRD that alignment of ferroelectric domains occurs locally near the film-electrode interface. Results were discussed in terms of Schottky barriers and strain gradients as a possible cause of the self-polarization via flexoelectric effect.

(EMA-S2-P011-2012) Dependence of Piezoelectric Properties on Structural Characteristics of (K, Na)NbO₃-based Ceramics

E. Kim*, J. Lee, Kyonggi University, Republic of Korea; J. Cho, B. Kim, Korea Institute of Ceramic Engineering and Technology, Republic of Korea

Effects of crystal structures on the piezoelectric properties of A- and B-site modified (K, Na)NbO₃ ceramics were investigated. For the sintered specimens, the orthorhombic-tetragonal phase transition temperature (T_{o-t}) and tetragonal-cubic phase transition temperature (T_c) decreased with increasing oxygen octahedral distortion, which was confirmed from the shift of Raman-active vibration modes. These results induced the increase of dielectric constant (ϵ_r), piezoelectric constant (d_{33}), electromechanical coupling factor (k_p) and temperature coefficient of k_p (TCk_p) of the specimens. With increasing Nb-site bond valence, the ϵ_r of the specimens decreased, while the k_p of the specimens increased. The mechanical quality factor (Q_m) of the specimens was affected by the relative density. The effect of composition on the electric-field-induced strain of the specimens was also discussed.

(EMA-S2-P012-2012) Dielectric and AC electrical conductivity studies of Ln₂CuO₄ (Ln=Nd, Gd) ceramics

P. H. Salame*, O. Prakash, A. Kulkarni, IIT Bombay, India

The semiconducting, layered cuprates Ln₂CuO₄ (Ln=Nd, Gd) in dense (> 95%TD) pellets form were prepared by ceramic solid state reaction and sintering route, using stoichiometric fine powder mix of high purity (> 99.9%) oxides of Cu, Nd, Gd. The samples as analyzed by their XRD patterns and SEM micrographs, revealed clean phase T'-type (Sp. Gp. I4/mmm). The frequency dependent dielectric constant (ϵ_r') and ac conductivity (σ_{ac}) of these Ln₂CuO₄ compounds in

preliminary experiments were found to be sensitive to lattice oxygen content, hence prolonged (> 10 days) annealing in oxygen ambience was carried out to stabilize the oxygen content in T'-type lattice. The dielectric properties (ϵ_r' , $\tan \delta = \epsilon_r'' / \epsilon_r'$) of Ln₂CuO₄ pellet were investigated in the temperature range -100 °C to 150 °C and frequencies 0.1 Hz to 1 MHz. The ϵ_r' values of both Nd₂CuO₄ and Gd₂CuO₄ were found to be very high ranging 10³ to 10⁴ for entire temperature and frequency range. The $\tan \delta$ values were found to vary from 0.1 for higher frequencies (> 10 KHz) to 100 for lower frequencies (<1 KHz) for the entire temperature range. The $\tan \delta$ plot in both the compound showed a peak around -25 °C, this was attributed to the antiferromagnetic ordering temperature of Cu(3d⁹). Further, σ_{ac} was found to be frequency dependent, and fairly obeyed the Jonscher's power law.

(EMA-S2-P013-2012) Integrated Humidity Sensor System Using Carbon Nitride Film Based on Analog Mixed CMOS Technology

S. Lee, J. Jung*, Kyungnam University, Republic of Korea

Integrated humidity sensor system with nano-structured carbon nitride film as humidity sensing materials is fabricated by 0.8 um analog mixed CMOS process. Integrated sensor system consists of differential humidity sensitive field effect transistors (HUSFET), operational amplifier, temperature sensor and resistive sensor. A differential humidity sensitive field effect transistor has a pair of transistors, i.e., humidity sensing transistor and non-sensing one (reference transistor) to eliminate the effect of other factors. Two types of integrated sensor chip are designed with 2x4 mm² area and 28 pin terminals. The process contains two poly, two metal and twin well technology. For the formation of CN_x film on Si₃N₄, the plasma etching was performed to Si₃N₄ layer as much as trench. CN_x films were deposited by reactive RF magnetron sputtering method and patterned by lift-off techniques. To fulfill the requirement of differential sensors, the water permeable gold layer was deposited only on the gate region of the sensing device. We can see that the drain current (I_d) is proportional to the dielectric constant, and slightly decreases with threshold voltage increase. The dielectric constant of HUSFET with W/L=20 is changed from about 3 to 12 in the relative humidity range of 10 %RH to 90 %RH.

(EMA-S3-P014-2012) Effect of different layer thickness on the Properties of 0.7BiFeO₃-0.3PbTiO₃-Based Multilayer Thin Films Prepared by Sol-gel Process

W. Zhang, Z. Xu, H. Liu, D. Xiao, J. Zhu*, Sichuan University, China

0.7BiFeO₃-0.3PbTiO₃(BFPT7030)multilayer thin films with different PbTiO₃ buffer layers were deposited on LaNiO₃/SiO₂/Si substrates by sol-gel processing. XRD patterns showed that the films exhibit single perovskite phase except for BFPT7030 thin films annealed in N₂ atmosphere. AFM images demonstrate that all the films show a dense, crack-free surface morphology. XPS analysis show that the BFPT7030 films annealed at 700 degree with heating rate of 5 degree per minute possess higher Fe³⁺ content than that of Fe²⁺. It was found that the BFPT7030 multilayer thin films with two PbTiO₃ buffer layers exhibit the highest remnant polarization of 36 μC/cm² with a low coercive field of 80 kV/cm.

(EMA-S4-P015-2012) Tunable Thermal Transport in Lithium-ion Battery Cathodes as Measured by Time-domain Thermal-reflectance

J. Cho*, M. Losego, D. Cahill, P. Braun, University of Illinois at Urbana Champaign, USA

Lithiation and delithiation of the electrode materials in lithium-ion batteries can induce significant variations in the properties of the electrodes. In some cases, this can even lead to plasticity, fracture and electrochemically driven solid-state amorphization. The thermal properties as a function of lithiation have not previously been measured, and may provide both an understanding of the fundamental behavior of battery electrodes, and if the change is significant, may provide a route to materials with tunable thermal properties. Here we present experimental thermal measurements of a lithium-ion cath-

ode as a function of lithiation. We have constructed an electrochemical device consisting of a Li foil as an anode, a liquid electrolyte containing a Li salt, and a thin film LiCoO₂ cathode which enables direct real time measurements of thermal properties during electrochemical cycling. By applying an external electric current, Li ions can be intercalated or deintercalated within the host materials during discharge or charge, respectively. The thermal conductance changes significantly as a function of the charging level (degree of lithiation). The dependence of thermal transport properties on potential difference between cathode and anode may be explained by considering the effect of lithiation and delithiation on the electron carrier density.

(EMA-S4-P016-2012) Characteristic of NiO/Li-La-Zr-O solid-state electrolyte by laser annealing for thin film battery

S. Lee*, S. Jee, Yonsei university, Republic of Korea; T. Kim, Korea Institute of Industrial Technology, Republic of Korea; Y. Yoon, Yonsei university, Republic of Korea

Solid-state electrolyte thin films have been studied for application in solid-state ionic power devices. Besides many improvements of solid-state electrolyte for ionic conductivity, an advanced solid-state electrolyte is still needed. In this study, nickel oxide (NiO)/lithium lanthanum zirconium (Li-La-Zr-O) thin films as solid-state electrolyte with laser annealing have been investigated. The NiO/Li-La-Zr-O thin film solid electrolyte is prepared by radio frequency (RF) magnetron sputtering under Ar gas atmosphere. We propose that the sandwich structure makes it possible to use the NiO/Li-La-Zr-O film as a thin film solid electrolyte without potential short circuit of the NiO/Li-La-Zr-O thin film. The NiO/Li-La-Zr-O thin film solid electrolyte with laser annealing is confirmed by X-ray diffraction (XRD) and field emission scanning electron microscopy (FESEM). Impedance measurement is conducted to confirm ionic conductivity of the NiO/Li-La-Zr-O thin film solid electrolyte at room temperature. The results show that the ionic conductivity of NiO/Li-La-Zr-O thin film solid electrolyte with laser annealing is enhanced. From the results, it can be confirmed that NiO/Li-La-Zr-O thin film is a potential candidate as solid state electrolyte to apply in thin film battery.

(EMA-S5-P017-2012) Improvement in thermoelectric properties by adding P2O5 in Fe2O3 ceramics

H. K. Hwang, G. W. Lee, K. Park*, Sejong Univ., Republic of Korea

Development of high-efficiency thermoelectric materials which convert thermal energy directly into electrical energy is expected to promote the efficient use of energy. Metallic oxides have been recognized as good candidates for applications in thermoelectric generation because of their excellent thermal and chemical stability, easy manufacture and low manufacturing cost. Nano-sized Fe_{2-x}PxO₃ (0 ≤ x ≤ 0.01) thermoelectric powders were synthesized by solution combustion process, using their corresponding nitrates as oxidizers and aspartic acid as combustion fuel. The combustion method was attractive for synthesizing nanocrystalline high-quality powders in shorter time. The green pellets were sintered at 1000 °C for 5 h. The sintered Fe_{2-x}PxO₃ bodies were α-Fe₂O₃-based single phase with a rhombohedral structure. The incorporation of P+5 led to a significant increase in electrical conductivity. The sign of the Seebeck coefficient was negative over the measured temperature range, i.e., n-type conduction. In this study, we discussed detailed thermoelectric properties of Fe_{2-x}PxO₃ ceramics, depending on P content.

(EMA-S6-P018-2012) Conceptual Design of a No-chamber, Bioethanol-fueled Solid Oxide Fuel Cell

J. L. Aguilar, Universidad Nacional de Colombia, Colombia; A. A. Oliveira, D. Hotza*, Universidade Federal de Santa Catarina, Brazil

Solid Oxide Fuel Cells are classified according to their conceptual design in three categories: dual-chamber, single-chamber and no-chamber. The performance of cells is compared based on literature, and advantages and disadvantages are discussed. It is found that to date the degree of development for the single-chamber cells is com-

parable to that of the dual-chamber in terms of the electro-chemical performance, but not in terms of the fuel conversion in the cells. A new no-chamber design is proposed for SOFC with the aim of using a porous burner for combustion of bioethanol as source of reducing fuels for the cell.

(EMA-S6-P019-2012) A novel route for the synthesis of nano-sized high-quality (Y0.5Gd0.5)PO4:Eu3+ red phosphors

K. Park*, K. Y. Kim, M. H. Heo, Sejong Univ., Republic of Korea

Spherical and nano-sized high-quality (Y0.5Gd0.5)PO₄:Eu0.06 phosphor powders were synthesized via solution combustion process, using citric acid (C₃H₄(OH)(COOH)₃) as combustion fuel and its corresponding metal nitrates as oxidizers. The combustion process was suitable for synthesizing complex (Y0.5Gd0.5)PO₄:Eu0.06 powders with ultra-fine size, high compositional homogeneity, and high purity, which was advantageous over the conventional solid-state method. In addition, the combustion process was a simple and cost-effective method. The synthesized powders were annealed at 600-1300 °C for 4 h in air. The crystal structure and microstructure of the annealed (Y0.5Gd0.5)PO₄:Eu0.06 powders were analyzed with an X-ray diffractometer and a field emission scanning electron microscope, respectively. The (Y0.5Gd0.5)PO₄:Eu0.06 phosphors annealed at 800-1000 °C and at 1200-1300 °C crystallized in the monoclinic monazite structure and the tetragonal xenotime structure, respectively. The crystallite size increased with an increase in annealing temperature. The most intense emission intensity at 619 nm was obtained for the (Y0.5Gd0.5)PO₄:Eu0.06 phosphors annealed at 1300 °C. In this study, we discussed detailed emission characteristics as a function of annealing temperature.

(EMA-S7-P020-2012) Dielectric Properties of MgNb₂O₆ / Polypropylene Composites at Microwave Frequencies

E. Kim*, C. Jeon, D. Im, Kyonggi University, Republic of Korea

Effects of MgNb₂O₆ content and crystallinity of semi-crystalline polypropylene (PP) on the microwave dielectric properties of MgNb₂O₆ / PP composites were investigated. The degree of crystallinity and different crystalline phases (α-monoclinic and γ-orthorhombic) of PP were determined by the different heat treatment processes of the composites. The dielectric constant (K), dielectric loss (tan δ) and temperature coefficient of resonant frequency (TCF) of the composites were dependent on the MgNb₂O₆ content and the crystalline phases of PP. For the composites with same amount of MgNb₂O₆, the K and tan δ increased with increasing crystallinity of PP. These results could be attributed to the increase of space charge trapped in the composites. The frequency dependence on dielectric properties of the composites was also discussed for frequency stability.

(EMA-S7-P021-2012) New theory to study metamaterials

Z. Wang*, Zhejiang Agriculture & Forestry University, China

Veselago introduced negative permittivity and permeability into Maxwell's equations and predicted a novel negative-phase-velocity (NPV) material [1] which has become a hot topic. The Poynting vector S is antiparallel to the wave vector k but this is in conflict with quantum mechanics and mass-energy relation $S/g = E/m = C^2$ ($g = \hbar k$). We would rather claim reversed physical laws than negative quantities, i.e. circuital theorem and induction rule is left-handed where permittivity and permeability is still positive. Difficulties will be overcome meanwhile correct contents of his theory such as negative refraction [2] and reversed Cherenkov effect [3] retained. In any event, Lorentz transformations break down and new transformations are necessary to explain above strange phenomena. For instance, the momentum within Veselago's materials should be expressed as $p = -mV$ opposite to the velocity. By this way, more metamaterials and curious effects are proposed. We hope they will be discovered soon.

(EMA-S8-P022-2012) Synthesis of cordierite dense glass-ceramic and its Structural Optimization using back-scattering Raman Spectroscopy

F. Jahantigh*, Tarbiat Modares University, Islamic Republic of Iran

In this article, the production and structural, optical and surface morphology of a type of amorphous $Mg_2Al_4O_3Si_5O_{18}$ glass-ceramic powder which was produced through the Pechini method is discussed. The obtained glass powders were pressed to form disk pellets which were sintered at 12000C, 12500C and 13000C. In order to identify the phases, structural and morphology of the glass-ceramics X-ray diffraction (XRD), back-scattering Raman spectroscopy and scanning electron microscopy (SEM) have been used. The XRD results revealed that by increasing temperature, the apparent adjacency of pellets phases become nearer to the desired glass-ceramic. The SEM-micrographs of the glass ceramic showed a uniform distribution of particles in the structure. The Raman spectra reveals the presence of broad band vibrations due to Al-O, Si-O and Mg-O.

(EMA-S8-P023-2012) A diffusionless transformation path relating Th3P4 and spinel structure: opportunities to synthesize ceramic materials at high pressures

A. Goswami*, UT Arlington, Texas, USA

Under high-pressure conditions, chemical reactivity of atoms and molecules increases manifold, significant shift in chemical equilibria observed and reaction rates get affected. On compression of any substance, distances between constituting atoms decrease and its electronic structure deforms. This leads to increase of the internal energy of the substance, and formation of denser structures could become energetically favorable on further compression. Shorter interatomic distances and/or higher coordination numbers of the constituent atoms characterize such structures when compared with the lower pressure phases. At high-pressure conditions, formation of compounds with elements in unusual oxidation states can take place. In many cases, these high-pressure phases can be quenched to ambient conditions where they may persist metastably due to slow kinetics of a reverse transformation. Such metastable products can have a number of unique physical and chemical properties, from high hardness and corrosion stability to interesting optoelectronic, magnetic or superconducting properties. Therefore, they can be of potential interest for various industrial applications.

(EMA-S8-P024-2012) Necessity of the Hanai method to evaluate concentrated dielectric slurries consisting of ceramic powders with high permittivity

W. Zhou*, J. Nino, University of Florida, USA

Traditionally the permittivity of ceramic powders is obtained through electrical characterization of a sintered pellet. However, the structure and the dielectric properties of the sintered products may differ from the initial loose powders. In recent years, the dielectric evaluation of ceramic slurries to characterize the dielectric response of particles has been of increasing interest. In this work, BaTiO₃ slurries and SrTiO₃ slurries were investigated by electrochemical impedance spectroscopy. Both the Lorentz-Lorentz (L-L) equation and Hanai equation were used in order to extract the permittivity of the particles. The permittivities of SrTiO₃ calculated from the two equations were similar, and close to the referenced value for concentrated slurries. Compared with the Hanai equation, the L-L equation considerably expanded the margin of error from the experimental apparatus and measurements. The permittivity of BaTiO₃ calculated from L-L equation was abnormal, while the results from Hanai equation were within a reasonable value region. It will be shown that increasing the solids loading of the slurry is required to increase the accuracy of the calculation. In addition, it will be demonstrated that for an accurate calculation of high permittivity particles within highly concentrated slurries the Hanai equation (instead of the L-L equation) is necessary.

(EMA-S8-P025-2012) High Temperature Piezoelectrics for Thermoacoustic Engines

B. Kowalski*, A. Sehirlioglu, Case Western Reserve University, USA

High temperature piezoelectric materials are sought after for power generation in aeronautic applications such as thermoacoustic engines. Piezoelectric energy converters need to work with >80% efficiency if cooling is required, but the development of high temperature piezoelectrics would eliminate the need for cooling which reduces the required energy conversion efficiency. In addition, the introduction of piezoelectrics for electromechanical energy conversion in thermoacoustic engines would create a system with no moving parts (i.e., pistons) and contribute significantly to the reliability of the engine. The output in current piezoelectric energy harvesting systems is in the mW range and it is necessary to increase the output efficiency, output power and operating temperatures for the intended applications. Recent studies by Grinberg et al and Eitel et al have predicted Curie temperatures (T_c) greater than that of PZT through solid solutions of BiMeO₃ with PbTiO₃(PT). In this study, solid solutions of PT with end members BiScO₃, BiInO₃, and Bi(Zn_{0.5},Zr_{0.5})O₃ are being investigated through both weak and high field studies to establish operating temperatures, dielectric and electromechanical properties as a function of temperature, frequency and electric field. The intention is to combine these high temperature piezoelectric materials with an energy harvesting circuit to output power in the 10-100W range.

(EMA-S8-P026-2012) Synthesis, characterization and magnetic properties of Li-Ca-Zn nanoferrite system

J. Singh*, B. S. Randhawa, Guru Nanak Dev University, India

Nanomaterials often have unique electrical, chemical, structural, and magnetic properties, with potential applications in information and high energy storage devices. Magnetic nanoparticle and nanostructural studies combine a broad range of synthetic and investigative techniques from physics, chemistry, and materials science. Further, magnetic properties of nanoparticles are of broad interest in fundamental science. Keeping in view, we have synthesized the Li_{0.25}Ca_{0.5}-XZnXFe_{2.25}O₄ ferrite system, where 'x' varies from 0→0.5 by using solution combustion method. This low temperature, self-propagating and gas producing exothermic combustion method is safe, simple economic and attractive. The capping agent i.e. Oxalyl-Dihydrazide used in this method as fuel acts to accelerate the process leading to the obtention of nanomaterials. X-ray diffraction confirmed the formation of cubic spinel nanophase ferrites and their crystallite size was calculated using Scherrer's formula. The particle size was also estimated using Transmission Electron Microscope (TEM) and was found to be in the range of 40 to 43 nm. Mossbauer studies have also been undertaken and are in good agreement with Neel's 'local molecular field' model. Magnetic properties, Curie Temperature (T_c), Saturation Magnetization (M_s), Coercivity (H_c) and Remanence (M_r) have also been carried out.

(EMA-S8-P028-2012) Liquid Hydrogen for Cryogenic Cooling and Aviation Fuel Additive

B. Pierce*, T. Haugan, WPAFB, USA

Hydrogen has long been heralded as a hot research topic among the automotive industry as a way to lower the greenhouse footprint established by their vehicles. BMW has done extensive research with building factory vehicles that can either run on a petroleum/hydrogen mixture or a stand-alone vehicle, with Toyota and other groups doing extensive research in the area of the storage technology. The aim of the investigation from WPAFB is to adapt the research and apply it towards aviation technology and apply it to cooling cryogenics and using the waste hydrogen as a fuel additive. By analyzing the logistics of SOFI and vacuum insulation as the two main viable approaches to slowing down boil-off, the analysis could then be done to

find the optimal liquid Hydrogen to storage ratio to satisfy the requirements of being both a manageable mass in the air vehicle and also providing adequate storage capacity for liquid hydrogen to prolonged trips. Further research has been done to intuitively optimize vessel wall thickness and the possibility of 2-stage cryogenic cooling within the vehicle to increase the longevity of the liquid hydrogen. Further analysis will be explained in the upcoming presentation and paper. This work supported by – AFRL Propulsion Directorate, and the Air Force Office Scientific Research (AFOSR)

Thursday, January 19, 2012

Plenary II

Room: Indian

8:00 AM

(EMA-PL-002-2012) Science to Energy (Invited)

H. Kung*, U.S. Dept. of Energy, USA

not available

S2: Advanced Dielectric, Piezoelectric and Ferroic Materials, and Emerging Materials in Electronics

Multiferroic Oxides, Heterostructures, and Thin Films

Room: Indian

Session Chair: Aiping Chen, Texas A&M University

9:30 AM

(EMA-S2-016-2012) Bi-based Piezoelectric Thin Films via Chemical Solution Deposition

Y. Jeon*, Oregon State Univ, USA; J. F. Ihlefeld, G. L. Brennecke, Sandia National Laboratories, USA; B. J. Gibbons, Oregon State Univ, USA

Bi-based perovskite materials have been investigated as promising candidates to replace lead-based piezoelectric materials. In particular, compositions near the morphotropic phase boundary in $(\text{Bi}_{0.5}\text{K}_{0.5})\text{TiO}_3 - (\text{Bi}_{0.5}\text{Na}_{0.5})\text{TiO}_3$ (BKT-BNT) display promising behavior such as high P_{max} and P_r . Recently, $\text{Bi}(\text{Zn}_{0.5}\text{Ti}_{0.5})\text{O}_3 - (\text{Bi}_{0.5}\text{K}_{0.5})\text{TiO}_3$ (BZnT-BKT) ceramics have also been explored for their piezoelectric response and showed a high dielectric constant ($K \approx 4,000$ at T_c) and P_{max} above $25 \mu\text{C}/\text{cm}^2$. Although bulk material research is useful, many applications require thin film embodiments, thus it is useful to explore whether these bulk properties can be replicated in thin films. Here, BKT-BNT near MPB composition and BZnT-BKT thin films are deposited on Pt-Si substrates via chemical solution deposition. Precursor solutions and process conditions have been varied to control the volatile elements. "Layer-by-Layer annealing" deposition resulted in single perovskite phase development and depending on the overdoping of cations, changes in grain size were observed. BZnT-BKT thin films showed $P_{\text{max}} > 20 \mu\text{C}/\text{cm}^2$. Process conditions were explored to improve the dielectric, ferroelectric, and piezoelectric properties. Sandia is a multiprogram laboratory operated by Sandia Corporation, a Lockheed Martin Company, for the United States Department of Energy's National Nuclear Security Administration under contract DE-AC04-94AL85000.

9:45 AM

(EMA-S2-017-2012) Localized Domain Structure in Ferroelectric Thin Films

M. Rogers*, Y. Jing, S. Leech, R. Garcia, J. E. Blendell, Purdue Univ, USA

The electromechanical coupling in ferroelectric materials arises from piezoelectric lattice strain, 180° and non- 180° domain wall

motion and elastic strain accommodation. Separating contributions from lattice strain and domain wall motion from the measured macroscopic piezoelectric properties has shown that intergranular interactions account for a significant portion of the electromechanical coupling. To examine this effect, lead zirconate titanate (PZT) thin films have been studied using Piezoresponse Force Microscopy (PFM). We have studied the domain motion within individual grains and domain interactions across grain boundaries under locally applied electric fields. The local structure of the grain boundaries within the thin films was determined using EBSD. These experiments provide an understanding of the intergranular interactions which contribute to the bulk piezoelectric properties. We are also studying lead-free piezoelectric systems for use as replacements due to environmental and health concerns for PZT-based ceramics. Investigation of the localized ferroelectric response in $\text{Na}_{0.5}\text{Bi}_{0.5}\text{TiO}_3$ (NBT) and $\text{Ba}(\text{Zr}_{0.2}\text{Ti}_{0.8})\text{O}_3 - (\text{Ba}_{0.7}\text{Ca}_{0.3})\text{TiO}_3$ (BZT-BCT) based materials provides an understanding of intergranular effects on the piezoelectric response in order to develop lead-free materials with optimum performance. The local ferroelectric response of the lead-free films will be reported.

10:00 AM

(EMA-S2-018-2012) Mapping and Statistics of Ferroelectric Domain Boundary Angles and Types

L. Ye, J. Desmarais, University of Connecticut, USA; J. F. Ihlefeld, Sandia National Laboratories, USA; T. Heeg, Cornell University, USA; J. Schubert, Research Centre Jülich, Germany; D. G. Schlom, Cornell, USA; B. D. Huey*, University of Connecticut, USA

Ferroelectric domain and domain boundary engineering is important for its potential to improve device performance, reliability, and energy efficiency. This work presents domain characterization methods for the measurement and analysis of populations of individual domain wall orientations, types, and cross-coupling. Domain orientations are first mapped using piezo-force microscopy, allowing the calculation and statistical analysis of interfacial polarization angles, the head-to-tail or head-to-head configuration, and any cross-coupling terms. Within $1 \mu\text{m}^2$ of an epitaxial $(001)_p$ -oriented BiFeO_3 film there are $>40 \mu\text{m}$ of linear domain boundary based on over 500 interfaces. 71° domain walls completely dominate the interfacial polarization angles, with a 2:1 preference for uncharged head-to-tail versus charged head-to-head domain boundary types. This mapping technique therefore offers a new perspective on domain boundary distributions, important for ferroelectric and multiferroic applications where domain wall parameters are critical.

10:15 AM

(EMA-S2-019-2012) Nd-doped BiFeO_3 thin films prepared by Pulsed Laser Deposition

W. Shen*, University of Sheffield, United Kingdom; A. Bell, University of Leeds, United Kingdom; S. Karimi, I. Sterianou, I. Reaney, University of Sheffield, United Kingdom

Undoped epitaxial $\text{Bi}_{1-x}\text{Nd}_x\text{FeO}_3$ ($x=0.1-0.25$) thin films were prepared by pulsed laser deposition (PLD) on SrTiO_3 substrates with SrRuO_3 bottom electrodes. According to XRD, all films were single phase with a low degree of mosaicity. Scanning electron and atomic force microscopy revealed a uniform surface microstructure but with debris typical of PLD. The leakage current was reduced by appropriately adjusted laser fluence which also gave precise control over film thickness. The microstructure and structure of the films were further characterized using transmission electron microscopy. Ferroelectric and piezoelectric response was determined using a combination of conventional electrode polarization – field measurements and piezo. force microscopy. Current-voltage studies were also performed in order to investigate the mechanisms in these systems.

10:30 AM

(EMA-S2-020-2012) Tunable Physical Properties of Self-assembled Manganite-Based Vertical Aligned Nanocomposite Thin Films

A. Chen*, Z. Bi, X. Zhang, Texas A&M University, USA; Q. Jia, Los Alamos National Laboratory, USA; J. L. MacManus-Driscoll, University of Cambridge, United Kingdom; H. Wang, Texas A&M University, USA

Two-phase manganite-based nanocomposite films such as $(\text{La}_{0.7}\text{Sr}_{0.3}\text{MnO}_3)_{0.5}:(\text{CeO}_2)_{0.5}$ (LSMO:CeO₂) and $(\text{La}_{0.7}\text{Sr}_{0.3}\text{MnO}_3)_{0.5}:(\text{ZnO})_{0.5}$ (LSMO: ZnO) were heteroepitaxially grown on SrTiO₃ (STO) (001) by pulsed laser deposition (PLD). X-ray diffraction (XRD) and transmission electron microscopy (TEM) results show that these nanocomposite films epitaxially grow on STO as self-assembled vertically aligned nanocomposite (VAN) structure. Physical properties measurements demonstrate that the LSMO phase in the VAN structure behaves differently from its epitaxial single phase counterpart, e.g., large tunable vertical lattice strain, greatly enhanced coercivity (HC) and tunable low-field magnetoresistance (LFMR). The enhanced properties in VAN system is attributed to the interaction between the perovskite and the secondary phase or phase boundary. The results suggest that the growth of functional oxide in another oxide matrix with vertical heteroepitaxial form is a promising approach to achieve new functionality that may not be easily realized in the single epitaxial phase.

10:45 AM

(EMA-S2-021-2012) Optimization of Magnetic and Ferroelectric Properties of $\text{MFe}_2\text{O}_4(\text{M}=\text{Ni}, \text{Co})/\text{Pb}(\text{Zr}_{0.52}\text{Ti}_{0.48})\text{O}_3$ Multilayer Composites

S. Tabei*, Georgia Institute of Technology, USA; S. Seifkar, F. Hunte, J. Schwartz, North Carolina State University, USA; N. Bassiri-Gharb, Georgia Institute of Technology, USA

We report multilayer composites of $\text{Pb}(\text{Zr}_{0.52}\text{Ti}_{0.48})\text{O}_3$ (PZT) and $\text{MFe}_2\text{O}_4(\text{M}=\text{Ni}, \text{Co})$, prepared via chemical solution deposition, for magnetoelectric applications. Effects of thermal treatment profiles (time and temperature) as well as sequence, thickness variation of the stack compared to active layer thickness variation have been studied. Increasing the annealing temperature from 650 to 800°C results in an increase in the average grain size and consequently enhances the remanent magnetization in the ferrite phase, without significant variation in the magnetic coercivity. Higher annealing temperatures (>850°C) lead to partial interdiffusion between the different chemistries and reduction of the ferroelectric properties. The saturation magnetization of Si/MFO/PZT and Si/MFO/Pt/PZT remarkably increases relative to Si/MFO films. Highly oriented (100) PZT on platinumized Si leads to enhancement of the magnetostrictive phase's microstructure and therefore its remanent magnetization. The effects of heat treatment in magnetic field on the magnetic properties of the MFO layers will also be discussed.

11:00 AM

(EMA-S2-022-2012) Spark plasma sintering (SPS) of nanostructured BaTiO_3 - CoFe_2O_4 multiferroic composites

D. Ghosh*, H. Han, A. Sakata, J. C. Nino, J. L. Jones, University of Florida, USA

A promising multiferroic composite architecture is the 0-3 composites, which can be fabricated by mixing a ferroelectric phase and a ferromagnetic phase, and then co-sintering them. The interface structure is extremely important since strain transfers across the interfacial areas. Using spark plasma sintering (SPS) technique, we have sintered dense and phase pure nanostructured BaTiO_3 - CoFe_2O_4 composites at temperature as low as 850 C and a sintering time of 5 min. In contrast, pressureless sintering (PS) did not produce phase pure composites as a result of reactions between BaTiO_3 and CoFe_2O_4 due to high sintering temperature (1150 C) and long consolidation time (120 min). X-ray diffraction measurements also revealed the evidence of iron diffusion into the BaTiO_3 phase from CoFe_2O_4 in the SPS composites. Permittivity measurements revealed a decrease in the Curie

temperature in the composites than pure BaTiO_3 ceramics, which is consistent with the Fe diffusion into the BaTiO_3 lattice. We showed that while Fe diffusion occurred in both SPS and PS methods, it was significantly higher in PS than SPS, resulting in a large decrease of the Curie temperature in the composites sintered by the PS method relative to the SPS technique.

11:15 AM

(EMA-S2-023-2012) Synthesis and characterization of $\text{xCo}_0.7\text{Zn}_0.3\text{Fe}_2\text{O}_4$ - $\text{Bi}_0.9\text{La}_0.1\text{FeO}_3$ multiferroic nanocomposites

K. Yadav*, Indian Institute of Technology Roorkee, India

As per the literature doping of Zn in CoFe_2O_4 at Co site improved the magnetic properties and small doping of La in Bismuth Ferrite (BFO) reduced the leakage current. Keeping this in mind we prepared $\text{xCo}_0.7\text{Zn}_0.3\text{Fe}_2\text{O}_4$ - $(1-x)\text{Bi}_0.9\text{La}_0.1\text{FeO}_3$ (with $x=0.1, 0.2, 0.3$ and 0.4) nanocomposites by sol-gel method and calcined at different temperature. XRD analysis of powder calcined at 700 OC shows the formation of composite phases. Particle size was found to be around 90 nm by TEM. Coercivity, saturation magnetizations were found to increase with increase in the concentration of ferrite content and pinning effect was observed in some samples. Variation of dielectric loss with temperature shows the conducting behavior of composite beyond 300 OC, which may be due to thermally activated process. Variation of dielectric constant with temperature shows transition peak around 394 OC for $x=0.1$. The peak was found to be shifted to higher temperature with increase in concentration of ferrite phase. Magnetocapacitance was also observed in the prepared composites which may be the sign of magnetoelectric coupling in the synthesized composites at room temperature. Furthermore magnetocapacitance were found to decrease with increase in the concentration of ferrite phase in $\text{Bi}_0.9\text{La}_0.1\text{FeO}_3$. Results will be discussed in details at the time of presentation.

11:30 AM

(EMA-S2-024-2012) Effect of annealing atmosphere on the structural and electrical properties of the $(\text{Na}_{0.5}\text{K}_{0.5})\text{NbO}_3$ thin film

B. Kim*, T. Seong, I. Seo, M. Jang, S. Nahm, Korea University, Republic of Korea

An amorphous $(\text{Na}_{0.5}\text{K}_{0.5})\text{NbO}_3$ (NKN) phase was formed for a film grown at 300°C. A crystalline NKN phase was developed in the films annealed at 800°C for 30 min under air atmosphere. However, the $\text{K}_{5.75}\text{Nb}_{10.85}\text{O}_{30}$ (KN) second phase was also observed in this film, probably due to the evaporation of Na_2O . The NKN film without the second phase was well formed when it was annealed at 800°C under NKN atmosphere. Moreover, this NKN film exhibited the good electric and dielectric properties: a high dielectric constant of 616.5 with a dissipation factor of 3 % at 100 kHz, a low leakage current density of 2.0×10^{-10} A/cm² at 0.16 MV/cm, and the high P_r values of 11.74 $\mu\text{C}/\text{cm}^2$. In this work, the effect of annealing atmosphere on formation of the NKN films will be discussed in detail and the piezoelectric properties of NKN films also presented.

11:45 AM

(EMA-S2-025-2012) $\text{BaZrxTi}_{1-x}\text{O}_3$ relaxors: self-assembled nanocomposite

T. Maiti*, Indian Institute of Technology Kanpur, India; R. Guo, A. S. Bhalla, The University of Texas at San Antonio, USA

In this paper the mechanism & nature of relaxor ferroelectric behavior in the environmental friendly lead free Barium Zirconate Titanate (BZT) system has been reported. A revised complete phase diagram of $\text{Ba}(\text{ZrxTi}_{1-x})\text{O}_3$, with compositions $0.00 \leq x \leq 1.00$ has been developed based on their crystallographic, dielectric, and ferroelectric properties. It has been shown that BZT system depending on the composition, successively depicts the properties extending from simple dielectric (pure BaZrO_3) to polar cluster dielectric, relaxor ferroelectric, 2nd order like diffuse phase transition, ferroelectric with pinched phase transitions & then to a proper ferroelectric (pure BaTiO_3). BZT relaxor compositions have been characterized

by measurement of their dielectric (under bias), pyroelectric, & thermal expansion properties in a wide range of temperatures. The structure of the BZT compositions has been evaluated by X-ray & neutron diffraction studies. Their local structure has been also probed by micro-Raman spectra. Two different kinds of relaxor behaviors are observed in the BZT system: one dominated by polar Ti-rich regions & another by non-polar Zr-rich regions. Finally BZT has been considered as an engineered material in which the self-assembled polar nano-regions exhibit some unusual properties, hard to be predicted from its constituents BT and BZ. In this context the BZT relaxors have been considered as self-assembled nanocomposite.

S4: Advanced Energy Storage Materials and Systems: Lithium and Beyond

Novel Electrode Architecture, Assembly and Design for Advanced Batteries

Room: Coral B

Session Chairs: Nancy Dudney, Oak Ridge National Laboratory; Jeff Sakamoto, Michigan State University

9:30 AM

(EMA-S4-012-2012) Design and Fabrication of 3D Electrodes and Battery Architectures (Invited)

N. Cirigliano, E. Perre, B. Dunn*, UCLA, USA

Three-dimensional battery architectures offer original solutions to powering modern-day portable electronics. The defining characteristic of 3D battery designs is that transport between electrodes remains one-dimensional (or nearly so) at the microscopic level, while the electrodes are configured in non-planar geometries. The design rules developed for 3D battery architectures indicate that it is possible to achieve both high energy density and high power density within a small footprint area. These properties are particularly important for integrated microsystems where the available area for the power source is limited to millimeter dimensions. The present paper reviews recent advances in the development of 3D microbatteries which are based on using periodic electrode arrays. Methods for fabricating the positive and negative electrodes have been demonstrated. 3D carbon arrays are fabricated by combining silicon micromachining with colloidal processing while LiCoO₂ electrodes are prepared through sedimentation of a colloidal solution between the rods of the array. In half-cell experiments, lithium cycles reversibly at rates of C/5 or higher with areal energy densities in the range of 5 mAh/cm². The results presented here illustrate both the advantages offered by 3D architectures as well as the challenges facing this technology.

10:00 AM

(EMA-S4-013-2012) Carbon-Containing Nanocomposite Materials for Energy Storage (Invited)

G. Yushin*, Georgia Institute of Technology, USA

High power energy storage devices, such as supercapacitors and Li-ion batteries, are critical for the development of zero-emission electrical vehicles, large scale smart grid, and energy efficient cargo ships and locomotives. The energy storage characteristics of supercapacitors and Li-ion batteries are mostly determined by the specific capacities of their electrodes, while their power characteristics are influenced by the maximum rate of the ion transport. The talk will focus on the development of nanocomposite electrodes capable to improve both the energy and power storage characteristics of the state of the art devices. Advanced ultra-high surface area carbons, carbon-polymer, and carbon-metal oxide nanocomposites have been demonstrated to greatly exceed the specific capacitance of traditional electrodes for supercapacitors. Rationally designed Si-C composites showed up to 8 times higher specific capacity than graphite, the con-

ventional anode material in Li-ion batteries, and stable performance for over 1000 cycles. In order to overcome the limitations of traditional composites precise control over the materials' structure and porosity at the nanoscale was required.

10:15 AM

(EMA-S4-014-2012) Lead-Carbon Hybrid Ultracapacitors and their Applications (Invited)

A. K. Shukla*, Indian Institute of Science, India

Most ultracapacitors rely on carbon-based structures utilizing non-faradaic electrochemical-double-layer capacitance for charge storage. By contrast, pseudo-capacitive ultracapacitors are based on charge storage brought about by faradaic charge-transfer through surface adsorbed species. In the taxonomy of ultracapacitors, an ultracapacitor employing a non-faradaic double-layer electrode and a faradaic battery-type electrode is referred to as battery-type hybrid ultracapacitor (HUC). HUCs are attractive as these could overarch the pulse power characteristic of an electrical-double-layer ultracapacitor and the sustained energy characteristic of a battery. Accordingly, charge-storage mechanism in a hybrid ultracapacitor combines the mechanism of energy storage in a battery and a double-layer ultracapacitor. These HUCs have the benefits of both the batteries and ultracapacitors, namely the high energy density of batteries and high power density with high cycle-life of ultracapacitors. Keeping the technology need, availability and cost, lead-carbon ultracapacitors are set to play a seminal role in future energy storage and management. Prismatic 12 V Lead-carbon hybrid ultracapacitors (Pb-C HUCs) with flooded, adsorbent-glass-mat (AGM) and silica-gelled sulphuric acid electrolyte are designed, developed and performance tested. Some possible applications of these HUCs will be highlighted.

10:45 AM

(EMA-S4-015-2012) Fe based fluoride nanocomposite cathode for lithium rechargeable batteries (Invited)

K. Kang*, Seoul National University, Republic of Korea

We report the fabrication of a new hierarchical nanostructure composed of FeF₃ nanoparticles and carbon nanotubes (CNTs), and its superior electrochemical properties in Li rechargeable batteries. The nanostructure fabricated by functionalizing CNT has a unique morphology, which has the appearance of FeF₃ nanoflowers on CNT branches. The heterogeneous nucleation of FeF₃ on CNT ensures intimate contact between the active material and the conductive agent as well as fast electron transport along the CNT. The nanowires provide a three-dimensional electronic path, which allows faster charge transport. Moreover, it also ensures the structural stability of the electrode during cycling. In the second part of the talk, we will discuss on the possibility of Li-free cathode material including FeF₃ in a lithium ion batteries. A conventional lithium ion cell is composed of a lithium-containing cathode and a lithium-free anode. Because the early lithium batteries that used elemental lithium as a negative electrode caused safety concerns, the shuttlecock battery used a cathode as a lithium source. Although several lithium-free materials have showed excellent electrochemical performance, they have not been practical for application in lithium-ion batteries due to this reason. Here, we will suggest a novel strategy to use lithium-free transition metal ionic compounds as a cathode for lithium-ion batteries.

11:15 AM

(EMA-S4-016-2012) Metal Free, Binder Free Silicon- Carbon Fiber Composite Anode Architecture

S. K. Marthia*, J. Nanda, R. R. Unocic, W. D. Porter, N. J. Dudney, Oak Ridge National Laboratory, USA

We report a silicon-carbon (Si-C) nano-composite material supported on carbon fiber (CF) network as a high performance anode for rechargeable lithium-ion batteries. Highly conductive CFs of 5-7 μm in diameter have been used to replace a conventional copper

(Cu) foil current collector. We demonstrate that the carbonized mesophase pitch performs the role of a conducting binder between the CFs and amorphous silicon nano-powders. The usual organic binder and current collector can be replaced by the high temperature binder of carbonized mesophase pitch and CFs, respectively. Together these replacements increase the specific energy density and capacity per unit area of the electrode. The carbonized mesophase pitch makes uniform continuous layer of 5-10 nm thick coating along the surface of the nano silicon powders. Stable capacities up to 800-1200 mAh/g can be achieved at 5C-1C charge-discharge rates for several hundreds of cycles with minor loss in capacity. The stable electrochemical performance is likely due to the formation of a uniform coating of mesopitch amorphous carbon around the Si particles and strong adhesion to the highly conductive carbon nano-fiber matrix. The microstructural mechanisms of alloying and subsequent amorphization of the Si-C composite anode were characterized by several surface sensitive techniques and thermal stability at different SoCs by Differential Scanning Calorimetry.

11:30 AM

(EMA-S4-017-2012) Three-dimensional Bicontinuous Composite Electrodes for High Power and Energy Density Batteries

H. G. Zhang*, P. V. Braun, University of Illinois at Urbana-Champaign, USA

High power and energy density has been long sought-out features of electrical energy storage devices. However, there are two huge challenges for high power and energy batteries. Rapid charge and discharge rates lead to dramatic capacity reductions in most rechargeable batteries. High energy density batteries entail a huge lithium storage capability which causes large volume change in electrodes and then a capacity decay during cycling. A storage technology that increases the power and energy density of batteries would revolutionize portable and distributed power. We demonstrate 3D bicontinuous electrodes which could either reduce the transport resistance at rapid charge and discharge or accommodate the volume change. The well-engineered 3D composite electrode enables charge and discharge rates of up to 400C and 1,000C for lithium-ion and nickel-metal hydride chemistries, respectively, with minimal capacity loss using a three dimensional bicontinuous nanoarchitecture consisting of an electrolytically active material sandwiched between rapid ion and electron transport pathways. The inert metal network could also accommodate the volume change. A thin silicon/3D scaffold composite electrode demonstrates high capacity retention of 85% after 100 cycles. The 3D bicontinuous electrode approach presented here is quite general, and is applicable to many battery chemistries.

11:45 AM

(EMA-S4-018-2012) High Capacity Prismatic Li-Ion Cell Alloy Anodes for Electric Vehicle Applications (Invited)

S. Lopatin*, R. Bachrach, D. Brevnov, S. Thirupapuliyur, K. Chen, L. Chen, Applied Materials, USA

A transformation of Li-ion battery volume manufacturing technology is necessary to enable large scale commercialization of electric vehicles. Key parameters include cycle life (300-1000 cycles at 80% depth of discharge), calendar life (5-10 years), and durable cell design capable of being affordably mass produced. The battery cost per kWh needs to be reduced while the energy density needs to increase. The purpose of this work is to develop high capacity anodes that are capable of achieving an energy density of at least 500 Wh/l and a power density of at least 500 W/l. The experimental work has developed electrodes with embedded active material in an inactive and conductive matrix of 3D current collector. The approach uses micro-cell porous Cu as the host structure for Li alloy electrodes. To overcome the large irreversible capacity loss in Si and Sn, we explored various electrochemical pre-lithiation processes, minor alloy compositions, and their effects on grain size. This approach produced nano-dimensional active material and enhanced the volumetric use efficiency.

The resultant Si-Sn composite material showed measured capacity in the range of 900 - 1400 mAh/g. In conclusion, we have demonstrated the feasibility of high-capacity alloy anodes using high rate deposition suitable for the micro-cell porous 3D Cu-Li alloy architecture.

S7: Metamaterials and Microwave Materials

Microwave Composites and Metamaterials

Room: Pacific

Session Chair: Paul Clem, Sandia National Laboratories

9:30 AM

(EMA-S7-001-2012) Engineering of High-K, High-Q Microwave Dielectrics

D. Suvorov*, B. Jančar, Jozef Stefan Institute, Slovenia

The development of a microwave dielectric material that would exhibit combination of a high dielectric constant and a high quality factor has been baffling the dielectric research community for decades. Most widespread ceramic microwave resonators with temperature stable resonant frequency are based on either complex perovskites with B-site cation ordering that exhibit very high quality factors ($Q_{xf} > 100000$ GHz) and dielectric constant of $K \approx 30$, or on tungsten-bronze-type 114 solid solutions that exhibit K from 70 to 90 with Q_{xf} values ≤ 11000 GHz. A successful compromise between the two groups of materials is represented by $\text{CaTiO}_3 - \text{REAlO}_3$ ($\text{RE} = \text{La}, \text{Nd}$) perovskite ceramics that combine a relatively high $K > 40$ and a high $Q_{xf} > 40000$ GHz. Recently a new demand for miniaturization has emerged which presents a need for a material that would exhibit K of at least 64 and Q_{xf} above 15000 GHz with a temperature coefficient of resonant frequency within ± 10 ppm/K. The closest of the known materials to the required combination of properties are solid solutions based on incipient ferroelectric perovskites CaTiO_3 and SrTiO_3 . Unfortunately, however, the temperature coefficient of compositions with K above 50, is far too high for most applications. In the contribution our approach towards such a material, based on two-phase ceramics with compositions in the vicinity of $\text{Ba}_6-3x(\text{Sm},\text{Nd})_8+2x\text{Ti}_{18}\text{O}_{54}$ will be presented.

9:45 AM

(EMA-S7-002-2012) Dependence of Microwave Dielectric Properties on Structural Characteristics of AB_2O_6 (A = Ni, Mg, Zn, and B = Nb, Ta) Ceramics

E. Kim*, C. Jeon, Kyonggi University, Republic of Korea

Relationships between crystal structures and dielectric properties of AB_2O_6 (A = Ni, Mg, Zn, and B = Nb, Ta) ceramics were investigated at microwave frequencies. A single phase with the orthorhombic columbite structure and/or the tetragonal tri-rutile structure was detected for ANb_2O_6 (A = Ni, Mg, Zn) and/or ATa_2O_6 (A = Ni, Mg), respectively. However, ZnTa_2O_6 showed a single phase with the orthorhombic $\text{Tri-}\alpha\text{PbO}_2$ structure. With increasing A-site ionic size (Ni = 0.69Å, Mg = 0.72Å, Zn = 0.74Å) at coordination number of 6, the oxygen octahedral distortion of the specimens increased, which induced the decrease of temperature coefficient of resonant frequency (TCF) of the specimens. The ATa_2O_6 specimens showed higher dielectric constant (K) and lower quality factor (Qf) than the ANb_2O_6 specimens. These results could be attributed to the dielectric polarizabilities, bond valence between octahedral cation and oxygen ion, and sharing area between oxygen octahedra.

10:00 AM

(EMA-S7-003-2012) Flexible Polymer/Ferrite Composites for High Frequency Applications

L. Qin*, K. Shqau, H. Verweij, Ohio State University, USA

Z-type hexagonal ferrites with strong magnetocrystalline anisotropy are considered for applications at microwave frequencies. In particular, $\text{Ba}_3\text{Co}_2\text{Fe}_{24}\text{O}_{41}$ (Co_2Z) is expected to exhibit a high permeability and low loss at frequencies > 1 GHz. On the other hand, polydi-

methylsiloxane (PDMS) is considered to be one of the most widely used elastomer-ic polymers with inert nature. In the present work, we report the fabrication of Co_2Z in PDMS matrix with various volume ratios of PDMS: Co_2Z =10:1, 5:1, 2:1, 1:1, 1:2 and 1:5, respectively. Pure-phase Co_2Z was fabricated from precursor powders made by a modified-Pechini route and calcination at 1300°C, 1310°C or 1330°C. The uniform Co_2Z particles were dispersed in PDMS with steric stabilizers. Highly orientated single-crystalline ferrite particles along the easy axis (c-axis) are obtained by the application of a magnetic field during cross-linking. The magnetically oriented PDMS/ Co_2Z composites exhibit good flexibility and high permeability at microwave frequencies.

10:15 AM

(EMA-S7-004-2012) Electrical and Structural Properties of $\text{Ba}(\text{Y,Sb})_{0.05}\text{Ti}_{0.90}\text{O}_3$, a Dipole-like B-Site Substituted Material, Characterized as Functions of Temperature and Frequency

J. Morales*, T. Mion, University of Texas - Pan American, USA; D. Potrepka, F. Crowne, U.S. Army Research Laboratory, USA; A. Tauber, Geo-Centers, Inc. (retired), USA; S. Tidrow, University of Texas - Pan American, USA

An Army Research Laboratory engineered, microwave perovskite ceramic based upon B-site dipole-like substituted barium-titanate is characterized as a function of temperature and frequency. The temperature dependent dielectric constant, tunability, dissipation factor and material figure of merit for $\text{Ba}(\text{Y,Sb})_{0.05}\text{Ti}_{0.90}\text{O}_3$ are discussed. Electrical properties of $\text{Ba}(\text{Y,Sb})_{0.05}\text{Ti}_{0.90}\text{O}_3$ are discussed in terms of structural changes as a function of temperature using x-ray diffraction analysis. Scanning electron microscopy and Rietveld refinements of the ceramics provide a qualitative study of the material. *This material is based upon work supported by, or in part by, the U.S. Army Research Laboratory and the U.S. Army Research Office under contract/grant number W911NF-08-1-0353.*

10:30 AM

(EMA-S7-005-2012) Dielectric and X-Ray Diffraction Analysis of $\text{Ba}(\text{Lu,Ta})_{0.05}\text{Ti}_{0.90}\text{O}_3$

T. Mion*, M. Rivas, University of Texas - Pan American, USA; D. Potrepka, F. Crowne, U.S. Army Research Laboratory, USA; A. Tauber, Geo-Centers, Inc. (retired), USA; S. Tidrow, University of Texas - Pan American, USA

$\text{Ba}(\text{Lu,Ta})_{0.05}\text{Ti}_{0.90}\text{O}_3$ is investigated for its dielectric constant, tunability, dissipation factor and figure of merit of the material over the temperature range -50°C to 125°C and frequency range, 10 Hz to 2 MHz. SEM images and XRD with Rietveld refinement performed over a broad temperature range are utilized to comparatively analyze the electrical and structural properties for usefulness within the military specified temperature range. *This material is based upon work supported by, or in part by, the U.S. Army Research Laboratory and the U.S. Army Research Office under contract/grant number W911NF-08-1-0353.*

10:45 AM

(EMA-S7-006-2012) Structural Investigation of $\text{Ba}(\text{Yb,Ta})_{0.05}\text{Ti}_{0.90}\text{O}_3$ Grain Size Using SEM, XRD

T. Mion*, M. Rivas, University of Texas - Pan American, USA; D. Potrepka, F. Crowne, U.S. Army Research Laboratory, USA; A. Tauber, Geo-Centers, Inc. (retired), USA; S. Tidrow, University of Texas - Pan American, USA

Using a Zeiss SEM, we investigated the average grain size of $\text{Ba}(\text{Yb,Ta})_{0.05}\text{Ti}_{0.90}\text{O}_3$ and verified the findings through x-ray diffraction using a Bruker XRD with a 2D HISTAR. This material's electrical properties were compared to others of similar nature over a temperature range -50°C to 125°C and frequency range, 10 Hz to 2 MHz. Phase transition temperatures for $\text{Ba}(\text{Yb,Ta})_{0.05}\text{Ti}_{0.90}\text{O}_3$ are reported and compared to those for BaTiO_3 . *This material is based upon work supported by, or in part by, the U.S. Army Research Laboratory and the U.S. Army Research Office under contract/grant number W911NF-08-1-0353.*

11:00 AM

(EMA-S7-007-2012) Microwave dielectric metamaterials: influence of dielectric loss and permittivity variation on metamaterial performance

P. Clem*, M. P. Rye, Sandia National Laboratories, USA; E. Kim, C. Jeon, Kyonggi University, Republic of Korea

As an alternative to metal-based metamaterials, magnetodielectric metamaterials have recently been developed using resonant dielectric spheres and cubes of high permittivity microwave ceramics. Conventional approaches for obtaining metamaterial properties ($\pm\epsilon$, $\pm\mu$) are based on orientation-dependent, lossy metallic structures, such as split ring resonator/wire pairs, fishnet- and omega-shaped structures. This alternative dielectric route, via Mie resonances of magnetodielectric structures, provides a mechanism for engineered electrical and magnetic response. In this presentation, experimental results will be presented demonstrating an approach for achieving an isotropic, double negative (DNG) metamaterial composite at Ku band frequencies. In particular, the influence of microwave ceramic resonator properties, including Q, permittivity variation, ceramic microstructure, and dimensional tolerances will be discussed. Microwave ceramic properties and metamaterials comprised of MgTiO_3 , $(\text{Zr,Sn,Ti})\text{O}_2$, and SrTiO_3 will be presented. It is observed that resonator Q tracks closely with dielectric Q, and that low Q materials may prevent useful metamaterial development.

11:15 AM

(EMA-S7-008-2012) Design and Comprehensive Study of Compact LH Metamaterials CSRR and CSSR-Based BPWG Filter

E. K. Hamad*, H. A. Atallah, Faculty of Engineering, Egypt

In this paper, a compact band pass waveguide metamaterial filter based on complementary split ring resonator (CSRR) and complementary split square resonators (CSSR) are presented for metamaterial flat lens designs and beam focusing applications. The presented waveguide filter combines a conventional band pass filter characteristics and negative refractive index (NRI) metamaterial characteristics. The left handed metamaterial (LHM) is made of CSRR and CSSR, etched on the ground plane. The effects of varying the geometry of CSRR and CSSR with such resonant elements are analyzed. In addition the effective parameters of the CSRR unit cell are extracted using robust retrieval algorithm to verify the LHM characteristics. The CSRRs can be tuned to pass the signals at slightly different frequencies and thus, give rise to a pass band with a certain bandwidth, which can to some extent be controlled with the geometrical parameters. The frequency characteristics of the proposed filter are successfully optimized using numerical experimentation techniques. The important size reduction achieved with the use of CSRR, which is obviously very convenient. The results show that the compactness is achieved by using CSRR compared to use CSSR. Simulations results based on a 3D full-wave electromagnetic simulator based on the finite element method are presented in the paper.

S8 Highlights of Student Research in Basic Science and Electronic Ceramics

Future of Ceramics II

Room: Pacific

Session Chair: Elena Aksel, University of Florida

12:15 PM

(EMA-S8-004-2012) Development and Implementation of a Polarization and Strain Measurement System

C. Llano*, E. Aksel, S. Banavara Seshadri, J. Forrester, J. Jones, University of Florida, USA

In this project, we have developed a device that can accurately measure the polarization and strain of piezoelectric materials at

various electric fields and frequencies. Polarization is the electric displacement of a material to an applied electric field, while strain is the physical displacement. These properties provide insight into many of the structure-property relationships of a material. An apparatus that can accurately measure these properties within a laboratory environment has been implemented and calibrated using a variety of standard piezoelectric materials that have been measured using other established set-ups. A linear voltage displacement transducer (LVDT) been implemented and calibrated in order to accurately measure the polarization and strain of a material, while simultaneously applying an electric field. The LVDT has been used to measure different piezoelectric samples both Lead (Pb)-based and Lead (Pb)-free such as Lead Zirconate Titanate (PZT) and Sodium Bismuth Titanate- Barium Titanate (NBT-BT), respectively. By analyzing the data measurements for both types of piezoelectrics, we can display specific piezoelectric properties such as coercive field and remnant polarization. The LVDT has given great insight into the characteristics of the in-demand piezoelectric materials in use today and in the future use of the materials science world.

12:30 PM

(EMA-S8-005-2012) Optimizing Flux Pinning of YBCO Superconductor with Mixed Phase Nanoparticle Additions

M. Sebastian*, J. N. Reichart, M. M. Ratcliff, AFRL, USA; J. Burke, University of Dayton Research Institute, USA; T. Haugan, AFRL, USA

Adding nanophase defects to YBa₂Cu₃O₇ (YBCO) superconductor thin films is well-known to enhance flux pinning, resulting in an increase in current densities (J_c). Previously, most studies have focused on the addition of single-phase addition; however the addition of several phases simultaneously has shown strong improvements by combining different flux pinning mechanisms. This paper further explores the effect of mixed phase nanoparticle pinning, with the addition of insulating, nonreactive phases of BaSnO₃ and Y₂O₃. Processing parameters varied the volume % of BaSnO₃ and deposition temperature of films prepared by pulsed laser deposition on LaAlO₃ and SiTiO₃ substrates. The addition of Y₂O₃ = 3 volume % was constant. Results of comparisons of flux pinning, current densities, critical temperatures, and microstructures will be presented. This work supported by: AFRL Propulsion Directorate and the Air Force Office of Scientific Research (AFOSR)

12:45 PM

(EMA-S8-006-2012) Effects of Surface Step on Oxygen Distribution and Silicon Oxidation State Transformation on Si (001)

M. A. Pamungkas*, B. Kim, K. Lee, Korea Institute of Science and Technology, Republic of Korea

Effects of surface step on initial oxidation of Si(001) were investigated in atomic scale by molecular dynamic simulation. A reactive force field was used for the simulation owing to its capability in describing charge transfer as well as breaking and forming chemical bonds involved in oxidation process. Oxidation process in flat Si(001) surface is compared with that in Si(001) surface contains SA step edge (SA surface) and with that in the surface contains SB step edge (SB surface). SB surface can adsorb oxygen molecules more than other surfaces. Oxygen atom distribution and silicon oxidation state transformation profile in SA and SB are similar. Silicon oxidation transformation in flat surface is much faster than that in other two surfaces even though number oxygen uptake in flat surface is less than others. In order to know the origin of those phenomena, sticking coefficient of SA surface and SB surface are calculated by statistically 1000 times deposition of one oxygen molecule with different initial position and orientation. In addition probability of oxygen atom to migrate from lower terrace to upper terrace and vice versa is also investigated.

S2: Advanced Dielectric, Piezoelectric and Ferroic Materials, and Emerging Materials in Electronics

Pervoskite Dielectric, Mott Insulators, Ferroelectric and Piezoelectric Materials

Room: Indian

Session Chairs: Steve Dai, Sandia National Labs; Akansha Dwivedi, IIT-Mandi

1:30 PM

(EMA-S2-026-2012) Temperature Stability in High Temperature Capacitor BaTiO₃ – Bi(Zn_{1/2}Ti_{1/2})O₃ Based Solid Solutions

N. Raengthon*, D. P. Cann, Oregon State University, USA

Degradation of dielectric properties and insulation resistance limits the usage of ceramic capacitor materials at high temperatures. In the search for new materials for high temperature capacitor applications, a high dielectric constant, high insulation resistance, and temperature stable dielectric properties are ideal. Solid solutions of BaTiO₃ – Bi(Zn_{1/2}Ti_{1/2})O₃ – BiMO₃, where M is Sc and In, have shown excellent properties for high temperature capacitor applications. The stable perovskite phase of xBaTiO₃ – (100-x)(0.5Bi(Zn_{1/2}Ti_{1/2})O₃ – 0.5BiMO₃) solid solutions where x = 50, 55, and 60 for BiScO₃ ternary compounds and x = 75 and 80 for BiInO₃ ternary compounds were investigated. A dielectric measurement showed that all compositions exhibited highly broad and diffuse phase transitions with permittivity of more than 1,000. The temperature coefficient of permittivity (TC_ε) of the BT-BZT-BS (BiScO₃) ternary compounds were found on the order of -230 to -470 ppm/°C. By introducing Ba vacancies to the compounds, the temperature coefficient of permittivity were minimized to -182 ppm/°C. At high temperatures, T = 335 °C, a low dielectric loss of 0.007, a high resistivity of 4.1 GΩ-cm, and a large RC time constant of 0.44 seconds was observed for Ba-deficient BT-BZT-BS compounds. These materials are highly suitable for use in high temperature capacitor applications.

1:45 PM

(EMA-S2-027-2012) Ca(Zr,Ti)O₃ Ceramics for Energy Storage Applications

S. Dai*, B. A. Hernandez-Sanchez, T. Garino, P. Lu, N. Bell, J. Wheller, D. L. Moore, B. A. Tuttle, Sandia National Labs, USA

Development of high-energy density dielectrics with low temperature coefficients of capacitance that are integratable with underlying electronics are needed for extreme environment, defense and automotive applications. The presentation will emphasize sintering of Ca(Zr_{0.9}Ti_{0.1})O₃ ceramics from chemically synthesized powders in three forms: pellets, constrained single and multilayers on Al₂O₃ substrates, and free-standing single and multilayer structures. The dielectric properties, including dielectric constant, dielectric loss, electrical breakdown and temperature stability, will be reported. An array of microstructural analysis techniques provided insight as to the densification mechanisms of the chemically prepared Ca(Zr_{0.9}Ti_{0.1})O₃ ceramics. Sandia National Laboratories is a multi-program laboratory managed and operated by Sandia Corporation, a wholly owned subsidiary of Lockheed Martin Corporation, for the U.S. Department of Energy's National Nuclear Security Administration under contract DE-AC04-94AL85000.

2:00 PM

(EMA-S2-028-2012) High energy density (0.65+y)Pb(Zr_{0.47}Ti_{0.53})O₃- (0.35-y)Pb[(Ni_{1-x}Zn_x)_{1/3}Nb_{2/3}]O₃ceramics for energy harvesting devices

S. Nahm*, I. Seo, Y. Cha, I. Kang, J. Choi, Korea University, Republic of Korea

(0.65+y)Pb(Zr_{0.47}Ti_{0.53})O₃- (0.35-y)Pb[(Ni_{1-x}Zn_x)_{1/3}Nb_{2/3}]O₃ ceramics have an MPB of Rhombohedral and tetragonal structures. Their

e_{33}^T/e_0 value considerably decreased on the Rhombohedral side of the MPB composition, but the d_{33} and k_p slowly decreased on both sides of the MPB. Therefore, the maximum transduction coefficient ($d_{33}^*g_{33}$) was obtained from the composition on the Rhombohedral side of the MPB, because g_{33} is given by d_{33}/e_{33}^T . This result could be applied to other systems containing an MPB of Rhombohedral and tetragonal structures. Furthermore, a $d_{33}^*g_{33}$ value of $20,056 \times 10^{-15}$ m²/N, which is the highest value reported so far for polycrystalline ceramics, was obtained from the 0.68Pb(Zr_{0.47}Ti_{0.53})O₃-0.32Pb(Ni_{0.6}Zn_{0.4})/1/3Nb₂/3O₃ ceramic.

2:15 PM

(EMA-S2-029-2012) Electrical Properties of Bismuth Zinc Niobate Pyrochlore Relaxor

R. Osman, University Malaysia Perlis, Malaysia; N. Masó, A. R. West*, University of Sheffield, United Kingdom

Bismuth Zinc Niobate (BZN) pyrochlore exhibits frequency- and temperature-dependent permittivity and tan δ data, which are typical of relaxor materials. Such data are traditionally analysed as temperature sweeps of fixed frequency data. We show here that frequency sweeps at fixed temperature provide an alternative presentational approach which allows fitting of the data to possible equivalent circuits and then, the extraction of meaningful circuit parameters. An essential element in fitting such data is the frequency dependent admittance or Constant Phase Element, which is responsible entirely for the observed relaxor response. The significance of the various elements in the equivalent circuit including the variable admittances, will be discussed.

2:30 PM

(EMA-S2-030-2012) Piezoelectric Properties of High Temperature Ternary Perovskite Ceramics

T. Ansell*, J. Nikkel, D. Cann, Oregon State University, USA

Lead based piezoelectric ceramics continue to dominate the field of high temperature materials applications. Lead zirconate titanate (PZT) has dominated this field in the past, however, the transition temperature, and thus the maximum operating temperature of PZT is too low for emerging electronic ceramic requirements. Lead based ternary perovskites show promise as a material system with higher transition temperature and higher operating temperatures. Two such ternary systems include solid solutions of PbTiO₃-BiScO₃-Bi(X_{1/2}Ti_{1/2})O₃, where X stands for either Mg or Ni. The morphotropic phase boundary (MPB) of PT-BS-BMgT covers a range of 46 – 50 mol% PT content and for PT-BS-BNiT is found within the range of 50 – 60 mol% PT content. Both BMgT and BNiT systems have compositions close to the MPB with high relative permittivity and structural phase changes at temperatures of 450°C and 350°C respectively. The BNiT system is very promising for capacitor applications due to its low dielectric loss. Samples of BMgT with Ag co-fired electrodes were poled at fields up to 60 kV/cm² up to a temperature of 100°C. Excellent piezoelectric properties were recorded with a $d_{33} = 170$ pC/N and $QM = 0.65$.

3:15 PM

(EMA-S2-031-2012) Flexible Energy Harvesters Based on Laser Transferred Piezoelectric Micro-Ribbons (Invited)

S. Yoon*, H. Song, Y. Do, C. Kang, Korea Institute of Science & Technology, Republic of Korea

Recently, energy harvesting from ambient mechanical energy such as human motions, automobile vibrations, building vibrations and etc. have been much attention for powering nano/micro devices and mobile electronics. Especially, piezoelectric nano generator based on ZnO nano-wires has been intensively studied in recent several years. However, the ZnO nano-wire has very low piezoelectric properties comparing to conventional Pb-based piezoelectric materials. Therefore, it may be inappropriate to mechanical energy harvesting. Pb-based piezoelectric materials have high piezoelectric properties are generally hard to be made to nano-wires structure on flexible substrates due to their complex composition and

high annealing temperature. In this study, to produce a high performance flexible energy harvester we choose a noble laser lift-off and transfer process. High property piezoelectric thick film ribbons of 0.01Pb(Mg_{1/2}W_{1/2})O₃-0.41Pb(Ni_{1/3}Nb_{2/3})O₃-0.35PbTiO₃-0.23PbZrO₃ composition were deposited on sapphire substrate and then transferred to plastic substrate by the laser lift off process. An interdigitated electrode was formed on piezoelectric ribbons and poled in a vertical direction of bending motions. Energy generation properties were measured by bending the flexible generator.

3:45 PM

(EMA-S2-032-2012) Enhancement of the Electromechanical and Electrocaloric Effects Near the Critical Point in Relaxor Ceramics

Z. Kutnjak*, B. Rozic, Jozef Stefan Institute, Slovenia; B. Malič, H. Uršič, J. Holc, M. Kosec, Jozef Stefan Institute, Slovenia; R. Pirc, Jozef Stefan Institute, Slovenia; Q. M. Zhang, The Pennsylvania State University, USA

Electromechanical (EM) and electrocaloric effects (ECE) have attracted considerable attention in recent years due to their potential application in a new generation of actuators and heating/cooling devices, respectively. Until recently the ECE effect did not attract extreme attention, however, this situation changed dramatically with the indirect measurements of a giant electrocaloric effect in inorganic PZT thin film and P(VDF-TrFE)-type ferroelectric polymers [1,2]. A review of recent direct measurements of the giant ECE in solid and soft ferroelectric materials including thick and thin films of PMN, PMN-PT, PLZT ceramics, and P(VDF-TrFE)-based polymers will be given. It was found that the giant ECE is common in these systems. The effective ECE responsiveness $\Delta T/E$ exhibits a maximum in the vicinity of the liquid-vapour type critical point in bulk relaxor ferroelectrics [3,4]. The relevance of the critical point proximity for the enhancement of the giant ECE and giant EM responses [5] will be discussed. [1] A. S. Mischenko et al., Science 311, 1270 (2006). [2] B. Neese et al., Science 321, 821 (2008). [3] R. Pirc, Z. Kutnjak, R. Blinc, Q.M. Zhang, Appl. Phys. Lett. 98, 021909 (2011). [4] S.-G. Lu, B. Rozic, Q. M. Zhang, Z. Kutnjak, B. Malic, M. Kosec, Appl. Phys. Lett. 97, 162904 (2010). [5] Z. Kutnjak et al, Nature 441, 956 (2006).

4:00 PM

(EMA-S2-033-2012) Influence of Magnesium and Yttrium Codoping on the Intrinsic Piezoelectric Property of BST Ceramics

J. Zhu*, Z. Xu, W. Zhang, G. Liu, D. Xiao, P. Yu, Sichuan University, China

Different amounts of Mn-Y codoped BST67/33 powders were prepared by citric acid method, and BST ceramics were synthesized using the powders. It is found that Mn-Y codoped BST ceramics show the enhanced dielectric, ferroelectric and piezoelectric properties. The intrinsic maximum piezoelectric coefficient γ_{max} of 0.3%Mn+1.0%Y mol% codoped BST ceramics is about 700 nC/cm².K at room temperature, this value of γ is larger than that of single Mn or Y doped BST ceramics. The maximum figure of merit of detectivity F_d of 0.3%Mn+1.0%Y mol% codoped BST ceramics is about 88×10^{-6} Pa^{-1/2}. However, the Mn-Y codoped BST67/33 ceramics possess the good piezoelectric properties at room temperature, the γ and F_d of Mn-Y codoped BST ceramics were not stable, and they changed greatly with the temperature changing in the vicinity of RT. A initial doping mechanism was also discussed.

4:15 PM

(EMA-S2-034-2012) Flux-assisted growth of BaTiO₃ thin films

D. T. Harris*, M. Burch, P. G. Lam, E. C. Dickey, J. Maria, North Carolina State University, USA

In this presentation we demonstrate that by incorporating a low melting temperature flux into BaTiO₃, we can enhance grain growth, crystallization, and the nonlinear dielectric properties important for devices like ferroelectric varactors. BaTiO₃ films with BaO-B₂O₃ flux were grown on c-sapphire using PLD from ceramic target compositions containing between 1% and 5% of the flux. Films were prepared

at room temperature, then annealed at temperatures above the flux melting temperature of 869 °C. TEM cross-section analysis, X-ray diffraction, and atomic force microscopy was used to verify grain size and to search for microstructural signatures resulting from flux incorporation. Average grain sizes of 0.3 μm were observed in samples grown with 5% flux, compared to < 0.1 μm for conventional material. At 5% flux incorporation, evidence for residual flux was not observed. Interdigitated capacitors were fabricated and tested electrically. Capacitance and polarization measurements reveal a dramatic enhancement of the nonlinear electromechanical response with flux incorporation, presumably associated with improved crystallinity and larger grain size. Capacitors with 5% flux exhibit nearly 5:1 permittivity tuning at 35 V applied to a 3 micron gap with losses below 1%. Hysteresis measurements reveal saturating loops with remanent polarization values of 8 μC/cm². Current efforts focus on in situ TEM during annealing and new tellurium-based fluxes.

4:30 PM

(EMA-S2-035-2012) Electrochemical Response of Pb(Zr,Ti)O₃ Thin Films

L. J. Small*, Rensselaer Polytechnic Institute, USA; C. Apblett, J. Ihlefeld, Sandia National Laboratories, USA; D. Duquette, Rensselaer Polytechnic Institute, USA

Despite extensive research on fundamental and device properties, very little is known about the electrochemistry of Pb(Zr,Ti)O₃. This study utilized cyclic voltammetry (CV) and X-ray photoelectron spectroscopy (XPS) to investigate the electrochemical response of PZT thin films in 1 N H₂SO₄. PZT films fabricated onto platinized silicon wafers were measured via a custom-built scanning droplet system. With a PZT film as the working electrode, cyclic voltammetry was utilized to characterize the system. A bimodal distribution of data was observed. In most cases, a CV typical of a PZT capacitor was observed; at some surface sites, the CVs recorded were characteristic of the Pt-H₂SO₄ system, suggesting the existence of discontinuities in the PZT film. More interestingly, at the defect sites an anomalous pair of peaks was observed at about 0.4 V vs. Ag/AgCl. These peaks are believed to be due to PbSO₄ formation. In the defect regions, XPS analysis revealed a shift in the Pb 4f₇ and 4f₅ peaks and the addition of a S2p peak, consistent with SO₄²⁻. No shifts in Zr or Ti were noted. For the non-defect areas, XPS spectra appear similar to those never contacted with acid. From these data, it is postulated that Pb-rich areas in PZT, (most likely from processing), are vulnerable to corrosion via PbSO₄ formation.

4:45 PM

(EMA-S2-036-2012) Electric-field-induced structural changes in 111-oriented domain-engineered tetragonal BaTiO₃

A. Pramanick*, K. An, A. D. Stoica, L. G. Clonts, A. A. Parizzi, D. Maierhafer, Oak Ridge National Laboratory, USA; D. Damjanovic, Swiss Federal Institute of Technology, Switzerland; J. L. Jones, University of Florida, USA; X. Wang, Oak Ridge National Laboratory, USA

Domain-engineering has proved to be an effective technique to enhance piezoelectric properties, reduce hysteresis and increase reliability of piezoelectric single crystals. The origins of enhanced electromechanical properties of domain-engineered ferroelectrics – crystallographic and/or microscopic- are not well understood, particularly under the usual operating conditions of high-frequency electric fields. Various hypothesis including monoclinic crystallographic distortions, domain wall broadening, and ferroelectric domain interactions, have been proposed; however direct structural evidence is lacking. In this study, we used a novel asynchronous in situ neutron diffraction method to elucidate the structural changes in a 111-oriented domain-engineered tetragonal BaTiO₃ single crystal during the application of square-wave ac electric fields with frequencies ranging from 1 Hz to 480 Hz. Extrinsic contributions to macroscopic electric-field-induced strains, evident from time-dependent changes in intensities of (444) and (448) diffraction peaks, are proposed to arise from

domain wall broadening effects. These structural insights are expected to be critical in designing of a new class of lead-free piezoelectric materials with highly enhanced electromechanical coefficients.

5:00 PM

(EMA-S2-037-2012) Thermodynamic Theory of Inter-Ferroelectric Transitions in Binary and Ternary Ferroelectric Solid Solutions

G. A. Rossetti*, A. A. Heitmann, University of Connecticut, USA

A phenomenological theory has been developed for binary and ternary ferroelectric solid solution systems based on the end member compounds barium titanate and lead titanate. Though topologically distinct, pseudo-binary composition-temperature phase diagrams of the shifting, pinching, and morphotropic types can all be described by a classical truncated Landau polynomial using a common parameterization scheme. Parameters that quantify the degrees of inclination and curvature of the inter-ferroelectric transition lines in the composition-temperature plane have been deduced. For morphotropic systems, the stability fields of the monoclinic M_A, M_B, and M_C phases have been determined by adding higher-order terms to the classical truncated Landau series. The morphotropic phase diagrams of pseudo-ternary systems have been constructed from the corresponding pseudo-binaries and ternary property maps have been computed. The theory provides analytical free energy functions for ferroelectric solid solution systems useful for constructing constitutive models, carrying out phase field simulations, and in developing thermodynamic theories utilizing results from first-principles computations as input data.

5:15 PM

(EMA-S2-038-2012) Unusual Phase Transition Behavior in Rhombohedral xBi(Mg_{1/2}Ti_{1/2})O₃-yBi(Zn_{1/2}Ti_{1/2})O₃-zPbTiO₃ Ternary Ferroelectric System

A. Dwivedi*, W. Qu, C. A. Randall, The Pennsylvania State University, USA

In the course of searching for high temperature piezoelectric materials for various applications in aerospace and automotive industries, continuous research has been going on BiMeO₃-PbTiO₃ based binary and ternary solid solutions. Some of the works performed on BiMeO₃-PbTiO₃ ternary systems have also reported high temperature relaxor ferroelectric behavior in these materials. In the present work, one such ternary system, which shows very high paraelectric to ferroelectric transition temperature ~640 °C has been investigated. Studies carried out on a perovskite structured rhombohedral 0.6(BiMg_{1/2}Ti_{1/2})O₃ -0.05Bi(Zn_{1/2}Ti_{1/2})O₃ -0.35PbTiO₃ ceramic quenched from temperatures below 1000°C show that the dielectric properties can be dramatically altered by the thermal history. The results demonstrate that the dielectric and electromechanical response, observed at room temperature, can be varied between normal to relaxor behavior by changing thermal quenching conditions. Microstructures of these different quenched samples as observed in TEM studies indicate that the underlying defect structures and their interaction with polarization in these systems may be responsible for this unusual behavior.

S3: Symposium on Thin Film Integration and Processing Science

Physical Vapor Deposition and Strain Engineering

Room: Pacific

Session Chair: Yu Hong Jeon, Oregon State Univ

1:30 PM

(EMA-S3-001-2012) Magnetron sputter deposition of biaxial aligned thin films (Invited)

D. Depla*, M. Saraiva, J. Lamas, Ghent University, Belgium

The paper looks for a simple explanation for the growth mechanism of biaxial aligned thin films. A straightforward analytical

model is proposed. The model starts from the gathered knowledge on the influence of the energy per arriving particle on the thin film texture and microstructure during magnetron sputter deposition. A Monte Carlo based particle trajectory code combined with the results from a published Molecular Dynamics simulation, enables to compare the ideas behind the analytical model with experiments. The influence of pressure, target-substrate distance on the in-plane alignment is studied for different materials. The model fits for a wide range of materials, ranging from metals (Cr), over oxides (MgO, YSZ) to nitrides (InN, TiN). Further evidence for the proposed model is given by a detailed study on the growth of Mg(M)O (M=Al, Cr, Ti, Y and Zr) biaxial aligned thin films. In this study, a second source is added to the set-up, a technique described as dual reactive magnetron sputtering. The addition of the second source increases the complexity of the growth, but by careful analysis, the obtained results showed to be consistent with the proposed model. The model can be further extended to YSZ, deposited now from two sources. The overall conclusion from this study is that the presented ideas have a solid foundation as they can be applied to different materials and experimental conditions.

2:00 PM

(EMA-S3-002-2012) Optimizing Nanophase Additions to YBCO Superconductor to Enhance Low Temperature Flux Pinning

T. J. Haugan*, M. A. Sebastian, J. N. Reichart, M. M. Ratcliff, B. T. Pierce, J. L. Burke, E. L. Brewster, The Air Force Research Laboratory, USA

The addition of nanophase defects to YBa₂Cu₃O_{7-z} (YBCO) superconductor thin films have been studied by many groups world-wide, to enhance flux pinning and increase critical current densities (J_c's). This paper studies and optimizes the addition of varying nanophase defects particularly for low temperature applications < 50 K. Defects studied include nanoparticles, nanorods, nanolayers, and RE substitution. Nanophase defects were incorporated by pulsed laser deposition of (M/YBCO)_N multilayer and (YBCO)_{1-x}M_x single-target films. Processing parameters were systematically studied, including substrate type, M phase volume %, deposition temperature, and also multilayer layer thickness parameters. Systematic comparisons show that each defect optimizes J_c for different regions of temperature (T), magnetic field (H), and orientation angle (θ) operation space; e.g. nanolayers of BaZrO₃ have the highest J_c(T<50K) for H//c > 0.5 T, and rare-earth=Eu substitution enhances J_c(77K) for H//ab < 0.5T. Results and comparisons of flux pinning for different regions of T, H and θ will be presented, and correlated with microstructure studies. This work supported by – AFRL Propulsion Directorate, and the Air Force Office Scientific Research (AFOSR)

2:15 PM

(EMA-S3-003-2012) Ion-Beam Assist Nano-Texturing of MgO Films (Invited)

V. Matias*, Los Alamos National Laboratory, USA

We present a method for growth of single-crystal-like films that does not utilize epitaxy on single crystal substrates. Ion-beam assisted deposition (IBAD) texturing is used to obtain biaxial crystalline alignment in a several nanometer thick film. The IBAD texturing process can be applied to arbitrary, but smooth substrates, including flexible metal tapes, glass sheets, and plastic foils. With IBAD texturing of MgO and subsequent homoepitaxial growth we have demonstrated an in-plane mosaic spread FWHM below 2° and out-of-plane alignment of less than 1°. The IBAD-aligned films can be utilized as templates for epitaxial growth of functional layers such as high-temperature superconductors that are used for superconductor wire. Associated with the IBAD process we have developed an R&D methodology for exploring new epitaxial materials and combinations thereof. The deposition system we use includes reel-to-reel tape transport for a linear transport of substrate materials through the deposition zones. This allows for high-throughput experimentation via a linear combinatorial experimental

design. We use this experimental technique to gain insight into the fundamental mechanisms of the IBAD nano-texturing process.

3:15 PM

(EMA-S3-004-2012) Surfactant Assisted Growth of Smooth Epitaxial Oxides on GaN (Invited)

E. Paisley*, North Carolina State University, USA; M. Biegalski, Oak Ridge National Laboratory, USA; J. Lebeau, B. Gaddy, S. Mita, R. Collazo, Z. Sitar, D. Irving, J. Maria, North Carolina State University, USA

Epitaxial integration of polar oxides with wide band gap polar semiconductors presents the possibility of tunable 2D charge carriers at polar interfaces and integration of non-linear dielectric properties. However, many cubic oxides form (100)-oriented facets when grown in the (111) orientation compatible with (0002) GaN. Previously, we showed a new surfactant approach to MBE growth of rocksalt oxide CaO on GaN, where water vapor is utilized during growth to change the equilibrium habit from cubic to octahedral, eliminating the (100)-faceting tendency and providing a 1000x increase in resistance of MIS capacitors. But, MBE cannot access processing space to stabilize (111) MgO and MgO-CaO solid solutions. To do so, higher surfactant partial pressures are required. In this presentation we will show a companion experiment performed at the ORNL CNMS using PLD with similar outcomes, i.e., 2D growth and step-and-terrace morphology. For both MgO and CaO, temperature dependent ab initio surface energy calculations predict the observed temperature and pressure windows supporting layer-by-layer growth. TEM analysis of the lattice-matched interface will be presented. Finally, we will report an extension of this work to the BaTiO₃/GaN interface. XRD shows PLD growth of epitaxial BT on c+ and c- polarity-patterned GaN. PFM suggests that the permanently polar GaN can simultaneously template the BT polarity in adjacent regions.

3:45 PM

(EMA-S3-005-2012) Strain Analysis of LaAlO₃/SrTiO₃ Hetero-interfaces

W. Wei, A. Sehirlioglu*, Case Western Reserve University, USA

Quasi-two-dimensional electron gas (Q2-DEG) that forms at the interface between two perovskite band insulators LaAlO₃ (LAO) and SrTiO₃ (STO) has stimulated extensive research interest since its discovery in 2004. The physical origin of the Q2-DEG formation at the interface has been under intensive debate. Several mechanisms have been proposed to explain the formation of Q2-DEG, such as the polar catastrophe, cationic intermixing and structural distortions at the interface, and oxygen vacancies introduced during the growth of LAO. Epitaxially grown LAO film is strained in LAO/STO heterostructure due to the ≈3% lattice mismatch. Strain relaxation in the LAO/STO heterostructures was systematically investigated with the LAO film thickness in the range from 4.9 nm to 84 nm. The heterostructures were characterized using reciprocal lattice mapping and conventional high resolution rocking curve, as well as X-ray reflectivity. The lattice parameters, such as lattice constant, mismatch and strain, are independently determined for both out-of-plane and in-plane directions. The LAO/STO heterostructure is tetragonally distorted over the entire range of film thickness. The degree of tetragonality is reduced as the film thickness is increased. At the thickness of 84 nm, a plastic deformation occurred in the film. However, the tetragonal distortion is found to exist in the residual film.

4:00 PM

(EMA-S3-006-2012) Control of the Octahedral Tilts in Lanthanum Cobaltite and the Impact on Magnetic Properties (Invited)

M. D. Biegalski*, W. Siemons, Z. Gai, A. Hailemariam, V. Lauter, Oak Ridge National Lab, USA; A. Mehta, Stanford Synchrotron Radiation Lightsource, USA; Y. Kim, A. Borisevich, Oak Ridge National Lab, USA; Y. Takamura, University of California, USA; H. M. Christen, Oak Ridge National Lab, USA

Strain can be accommodated in two major ways in perovskite materials, via bond lengthening or the rotation of the relatively rigid BO₆,

octahedra. However, the effects of octahedral rotations on the magnetic properties have not been explored. To explore the effects of octahedral tilts, we have used epitaxy to control the octahedral tilting in the unit cell of $\text{La}_{0.5}\text{Sr}_{0.5}\text{CoO}_3$ (LSCO) by growth on orthorhombic and cubic perovskite substrates, where orthorhombicity originates from octahedral tilts in the substrate. A tetragonal structure can be template into the film through use cubic, whereas an orthorhombic substrate does not suppress the octahedral tilts in the LSCO material. To analyze the interplay between octahedral tilts and magnetic properties, LSCO films were grown on substrates that have nearly identical macroscopic lattice mismatch, with in-plane lattice parameters of ~ 3.87 Å. The two substrates chosen for these experiments were cubic $\text{La}_{0.3}\text{Sr}_{0.70}\text{Al}_{0.65}\text{Ta}_{0.35}\text{O}_3$ (LSAT) and orthorhombic NdGaO_3 . From X-ray diffraction, the films grown on LSAT were shown to have a tetragonal structure, whereas, the films grown on NdGaO_3 , show a triclinic distortion. Our results show that the changes in the crystal structure due to the epitaxial imposed symmetries (for the same macroscopic strain) alter the magnetism in these materials.

4:30 PM

(EMA-S3-007-2012) Luminescent, structural and compositional properties of thin garnet phosphor layer for light emitting diodes

D. Kundaliya*, M. Raukas, A. Scotch, D. Hamby, M. Stough, K. Mishra, OSRAM SYLVANIA, USA

The ubiquitous light emitting diode (LED) typically relies on phosphor innovation to make today's bright white LEDs more efficient with better color gamut. There are numerous types of LED phosphors that have been investigated including oxides/garnets, nitrides, orthosilicates, nitrodosilicates and sulfides. Among these, garnets are the most often used in LEDs due to their excellent chemical, spectral & other luminescent properties needed for better performance in LEDs. Garnets crystallize cubic structures and are synthesized mainly by techniques such as solid state reaction, sol-gel, hydrothermal, coprecipitation, and other methods. In this presentation, we discuss the luminescent, structural and compositional properties of thin layers of garnet phosphors (e.g. Ce doped $\text{Y}_3\text{Al}_5\text{O}_{12}$) through an examination of different processing environments that yield well-suited materials and structures for improving the overall efficiency of light emitting packages. Specifically, we will describe recent results on strain induced in the phosphor layer by the lattice mismatch that shifts the emission of the phosphor to longer wavelengths (red shift) when a tensile strain is induced and to shorter wavelengths (blue shift) when a compressive strain is induced.

4:45 PM

(EMA-S3-008-2012) Control of ZnO thin film polarity through interface chemistry

C. T. Shelton*, J. Maria, NCSU, USA

When grown epitaxially on sapphire substrates, ZnO thin films exhibit oxygen, or c-, polarity. Insertion of a few nm of MgO as a buffer layer, however, causes the polarity to switch to zinc-polar or c+. Other researchers have surmised that the polarity switching observed in ZnO with increasing buffer layer thickness is the result of a change in the crystal structure of the MgO buffer from an intermediate wurtzite phase to the more stable rock-salt structure. The results of this study indicate that the overriding effect regulating ZnO polarity, however, is coverage. MgO deposited on Al_2O_3 substrates grows Volmer-Weber and, at thicknesses on the order of single nanometers, may not completely cover the substrate. This results in ZnO films with mixed polarity. Dual AC resonance tracking piezoresponse force microscopy (DART-PFM) was used to observe the polarity of ZnO films as a function of buffer layer thicknesses over a range spanning island nucleation and coalescence. Furthermore we show also that Si substrates can be either oxide or nitride terminated and these terminations can be used to produce oxygen and nitrogen polar ZnO respectively. Collectively this research suggests that a interface chemistry, as opposed to epitaxy, provides a predominate influence on ZnO polarity.

S4: Advanced Energy Storage Materials and Systems: Lithium and Beyond

Interfacial Processes and In Situ Methods for Energy Storage Materials and Devices II

Room: Coral B

Session Chairs: Sreekanth Pannala, Oak Ridge National Laboratory; Kang Xu, Army Research Lab; Don Siegel, University of Michigan

1:30 PM

(EMA-S4-019-2012) Transitioning From LiCoO₂ to Layered-Layered Composite Li₂MnO₃-LiMO₂ (M=Mn, Ni, Co) Li-ion Cathodes: Benefits and Challenges (Invited)

R. Bugga*, W. West, M. Smart, J. Soler, Jet Propulsion Laboratory, USA; R. Staniewicz, C. Ma, J. Robak, SAFT America Inc., USA

The layered-layered composite Li_2MnO_3 - LiMO_2 (M=Mn, Ni, Co) materials system offers much higher specific capacity than the commercially employed LiCoO₂ cathodes for Li-ion batteries. Despite this key advantage, numerous well-known challenges have hindered infusion into commercial cells, namely high first cycle irreversible capacity, low rate capability, and low cycle life. Here, we present results showing alternative synthesis approaches for improved performance. In addition, we present findings from a study characterizing the nature of the first cycle irreversible capacity loss. We have measured by two independent approaches the amount of utilizable lithium that is transferred on charge from this cathode system, i) with MoS₂ anode lithiation plateau transition as a reference point to the amount of Li at anode and ii) by acid digestion of the carbon anode for Li content. Both the methods show that virtually none of the cathode first cycle irreversible charge capacity resulted in lithiation of the anode.

2:00 PM

(EMA-S4-020-2012) Neutron Computed Tomography of Lithium Distribution in Porous Carbon Foams and Discharged Li-Air Cathodes (Invited)

H. Bilheux*, J. Nanda, S. Voisin, G. Veith, L. Walker, S. Allu, S. Pannala, P. Mukherjee, N. Dudney, Oak Ridge National Laboratory, USA

Optimization of lithium-ion transport and diffusion across electrodes is important in improving battery performance. This work presents the ability of neutron computed tomography (nCT) to map and semi-quantify Li distribution in 3D porous carbon foams and discharged Li-air cathodes, with spatial resolution of 60 microns at the High Flux Isotope Reactor (HFIR) neutron imaging prototype facility of the Oak Ridge National Laboratory (ORNL). Neutron radiography measures the attenuation of a neutron beam in the presence of an object under investigation with a 2D position sensitive detector. Neutrons can be removed from the incident beam by scattering and absorption by the object. Due to their high sensitivity to light elements such as Li, neutrons are well suited to probe battery electrodes at different cycling stages. A series of neutron radiographs of the electrode placed at different angles in the neutron beam were measured to generate the nCT. This talk presents 3D investigations of Li distribution in C matrices using neutron imaging. Research sponsored by ORNL's Laboratory Directed Research and Development funds. HFIR supported by the Division of Scientific User Facilities, Office of Basic Energy Sciences, US Department of Energy, under contract DE-AC05-00OR22725 with UT Battelle, LLC.

2:30 PM

(EMA-S4-021-2012) Using in situ thin film stress measurements to understand fundamental lithiation mechanisms in battery electrode materials

B. W. Sheldon*, A. Mukhopadhyay, S. K. Soni, A. Tokranov, D. Liu, Brown University, USA

The electrodes used in most Li ion batteries are mixtures of powdered active components, conductive filler, and binders. These complex mi-

costructures make it difficult to study many of the mechanisms that dictate battery performance. With this in mind, thin films provide a convenient configuration to study fundamental processes. We are particularly interested in combining in situ stress data with conventional in situ electrochemical measurements. Three examples that demonstrate this approach will be highlighted: (1) the formation of the solid-electrolyte interphase (SEI) layer on graphitic carbon films, (2) the stress response of model Si-based composite structures, (3) the role of oxygen non-stoichiometry on diffusion limitations in vanadium oxide films.

3:15 PM

(EMA-S4-022-2012) Multiscale electronic transport mechanism and true conductivities in amorphous carbon-LiFePO₄ nanocomposites (Invited)

K. Seid, Université de Nantes, CNRS, France; J. Badot, Chimie ParisTech (ENSCP), CNRS, UPMC Univ Paris 06, France; O. Dubrunfaut, SUPELEC, UPMC Univ Paris 06, Univ Paris-Sud, CNRS, France; D. Guyomard, Université de Nantes, CNRS, France; S. Vlasseur, UMICORE Cobalt & Specialty Materials, Belgium; B. Lestriez*, Université de Nantes, CNRS, France

Composite and nanostructured materials have hierarchical architecture with different levels: a) macroscopic (substructure of porous clusters); b) mesostructural (particles constituting the clusters); c) microscopic and nanometric (coatings, bulk of the particles). The identification of the key parameters that play on the electronic transport across all observed size scales is required, but is not possible using conventional dc-conductivity measurements. In this paper, the powerful broadband dielectric spectroscopy (BDS) from low-frequencies (few Hz) to microwaves (few GHz) is applied to one of the most important composite material for lithium batteries. LiFePO₄ is wrapped by a carbon coating whose electrical properties, although critical for battery performance, have never been measured due to its nanometer-size and the powdery nature of such material. We achieve the description of the electronic transport mechanism from the nanoscale (crystallites of sp²-coordinated carbon atoms) up to the sample macroscopic scale for this material. Moreover, the absolute conductivities and their respective drop when going from one scale to another are given, for the very first time, in the case of a composite powdery material for lithium batteries.

3:45 PM

(EMA-S4-023-2012) Knock-off Mechanism of Li-ion Diffusion in Solid Electrolyte Interphase

S. Shi*, Brown University, USA; P. Lu, L. G. Hector, S. J. Harris, Y. Qi, General Motors R&D Center, USA

One of the most topical issues surrounding the solid electrolyte interphase (SEI) for Li-ion batteries is the diffusion mechanism of Li⁺ ion. In this Letter we investigate the Li⁺ ion diffusion in Li₂CO₃ as one of the main components of the SEI by combining ab initio calculations and time-of-flight secondary ion mass spectrometry (TOF-SIMS) experiment. The excess interstitial Li⁺ ion with five-fold Li-O bond is demonstrated to be the dominant charge carriers determining the ionic conduction. Rather than via the direct hopping through empty space between the lattice sites, we find the interstitial Li⁺ ion diffuses via repetitive knock-off with lattice Li sites. The knock-off mechanism is explained in terms of the stable Li-O coordination environment maintained during the process.

4:00 PM

(EMA-S4-024-2012) Surface and Subsurface Damage Characterization of Graphite Anodes Electrochemically Cycled in Lithium-ion Cells

S. Bhattacharya*, A. Riahi, A. Alpas, University of Windsor, Canada

Volume change of graphite anodes used in lithium-ion batteries is not severe. Yet, graphite electrodes exhibit a drastic capacity drop, which is accompanied by graphite exfoliation and removal of partic-

ulate graphite from the surface. Therefore, understanding microstructural aspects of damage in cycled graphite will facilitate identification of electrochemical cycling-induced degradation mechanisms. To study the effect of applied voltage on graphite damage, cyclic and linear sweep voltammetry were performed. *In-situ* optical microscopy revealed graphite surface damage in the form of particle removal. FIB-milled cross-sectional microstructures of graphite electrodes exhibited partial delamination of graphite layers adjacent to solid electrolyte (SEI)/graphite interface by formation of interlayer cracks. Deposition of Li₂C₆, Li₂CO₃ and Li₂O near the crack tip caused partial closure of propagating graphite cracks during electrochemical cycling reducing the crack growth rate. Interconnecting graphite fibres bridged crack faces and retarded crack propagation. HR-TEM techniques revealed coexistence of crystalline (~ 5-20 nm) and amorphous regions within SEI. Fractured graphite particles comminuted to nano-size fragments were mixed with the decomposition products of SEI forming a protective layer, and prevented further damage to electrode surface during subsequent cycling.

4:15 PM

(EMA-S4-025-2012) Study of the ions and ion pair transport and component interactions in PPG-LiTFSI complexes

C. Sun*, Y. Wang, T. Zawodzinski, A. Sokolov, Oak Ridge National Laboratory, USA

To investigate the mass transport mechanism and component interactions in the salt-in-polymer system, we attempt to analyze the transport properties for each species by combining dielectric and NMR measurement. PPG-LiTFSI complexes were prepared with [O]/[Li]=40, 80, and 300. Conductivity was measured through dielectric measurement; on the other hand, the diffusion coefficient and the spin-lattice relaxation time for ⁷Li and ¹⁹F were probed using NMR methods. Experimental data was obtained as a function of temperature. Our first step is to estimate the "true" diffusion coefficient and concentration for each species through the experimental data incorporating with the model proposed by Stolwijk et al. However, it is observed that our data can be fitted either enthalpy of pair formation is positive or negative with acceptable statistic error and lead to different trends. This observation indicates that it is crucial to assign the reasonable fitting coefficients to obtain a more reliable result. To assess this point, we will demonstrate the way to determine the coefficient more precisely.

4:30 PM

(EMA-S4-026-2012) Computational Modeling for Cycling Characteristics of Various Electrolytes in Lithium-Ion Battery Cells (Invited)

K. Tasaki*, Mitsubishi Chemical America, USA

Despite the rapid developments of advanced electrolytes, little is known on the differences in cycling behaviors of lithium-ion batteries using various solvents. For example, the lithium intercalates into graphite in the dimethyl carbonate (DMC)- or ethyl methyl carbonate (EMC)-based electrolyte, while no lithium intercalation has been observed in the diethylene carbonate (DEC)-based electrolyte. In this study, density functional theory (DFT) calculations and classical molecular dynamics (MD) simulations have been performed for a series of carbonate-based electrolytes including ethylene carbonate (EC), propylene carbonate (PC), DMC, EMC, and DEC as the solvent. It was shown that the minimum-energy lithium ion solvation by each solvent all had a tetrahedral structure around the lithium ion and there was little difference in the solvation energy in the bulk electrolyte among the solvents investigated. However, there were significant differences in the stability of the lithium solvation when the solvated lithium ion was inserted into graphite in which the solvation structure became flat. The results suggest that the structural transformation of the DEC-solvated lithium ion prior to graphite intercalation is thermodynamically unfavorable. We discuss the approach taken and the differences in the characteristics of the ternary GIC's.

Friday, January 20, 2012

Plenary III

Room: Indian

8:00 AM

(EMA-PL-003-2012) Future Opportunities in Materials Design (Invited)

J. T. Prater*, U.S. Army Research Office, USA

In the early 1990's the Materials Sciences Division at Army Research Office launched the Smart Materials and Structures Initiative, an ambitious effort to push the limits of materials science. The Smart Materials concept envisioned material systems where sensors, actuators and control mechanisms could be integrated into the material via its microstructure such that the material would have the apparent ability to "sense and respond" to its environment. At the time, progress in the area was largely stymied by the lack of expertise in the areas of materials integration and microstructural control. However, the initiative established a long-term commitment within the Materials Division to advance our capabilities in the area of nanoscale engineering and directed self assembly of materials. Over the past decade researchers have made significant advances across the whole of materials science, bringing us much closer to realizing that original dream. In this presentation, several case studies will be included that highlight the advances that have been made and the potential benefits that can potentially be accrued. Lessons learned from studies on biological systems will also be reviewed. All of this suggests that large long-term advances in materials science may be possible through the judicious design and engineering of phase transforming materials. Opportunities for future research and potential relevance to Army needs will be discussed.

S2: Advanced Dielectric, Piezoelectric and Ferroic Materials, and Emerging Materials in Electronics

Microwave Dielectrics, Metamaterials and Frequency Tunable Devices and Nanoscale Phenomena in Dielectric, Ferroelectric and Piezoelectric Materials

Room: Indian

Session Chairs: Nazanin Bassiri-Gharb, Georgia Institute of Technology; Robert Freer, University of Manchester

9:30 AM

(EMA-S2-039-2012) Dielectric and Structural Characterization of Co-doped Ba_{0.6}Sr_{0.4}TiO₃ Thin Films for Tunable Passive Microwave Applications

F. Stemme*, H. Gesswein, C. Azucena, Karlsruhe Institute of Technology, Germany; M. Sazegar, Darmstadt University of Technology, Germany; J. R. Binder, M. Bruns, Karlsruhe Institute of Technology, Germany

Barium strontium titanate (BST) is a very promising material for tunable microwave applications like phase-shifters and tuneable filters. In contrast to screen printed BST thick films, we show the influence of fluorine doping in iron and undoped BST thin films without any influence of the microstructure. To achieve such iron and fluorine co-doped thin films we modified a RF magnetron sputter process with a co-sputter target and a two step annealing process after deposition. The first annealing process provides the crystallinity of the films. In the second annealing process the fluorine co-dopant is introduced into the BST thin films by a diffusion controlled process. The present contribution focuses on the processing and characterization of the undoped and iron doped BST thin films with fluorine co-dopant. The characterization of the thin films by X-ray photoelectron spectroscopy (XPS) provides chemical binding states and film composition. XPS sputter depth profiles prove the chemical homogeneity and the film thickness. Grazing incident X-ray diffraction (XRD) validates the crystallinity and the identification of chemical phases. Di-

electric measurements to investigate the influence of the donor and acceptor co-doping on the dielectric performance were carried out in metal insulator metal (MIM) structures with ground signal ground probes.

9:45 AM

(EMA-S2-040-2012) The effect of ZnO-B₂O₃ addition on the dielectric properties of screen-printed low-sintering Barium Strontium Titanate (BST) thick-films

C. Kohler*, X. Zhou, Karlsruhe Institute of Technology (KIT), Germany; M. Sazegar, R. Jakoby, Technische Universität Darmstadt, Germany; F. Stemme, J. Hausselt, J. R. Binder, Karlsruhe Institute of Technology (KIT), Germany

Barium Strontium Titanate (Ba_xSr_{1-x}TiO₃) has gained great attention as a tunable material for microwave devices. Among the different technologies for film fabrication, screen-printed BST thick films are distinguished by their low fabrication cost and simple processing. Additionally, thick-film technology enables the opportunity to integrate BST based components in LTCC (low temperature co-fired ceramics) substrates. However, the sintering temperature of pure BST thick-films with approximately 1200°C is too high for the required low sintering temperature of LTCC tapes (~900°C). Therefore, different amounts of a ZnO-B₂O₃ mixture were added to sol-gel-derived BST-powders in this study, in order to reduce the sintering temperature. After mixing and drying of the powders, thick-film pastes with an organic vehicle were prepared, screen-printed on alumina substrates and sintered at different temperatures (800-1000°C). The dielectric properties of the thick-films were extracted up to 40 GHz. Compared to pure undoped BST thick-films similar tunabilities and dielectric losses were achieved with permittivities lower than 200. X-ray diffraction and scanning electron microscopy revealed the dependence of the dielectric properties of the thick-films on their microstructure and phase content.

10:00 AM

(EMA-S2-041-2012) Integration of Fluxed-Barium Strontium Titanate Thin Films in Bandpass Tunable Filter

P. Lam*, V. Haridasan, M. B. Steer, J. Maria, North Carolina State University, USA

Barium strontium titanate (BST) thin films have been widely used for microwave devices. The strong non-linear response of the permittivity with an applied external bias allows for a direct tuning of the frequency response of an LCR circuit. Access to a higher tunability is limited by the thermal restriction of the system, i.e. for BST films in alumina, annealing above 900°C results in formation of second phases and cracking. Potential enhancement of the crystal structure at a lower temperature can be achieved by addition of a flux with a lower melting point than the sintering temperature of the ceramic. When melted, the flux serves as a medium for enhancing the crystal growth of the matrix ceramic providing lower thermal pathways for crystal densification. For this study we investigate a flux composed of 58% wt B₂O₃ and 42% wt BaO, which has a melting temperature of 869°C. Preliminary results of 5% fluxed-BT deposited by pulsed laser deposition show a substantial increase of the grain size with a corresponding enhancement in dielectric properties, almost 50% higher capacitance tuning. PLD films are limited to a small area which is unsuitable for device applications. The aim of this study is to translate those results to a co-sputtering system. We will present characterization data and dielectric results of the BST-fluxed films, and microwave data for a bandpass tunable filter.

10:15 AM

(EMA-S2-042-2012) Atomic-Resolution Transmission Electron Microscopy (HAADF-STEM) Z-Contrast Imaging and EELS of Microwave Dielectrics

R. Freer*, F. Azough, B. Schaffer, University of Manchester, United Kingdom

Atomic-Resolution High-Angle Dark-Field (HAADF) STEM Z-Contrast Imaging coupled with Electron Energy Loss Spectroscopy

(EELS) is a powerful tool for determining structure-property relationships at sub-grain interfaces and grain boundaries. We have employed this technique to characterise the sub-grain structure of microwave dielectrics to improve our understanding of intrinsic and extrinsic dielectric loss at microwave frequencies. A-site vacancies in La₂/3TiO₃ ceramics have been imaged. The vacancies and La1 atoms occupy the 4(h) sites and the 4(g) site is fully occupied by La2 atoms in the orthorhombic Cmmm structure of La₂/3TiO₃. The microtwin boundaries in the microstructure of La₂/3TiO₃ lie on the La2 atomic planes. On twinning, La2 and La1 atoms share the same site. The distribution of A-site vacancies, Ca and Nd in Ca(1-x)Nd₂/3TiO₃ (x=0.39 and 0.48) ceramics were imaged and analysed. Cation vacancies, Ca and Nd are randomly distributed in the perovskite structure. The structure of transformation induced twin boundaries and anti-phase boundaries due to A-site cation shifting will be presented. The site occupancy of Ba and Nd in Ba₆-3xNd₈+2xTi₁₈O₅₄ (x=0.3, 0.5 and 0.75) were determined using HAADF imaging and EELS. The ambiguity of occupancy of Ba and Nd in pentagonal tunnels and tetragonal tunnels in the tungsten bronze structure has been resolved.

10:30 AM

(EMA-S2-043-2012) Dielectric Properties of Complex Barium Neodymium Titanates in Microwave Regime

D. K. Dhanjal*, Punjab Technical University, India

Complex polycrystalline titanates of Ba₆-3xNd₈+2xTi₁₈O₅₄ with x = 0.0 - 0.7, in steps of 0.1, have been synthesized and characterized. X-Ray Diffraction (XRD) analysis confirmed that the crystal symmetry was orthorhombic with a possible space group of Pbam. The lattice parameters decreased linearly with an increase in the Nd content. Elongated bar shaped grains in the vicinity of Ba₆-3xNd₈+2xTi₁₈O₅₄ phase has been observed with the help of Scanning Electron microscopy (SEM). It was also observed that ceramics have been sintered above 95% of theoretical density. Dielectric investigations have been carried out in the frequency range of 0.3GHz-3.0GHz at room temperature. These dielectrics showed a high dielectric constant of 85 and a low loss tangent of 2 10⁻⁴. Temperature co-efficient of resonant frequency (92.7828 ppm/C) has been estimated in the temperature range of 20-80C. The relationship between the structure and dielectric properties has also been stated.

10:45 AM

(EMA-S2-044-2012) Analysis of Ba(Sc,Ta)_{0.05}Ti_{0.90}O₃ as a Frequency Agile Microwave Material

T. Mion*, M. Rivas, University of Texas - Pan American, USA; D. Potrepka, F. Crowne, U.S. Army Research Laboratory, USA; A. Tauber, Geo-Centers, Inc., USA; S. Tidrow, University of Texas - Pan American, USA

Ba(Sc,Ta)_{0.05}Ti_{0.90}O₃ over a temperature range -50°C to 125°C and frequency range, 10 Hz to 2 MHz has been investigated as a possible frequency agile microwave material. Phase transitions from -100°C to 900°C found using a Bruker D8 X-Ray Diffractometer show the structural changes over the temperature range including space group and lattice constants. SEM images with resolution up to 5 nm were implemented to investigate grain size and ordering. *This material is based upon work supported by, or in part by, the U.S. Army Research Laboratory and the U.S. Army Research Office under contract/grant number W911NF-08-1-0353.*

11:00 AM

(EMA-S2-045-2012) Synthesis of the Na_xK_{1-x}NbO₃ nanowires using hydrothermal method

X. HaiBo*, J. Mi-Ri, S. In-Tae, N. Sahn, Korea university, Republic of Korea

The lead-free Na_xK_{1-x}NbO₃ nanowires have been successfully synthesized by hydrothermal method using the (14-y)NaOH-yKOH solution with 0.0 ≤ y ≤ 14.0. For the specimens with 0.0 ≤ y ≤ 1.0, Sandia Octahedral Molecular Sieve (SOMS) and Na₈Nb₆O₁₉ 13H₂O transient phases

were formed after heating at low temperatures (140~180°C) and they were changed to NaNbO₃ nanowires after annealing at high temperatures (>350°C). The K₈Nb₆O₁₉ 13H₂O transient phase was formed for the specimens with 2.0 ≤ y ≤ 3.0 when the solution was heated at low temperatures (140~180°C) and they were changed to the NKN nanowires after the annealing at high temperatures. The NKN nanowires have the orthorhombic structure and their diameter and length were 90~100 nm and 70~80 μm, respectively. However, when y exceeded 3.0, the K₃Nb₆O₁₉ and KNbO₃ were produced instead of the K₈Nb₆O₁₉ 13H₂O transient phase and they changed to KNbO₃ nanoparticles after the heating at high temperature. In this work, the formation mechanism of the NKN nanowires will be discussed in detail and their piezoelectric properties will be also presented.

11:15 AM

(EMA-S2-046-2012) Piezoelectric response of lead zirconate titanate nanotubes processed via soft template infiltration

N. Bassiri-Gharb*, A. Bernal, Georgia Inst. of Technology, USA

Ferroelectric materials are subject to intrinsic and extrinsic size effects. Although the theoretical studies on limits of intrinsic ferroelectricity and domain walls' contribution to the piezoelectric response of ferroelectric materials have flourished, experimental studies have been mostly lacking, specially in Pb-based systems. Studying size effects in ferroelectric thin films is inherently difficult due to the inability of separating true size effects from microstructural heterogeneities, variations in crystalline quality and mechanical stresses imposed on the film by the underlying substrate that change with film thickness. We report a bottom-up patterning approach for creating sub-micron PbZr_{0.52}Ti_{0.48}O₃ (PZT) nanotubes by soft-template infiltration of a sol-gel solution. PZT nanotubes with aspect ratios (height to outer diameter) from 1:1 to 4:1 were produced. It is found that the thin (<10 nm thick) Al₂O₃ template leads to an order of magnitude decrease in the electric field developed in the PZT nanotubes with respect to thin film configuration. The effects of constraint to the substrate (aspect ratio of the nanostructures), critical size (thickness of the PZT tube wall), as well as lateral constraint (comparison with hard-template grown nanotubes as well as thin films of similar thickness) will be discussed.

11:30 AM

(EMA-S2-047-2012) Crystal Structure and Ferroelectric property of Epitaxial Rhombohedral Pb(Zr,Ti)O₃ Films

Y. Ehara*, S. Yasui, T. Oikawa, M. Nakajima, Tokyo Institute of Technology, Japan; T. Yamada, Nagoya University, Japan; T. Iijima, Advanced Industrial Science and Technology, Japan; H. Funakubo, Tokyo Institute of Technology, Japan

Crystal structure of PZT and ferroelectric properties depend on Zr/(Zr+Ti) ratio. Crystal symmetry is rhombohedral (polar-axis is <111> direction) when Zr/(Zr+Ti) > 0.52, while tetragonal symmetry (polar-axis is <001> direction) below for Zr/(Zr+Ti) > 0.50. However, due to the limited growth of the single crystal, especially rhombohedral case, some fundamental data of are still lacking experimentally such as ferroelectric and piezoelectric properties. Our approach is to get fundamental data is used the epitaxially grown polar-axis oriented films. Thus, we grew the epitaxial (111)/(11-1)-oriented rhombohedral Pb(Zr,Ti)O₃ (PZT) films on SrRuO₃-covered (111) KTaO₃, (111) [(LaAlO₃)_{0.3}-(SrAl_{0.5}Ta_{0.5}O₃)_{0.7}], (111) SrTiO₃, and (111) CaF₂ substrates by metal organic chemical vapor deposition. The volume fraction of the (111)-orientation almost linearly increased with the increase of the thermal strain during the cooling process from the deposition temperature to the Curie temperature as same as tetragonal PZT case. Consequently, perfectly (111)-oriented (i.e., polar-axis-oriented,) rhombohedral PZT film was obtained on CaF₂ substrate. Well saturated polarization-electric-field hysteresis loops were observed for the polar-axis-oriented films, and the saturated polarization value ($P_{sat} = 61 \text{ vC/cm}^2$) is similar to the theoretical predictions for PZT single crystals.

11:45 AM

(EMA-S2-048-2012) Solar air conditioning using ceramic composite and nano-structured materials

G. Singh*, P. Singh, P. Vyas, G. Sharma, College of Engineering & Technology, Bikaner, India

The research in the group is focused on the design and development of ceramic composite and nano-structured materials for solar air conditioning. Reinforcement of BaTiO₃ particles in ceramic composites body by using Thermoelectric cooling and ferroelectric effect in multilayer structure, the temperature significantly decreases. This paper deals with the fundamental energy conversion principles. Using this process in zero energy building as a roofing tiles, the temperature of building can be maintained in solar cycles heating as well as cooling via active solar thermal energy conversion.

12:00 PM

(EMA-S2-049-2012) Another Look at Goldschmidt's Tolerance Factor for Design of Advanced Material

S. Tidrow*, University of Texas - Pan American, USA

There are increasing numbers of publications and reports in which Goldschmidt's tolerance factor has not provided and does not provide an adequate model for understanding material parameters. We as a community need to develop improved methods for guiding material research to better support society through more time efficient discovery and development of materials that adequately address complex issues including but not limited to energy conversion and environmental sustainability. In this presentation, a physically significant construct for improving material parameter prediction is explored and compared with Goldschmidt's tolerance factor, a semi-empirical relation, using "simple" perovskites for visual illustration. This new approach, which uses a mapping transformation, yields some results similar with Goldschmidt's tolerance factor yet provides a more accurate, although still deficient, physical model for understanding of material parameters. The discussed construct is a reasonable starting point for improving our ability to rapidly discover and develop new materials in support of society. *This material is based upon work supported by, or in part by, the U.S. Army Research Laboratory and the U.S. Army Research Office under contract/grant number W911NF-08-1-0353.*

S3: Symposium on Thin Film Integration and Processing Science

Low Temperature Processing

Room: Pacific

Session Chair: Elizabeth Paisley, North Carolina State University

9:30 AM

(EMA-S3-009-2012) Bio-Integrated Soft Electronics (Invited)

N. Lu*, University of Texas at Austin, USA

Strategies for bio-integrated electronics must overcome challenges associated with the mismatch between the hard, planar surfaces of brittle semiconductor wafers and the soft, curvi-linear tissues of dynamic biological systems. This talk introduces the strategic integration of metallic and ceramic thin films onto soft polymeric substrates. Two examples of bio-integrated electronics will be discussed. Balloon catheters as minimally invasive surgery tools are instrumented with EKG, temperature and tactile sensors which can survive inflations as large as 200% and are tested within live animal models. As another example, ultra-thin, ultra-soft tattoo-like epidermal electronics are created to achieve conformal contact and compatible deformation with human skin for non-invasive transcutaneous sensing and stimulation.

10:00 AM

(EMA-S3-010-2012) Optical and Electrical Transport Properties of Chemically Deposited Antimony – Cadmium Selenide Thin Film Structures

E. U. Masumdar*, Rajarshi hahu College, Latur, India

Abstract: CdSe : Sb thin films with Sb³⁺ doping concentration varied from 0 to 5 mol% were obtained onto the amorphous glasses by a chemical bath deposition. The deposits were smooth, well adherent to the substrate support, uniform and diffusely reflecting with colour changing from dark-orange red to yellowish orange as doping concentration was increased from 0 to 5 mol%. Thickness increased with doping concentration from 0 to 0.1 mol% and then decreased with further increase in doping concentration. The XRD studies revealed polycrystalline nature of the samples. The optical gaps were determined and found to be decreased from 1.79 eV to 1.61 eV for the increase in Sb³⁺ doping concentration from 0 to 0.1-mol% and further it increased with increase in doping concentration. The transitions in these films were of the band-to-band direct type. The electrical conductivity is found to be enhanced with Sb³⁺ doping concentration from 0 to 0.1 mol% and then decreased with further addition of antimony content in CdSe. The activation energies were calculated in both the conduction regions. The other material characteristics such as thermoelectric power, carrier concentration (n), mobility (μ), barrier height (Φ_B) were studied as a function of working temperature and antimony doping concentration in CdSe. * Crospondng author: email-emasumdar@yahoo.com

10:15 AM

(EMA-S3-011-2012) Templating Nanostructured Cadmium Sulfide Thin Films (Invited)

E. Spoecker*, Sandia National Laboratories, USA

Cadmium sulfide (CdS) is a wide band gap semiconductor with optoelectronic properties valuable in applications ranging from photovoltaics to sensing. Integrating CdS into these applications, particularly when nanoscale thickness and uniformity are important, requires strict control of CdS materials chemistry. We have developed a room temperature, solution-phase growth process we call Nanocrystal Layer Deposition (NCLD) that produces dense, conformal nanocrystalline films of CdS, only 10-20nm thick, selectively templated on basic oxides such as zinc oxide or magnesium oxide. Governed by the surface chemistry of the growth surface and the controlled reactivity of the growth reagents, the unique NCLD process also enables the selective patterning of the CdS and the growth of conformal nanocrystalline CdS thin films on three-dimensional nanostructures. Furthermore, the low-temperature, solution-phase process is ideal for the incorporation of organic crystal growth modifiers capable of modifying crystal structure, crystal orientation, and optoelectronic properties of the CdS films. This talk describes the synthesis, chemistry, and characterization of these engineered CdS thin films and their potential applicability in current optoelectronic applications. Sandia is a multiprogram laboratory operated by Sandia Corporation, a Lockheed Martin Company, for the United States Department of Energy under contract DE-AC04-94AL85000.

10:45 AM

(EMA-S3-012-2012) Nanoscale ceramic thin film integration on fibrous materials (Invited)

J. S. Jur*, C. J. Oldham, W. J. Sweet, G. N. Parsons, North Carolina State University, USA

Inorganic surface coatings on complex fibrous systems are attracting interest for hybrid electronic device systems. Atomic layer deposition (ALD) is examined as a means for producing conformal coatings on polymer fibrous substrates with nanoscale precision at compatible temperatures. For example, the growth of alumina, zinc oxide, alu-

minum-doped zinc oxide, and tungsten on natural and synthetic fiber systems such as woven cotton, nonwoven polypropylene, nonwoven nylon-6, and cellulose paper are examined. Control over the nucleation behavior of the ALD thin films leads the unique ability to engineer the electrical behavior of the hybrid materials. Nonwoven polypropylene with a sub-50 nm ZnO coating shows a conductivity as high as 65 S/cm, whereas a W coating on nonwoven nylon-6 shows values as high as 1000 S/cm. The use of a modified 4-probe resistance measurement method provides the ability to relate the electrical behavior of fiber mat to the inherent properties of the fiber mat (i.e. fiber orientation, fiber density, etc.), a necessity for using these materials platforms in new hybrid electronic devices. The functional importance of conductive coatings on fibers is demonstrated by examining chemical sensors consisting of an "all-fiber" structure.

11:15 AM

(EMA-S3-013-2012) The influence of a Bi-precursor on the formation of β -Bi₂O₃ thin films

A. Veber*, Institut "Jožef Stefan", Slovenia, Institut "Jožef Stefan", Slovenia; Jožef Stefan Institute, Slovenia; S. Kunej, Institut "Jožef Stefan", Slovenia, Institut "Jožef Stefan", Slovenia; Jožef Stefan Institute, Slovenia; D. Suvorov, Institut "Jožef Stefan", Slovenia, Institut "Jožef Stefan", Slovenia; Jožef Stefan Institute, Slovenia

This work examines the synthesis and characterization of crack-free, β -Bi₂O₃ thin films, prepared on Pt/TiO₂/SiO₂/Si or corundum substrates using the sol-gel method. We observed that the Bi-based precursor has a pronounced influence on the β -Bi₂O₃ phase formation. Well-crystallised, single β -Bi₂O₃ thin films were obtained from Bi-2ethylhexanoate at a temperature of 400°C. In contrast, thin films deposited from Bi-nitrate and Bi-acetate resulted in non-single Bi₂O₃ phase formation. TEOS was used for the stabilization of the β -Bi₂O₃ phase. The phase composition of the thin films was characterized by means of X-ray diffraction (XRD) and transmission electron microscopy (TEM), whereas the morphology and thickness of the thin films were studied with scanning electron microscopy (SEM) and atomic force microscopy (AFM). The β -Bi₂O₃ films' dielectric properties were characterized utilizing microwave-frequency measurement techniques: 1) the split-post dielectric resonator method (15 GHz) and 2) the planar capacitor configuration (1–5 GHz). The dielectric constant and dielectric loss measured at 15 GHz were 120 and 9.6 10⁻³, respectively.

11:30 AM

(EMA-S3-014-2012) Low temperature synthesis of epitaxial KNbO₃ thick films grown by hydrothermal Method (Invited)

H. Funakubo*, T. Shiraishi, H. Einish, T. Hasegawa, M. Ishikaw, Tokyo Institute of Technology, Japan; T. Morita, The University of Tokyo, Japan; M. Kurosawa, Tokyo Institute of Technology, Japan

Low temperature growth of functional oxide is an very important issues for the application compatible to the organic electronics. Our groups grew KNbO₃ films grown at 240°C by the hydrothermal method using KOH and Nb₂O₅ as source materials. Film thickness increased with reaction time up to 3 h, however decreased for longer reaction times. A 16- μ m-thick epitaxially grown KNbO₃ films with (100)_{pc} orientation were successfully grown on (100)_cSrRuO₃//(100)SrTiO₃ substrates for 3 h. The relative dielectric constant and dielectric loss at 100 kHz were 415 and 8%, respectively. Clear hysteresis loops originating from ferroelectricity were observed and the remanent polarization was 20 μ C/cm² at the maximum applied electric field of 220 kV/cm. The effective longitudinal piezoelectric constant obtained using a Laser Doppler velocimeter, was 86 pm/V. Film thickness can be extended to beyond 100 μ m. This process can be also used as the process to obtain bulk materials with three-dimensionally orientation control. In addition, we demonstrated the preparation films of KNbO₃-NaNbO₃ solid solution on flexible metal foils that is useful for the energy harvesting applications.

S4: Advanced Energy Storage Materials and Systems: Lithium and Beyond

Next Generation Advanced Energy Storage Devices: Lithium-air, Lithium-sulfur and All Solid State Batteries II

Room: Coral B

Session Chairs: Anton Van der Ven, University of Michigan; Jagjit Nanda, Oak Ridge National Lab; Jack Wells, Oak Ridge National Lab

9:30 AM

(EMA-S4-027-2012) Improving Performance in Vanadium Flow Batteries (Invited)

T. Zawodzinski*, Z. Tang, D. Aaron, J. Lawton, R. Counce, M. Moore, J. Watson, M. Mench, A. Papandrew, U. Tennessee-Knoxville, USA

Redox flow batteries (RFBs) have been the subject of low-level research and development over the past few decades (1). They would seem to be ideal candidates for use in large-scale energy storage applications. However, deployment has been hampered by cost and performance issues. While much of the effort to date has focused on improving energy density of the systems, the power density is the most important handle on cost since it determines the size of the relatively expensive cell stacks, especially membranes. For most conventional grid applications, the most important focus of research would logically be factors related to power density and operating efficiency. In this work, we demonstrate our recent advances in improving the power density of VRBs. Relative to performance reported in the literature (2), more than an order of magnitude increase in the achievable power density has been achieved. We will also summarize an array of tools we have developed to provide the insight into critical voltage losses in the RFBs. As a model system, we are developing these analysis methods using vanadium redox flow batteries (2), membrane-separated RFBs. References: 1 C Ponce de Leon, A Frias-Ferrer, J Gonzalez-Garcia, D Szanto, and F Walsh, Journal Of Power Sources 160, 716-732 (2006). 2 B. Sun and M. Skyllas-Kazacos, Electrochimica Acta 37, 1253-1260 (1992).

10:00 AM

(EMA-S4-028-2012) A Practical, Rechargeable Lithium-Oxygen Battery (Invited)

B. Kumar*, UDRI, USA

This presentation will cover research activities on solid state, rechargeable lithium-oxygen batteries conducted at the University of Dayton Research Institute. Specifically, the presentation will describe open circuit voltage measurements, reversible electrochemical reaction and an approach to design a functional, practical cell. Based on the approach, lithium-oxygen cells have been fabricated and characterized. The cells provide high capacity and rate, a wide temperature range of operation, and a moderate cycle life (>400). The cell design also eliminates issues arising from the atmospheric constituents such as CO₂ and H₂O. The presentation will cover a detailed discussion of cell attributes.

10:15 AM

(EMA-S4-029-2012) Fast ion conducting ceramic electrolyte based on Li₇La₃Zr₂O₁₂ garnet (Invited)

J. Sakamoto*, Michigan State University, USA

Lithium ion battery technology has advanced significantly in the last two decades. However, future energy storage demands will require safer, cheaper and higher performance electrochemical energy storage. While the primary strategy for improving performance has focused on electrode materials, the development of new electrolytes has been overlooked as a potential means to revolutionize electrochemical energy storage. This work seeks to explore a new class of ceramic electrolyte based on a ceramic oxide with the garnet structure that exhibits the unprecedented combination of high ionic conductivity (4 x 10⁻⁴ S/cm at 298 K) and

chemical stability against metallic lithium and air. Examples of technologies that could be enabled by this class of electrolyte include: solid-state lithium ion batteries that are non-flammable and do not require hermetic packaging, lithium-air semi fuel cells and lithium-sulfur batteries. Initial investigations indicate that LLZO has several key attributes that make it appealing for use in conventional and advanced electrochemical energy storage technology. Ongoing fundamental studies are focused on understanding the mechanisms that stabilize the cubic garnet phase and enable fast ionic conductivity. Of particular interest are the roles that the synthesis conditions and dopants play in controlling defect concentrations.

10:45 AM

(EMA-S4-030-2012) Investigation on solid electrolyte materials for micro electronic devices

S. Jee*, Y. Yoon, Yonsei Univ, Republic of Korea; D. Kim, Auburn University, USA

Thin film lithium ion rechargeable batteries have been researched for their application in miniaturized ionic power devices such as electronic paper, smart cards, and RFID-Tag. Besides, development of an advanced solid electrolyte is greatly needed. Especially, Ultra-thin electrolyte is being required for the microelectronic devices. In this study, the feasibility of applying lithium Lanthanum Metal oxide (Li-La-M-O) thin films as solid-state electrolytes in solid-state ionic energy systems such as thin film batteries and super-capacitors was evaluated. The Li-La-M-O thin film electrolyte with garnet structure was prepared by radio frequency (RF) magnetron sputtering under atmosphere of argon (Ar) gas. We propose that the sandwich structure makes it possible to use a Li-La-M-O thin film as a thin film solid electrolyte without potential short circuiting of the Li-La-M-O thin film. For the final cell structure of SUS / Li-La-M-O / SUS / SiO₂ / Si, impedance measurements conducted at room temperature revealed ionic conductivities in the range of $10^{-6} \sim 10^{-7}$ S/cm for the various M composition (Nb, Ba, and Ta) of the Li-La-M-O thin films. This result suggests that the Li-La-M-O ultra-thin film electrolyte has potential as a solid oxide thin film electrolyte in micro thin film battery.

11:00 AM

(EMA-S4-031-2012) All Silicon Based Lithium Battery (Invited)

G. Nazri*, Wayne State University, USA

Silicon-based Energy Storage Battery Gholam-Abbas Nazri Frontier Applied Sciences and Technologies, LLC and Physics Department, Wayne State University, Detroit, Michigan 48202 The silicon physics has served the electronic industry for decades with great success, silicon chemistry may serve the next generation of energy storage devices. Current civilization is highly dependent on the daily use of electrical energy and battery as an electrical energy storage device is a main components of the future energy-based economy. In this work, a new energy storage technology based on silicon chemistry will be reported. This all silicon based lithium battery consists of composite lithium-silicon alloy anode, lithium transition metal silicate as cathode, and silicon based membrane and sput as an electrolyte. The all silicon-based battery has significantly higher energy density as compared with the current lithium-ion battery. This new technology will significantly reduce the cost, and improve safety of the lithium battery. We will discuss preparation methods, detail characterization, cell fabrication and performance of the all silicon based electrodes. Challenges and new opportunity for developing a reliable silicon based battery will be reviewed. The economic viability of all silicon-based battery versus current lithium-ion technology also will be presented.

11:30 AM

(EMA-S4-032-2012) Identifying Performance-Limiting Phenomena in Li-air Batteries via First-Principles Simulation (Invited)

D. Siegel*, M. Radin, F. Tian, J. Rodriguez, University of Michigan, USA

Thanks to their high theoretical specific energy densities, Li-air batteries are attracting increasing attention as a potentially transformative

energy storage technology. Despite this potential, Li-air technology remains in its infancy, and attaining a viable secondary Li-air battery will require that several challenges be overcome. These include: low efficiencies, slow discharge rates, and capacity fade upon long-term cycling. To accelerate the development Li-air batteries, we apply density functional theory calculations to identify performance-limiting phenomena. Our recent work has focused on characterizing the surface and bulk thermodynamics of Li-O discharge phases, and on predicting the formation and migration energies of defects in Li₂O₂. Regarding surfaces, we find that the stable surfaces of Li₂O₂ are metallic, even though bulk Li₂O₂ is an insulator. This behavior differs from that of Li₂O, whose stable surfaces are insulating, and is consistent with experiments showing reversibility in cells where Li₂O₂ is the discharge product. We conclude that the surface electronic structure is important for understanding reversibility in these systems. Regarding bulk properties, we find that Li vacancies mediate mass transport in Li₂O₂. In contrast, mass transport of oxygen is severely limited. These results are discussed in light of the high overpotentials observed during charging.

S1: New Frontiers in Electronic Ceramic Structures, Advanced Electronic Material Devices and Circuit Integration

Electronic Ceramic Structures

Room: Indian

Session Chairs: Vojislav Mitic, Faculty of Electronic Engineering; Amar Bhalla, University of Texas, San Antonio

1:30 PM

(EMA-S1-001-2012) High-Temperature Nanomaterials for Electrochemical Micro-Sensors

E. M. Sabolsky*, C. Wildfire, E. Ciftiyurek, K. Sabolsky, West Virginia University, USA

The objective of this proposed work is to develop micro-scale, chemical sensors and sensor arrays composed of nano-derived, metal-oxide composite materials to detect gases such as H₂ within high-temperature environments (>500°C). The long-term goal of this program is to demonstrate sensor materials and processing strategies that can also be used on micro-sensor arrays that monitor other chemicals (besides H₂), such as carbon dioxide, carbon monoxide, methane, and nitrogen oxides levels within a similar environment. The impact of this work will enable the inexpensive implementation of sensor arrays within broad sensor nets. Hydrothermal synthesis experiments were completed in order to form doping of refractory oxide compositions. A range of baseline and A-site and B-site doped compositions were successfully synthesized with no secondary phases. In order to evaluate the sensing properties of the new refractory nanomaterials, chemi-resistive sensors were fabricated on polished alumina substrates, and the stability, sensitivity, and selectivity of the nanoparticle were evaluated. The pure and promoted A-site and B-site doped, nano-derived electrodes showed rapid response to 0.05-5% H₂, and showed remarkable stability at testing temperatures between 600-1000°C over a 24 hour period.

1:45 PM

(EMA-S1-002-2012) Optimum Conditions For Deposition of ZnO Semiconductor Films By RF Sputtering

T. Oder*, A. Smith, M. McMaster, N. Velpukonda, Youngstown State University, USA; M. L. Nakarmi, Brooklyn College, USA

We present results on work done to optimize the deposition conditions of ZnO films needed for successful achievement of p-type doping, which is currently the impediment to device developments. The films were deposited on sapphire substrate by RF magnetron sputtering using a mixture of argon and oxygen. Prior to deposition, the sapphire substrates were heated in oxygen and/or in vacuum. The deposition conditions varied included substrate temperature, the gas

pressure and flow rate. The resulting films were annealed in a rapid thermal processor in nitrogen at 900 °C for 5 min and analyzed using photoluminescence spectroscopy, X-ray diffraction and Hall effect measurements. The results obtained indicate that films deposited on sapphire heated in oxygen prior to deposition had greatly improved optical properties. Other optimum conditions were a deposition temperature of 300 °C, a pressure of 10 mTorr and a gas flow rate of 20 standard cubic centimeter per minute. This film had a luminescence peak at 3.347 eV with a full-width-half maximum (FWHM) value of 15 meV when measured at 10 K. The XRD 2 θ -scans had peaks at about 34.5° with the best FWHM value of only 0.10°. Results from p-type doping currently being performed using these optimized growth conditions will be also presented.

2:00 PM

(EMA-S1-003-2012) Fibrous BaTiO₃ Filler / PVDF Composite Sheet for Transducer Application

K. Fukata*, K. Kakimoto, Nagoya Institute of Technology, Japan; H. Ogawa, Otsuka Chemical Co., Ltd, Japan

Piezoelectric ceramic filler / polymer composite sheet shows high bending flexibility in comparison to monolithic ceramics, hence it can be applied to transducer devices such as touch panel sensors and vibration energy harvesters. In this work, fibrous BaTiO₃ / polyvinylidene fluoride (PVDF) composite sheets were fabricated for the first time, and their electric-field-induced strain curves and piezoelectric output voltages were measured. Fibrous BaTiO₃ powder, fabricated by the molten salt method, was mixed with the ratio of 0~30 vol% in the PVDF solution dissolved in dimethylsulfoxide at 140 °C. The mixture was spin-coated to make thin film, then the stacked films were thermally pressed and extended toward an uniaxial direction by a hot rolling technique with a temperature kept at 90 °C. The extension ratio is 3 times and larger to form a piezoelectric β phase of PVDF. The measured electric-field-induced strain in the 31 direction was enhanced in the sheet having higher volume ratio of fibrous BaTiO₃ powder, which was more obvious than the case of the reference specimens using spherical BaTiO₃ powders. The effect of filler shape on the piezoelectric property in the PVDF matrix composite sheet was discussed.

2:15 PM

(EMA-S1-004-2012) Contribution of non-180° domain wall motion and lattice strain to the frequency dependence of the piezoelectric coefficient in ferroelectric ceramics

S. Banavara Seshadri*, A. D. Prewitt, University of Florida, USA; D. Damjanovic, Swiss Federal Institute of Technology - EPFL, Switzerland; A. J. Studer, ANSTO, Australia; J. L. Jones, University of Florida, USA

Thus far, all descriptions of the logarithmic frequency dependence of the macroscopic piezoelectric coefficient, d_{33} , have been phenomenological in nature. In this work the extent of the contribution of non-180° domain wall motion to the frequency dependence of the macroscopic d_{33} has been determined experimentally using time resolved, in-situ neutron diffraction measurements. Lattice strains and domain wall motion were measured as a function of frequency in a soft commercial PZT material. These results were then compared to macroscopic d_{33} measured as a function of frequency. It was found that both lattice strain and non-180° domain wall motion show a linear decrease with the logarithm of the frequency of applied field indicating that they contribute to the frequency dependence of macroscopic d_{33} . The magnitude of the contribution of non-180° domain wall motion and lattice strain to the macroscopic d_{33} was also quantitatively established.

2:30 PM

(EMA-S1-005-2012) Microstructure Fractal Analysis of Er Doped BaTiO₃-ceramics

V. Mitic*, V. Paunovic, J. Purenovic, L. Kocic, Faculty of Electronic Engineering, Serbia; S. Jankovic, Faculty of Mathematics, Serbia; V. Pavlovic, Faculty of Agriculture, Serbia

In this paper the influence of Er₂O₃ on microstructure and dielectric properties of BaTiO₃-ceramics has been investigated. BaTiO₃-ceramics doped with 0.01 up to 1 wt% of Er₂O₃ were prepared by conventional solid state procedure and sintered at 1320°C for four hours. Microstructural investigations were carried out by using scanning electron microscopy (JEOL-JSM 5300) equipped with EDS (QX 2000S) system. The new correlation between microstructure and dielectric properties of doped BaTiO₃-ceramics based on fractal geometry and contact surface probability has been developed. Using the fractals and the grains contact surface statistics, a reconstruction of microstructure configurations, like grains shapes, or intergranular contacts has been successfully done. The presented results indicate that fractals analysis and statistics model of contact surfaces different shapes are very important for BaTiO₃-ceramics microstructure and dielectric properties prognosis in function of intergranular and total impedances in higher level of circuit packaging integrations.

3:15 PM

(EMA-S1-006-2012) Atom Probe Tomography of Oxide Ceramics

R. Kirchhofer, D. R. Diercks, B. P. Gorman*, Colorado School of Mines, USA

Atom Probe Tomography (APT) has the unique ability to provide chemical composition information (chemical resolution <1 ppm) paired with high spatial resolution (~2 Å). This unique characterization technique enables quantitative determination of internal interfaces and nanostructures with unprecedented accuracy. Traditionally, field evaporation using pulsed electric fields has limited the applicability of APT to highly conductive materials. The introduction of a laser to assist the field evaporation has opened up the technique to ceramic materials; however, challenges arise from the effect of the laser on the specimen. Poor heat dissipation from the tip results in delayed evaporation that limit the mass resolving power and ultimately affect the compositional information. Significant loss of spatial resolution due to surface diffusion has also been observed at high laser powers. For these experiments a focused, low power laser (1-10 pJ/pulse) was used to assist in field emission of ions to avoid surface diffusion and ion clustering. Combining experimental modifications to the specimen geometry during sample preparation and revised laser pulsing strategies has improved the cation / oxygen stoichiometry and spatial resolution. Specific examples include ion conducting ceramics, transparent conducting oxides, dielectric and ferroelectric thin films, and grain boundary effects in conducting oxides.

3:30 PM

(EMA-S1-007-2012) Mechanically Activated BaTiO₃ Microstructure Fractal Nature

V. Mitic*, Faculty of Electronic Engineering, Serbia; V. Pavlovic, Faculty of Mechanical Engineering, Serbia; L. Kocic, V. Paunovic, J. Purenovic, J. Nedin, Faculty of Electronic Engineering, Serbia; V. Pavlovic, Faculty of Agriculture, Serbia

Increasing demands on the quality of electronic ceramics requires a well-controlled correlation between particle morphology and processing conditions. Since mechanical activation is one of the methods for modification of physico-chemical properties of dispersed systems, in this study a correlation between the densification rate microstructure evolution and fractal nature of mechanically activated BaTiO₃ has been analyzed. The high purity commercial BaTiO₃ powder was mechanically activated in a planetary ball mill in a continual regime for 60 and 120 minutes. Sintering under non isothermal conditions was carried out up to 1380°C. The shrinkage behaviour of mechanically activated samples, has been analyzed by a

sensitive dilatometer. Densification rate as a function of relative density for different activation times has been calculated. Microstructure investigations of sintered samples were carried out, using a scanning electron microscope (SEM). The presented results enable establishing processing parameters that are indispensable for obtaining materials with advanced properties.

3:45 PM

(EMA-S1-008-2012) Intense cooperative upconversion emission in Yb/Er : TeO₂-Li₂O-WO₃ oxyfluoride glass ceramics

G. F. Ansari, All Saints' College of Technology, Bhopal (M.P.) 462036 India, India; S. K. Mahajan*, Samrat Ashok Technological Institute, Vidisha (M.P.) 464001 India, India

There has been a great deal of interest in cooperative upconversion of Yb³⁺ ions advantage over Tm³⁺ doped glass ceramics for blue emission in display technology. We have fabricated transparent glass-ceramics based on selected glass of (70-x)TeO₂-16.5Li₂O-13WO₃-0.5ErF₃-xYbF₃ (where x = 1-3 mol%) by melt quenching and subsequent heating at first crystallization temperature. The crystallinity of the glass ceramic has been examined by X-ray technique. Under 980 nm diode laser excitation of 2 mol% Yb³⁺ sample produced an intense blue at 487 nm, very weak green at 525 nm and 550 nm, and red at 650 nm emission signals. This intense blue emission attributed through cooperative upconversion due to Yb³⁺-Yb³⁺ clusters and LiErF₄ crystalline phase precipitation. The red and green emissions are mainly attributed to energy transfer from Yb³⁺ ions to Er³⁺ ions. The cooperative upconversion mechanism for the couple of Yb³⁺ ions is dominated over the excited state absorption process at less than 0.5 mol% of Er³⁺ content. The dependence of 487 nm intensity versus laser power is equal to 1.75 confirm that two-photons contribute to blue cooperative upconversion. In addition, these oxyfluoride materials were robust, easy and flexible to process, and possible to be fabricated in the fiber form for device applications.

4:00 PM

(EMA-S1-009-2012) Analytical model for ion-implanted 4H silicon carbide metal-semiconductor field-effect transistors

S. Wang*, Northwest University, China

In order to design ion-implanted 4H-SiC MESFETs (Silicon Carbide Metal-Semiconductor Field-Effect Transistors), an analytical model is present. The implant depth profile is simulated using the Monte Carlo simulator TRIM. The calculation methods for the channel depth, the pinch-off voltage and the output current-voltage characteristics of ion-implanted 4H-SiC MESFETs are given. The effects of parameters such as the ions activation rate, the acceptor density of the epitaxial layer and temperature on the channel depth have been studied. The output current-voltage characteristics for the multiple ion-implanted 4H-SiC MESFETs designed and the drain current with the effect of temperature are given. The model can be used to give some helps to the designers of ion-implanted SiC MESFETs before the fabrication process.

S3: Symposium on Thin Film Integration and Processing Science

Complex Oxide Thin Film Synthesis

Room: Pacific

Session Chair: Christopher Shelton, NCSU

1:30 PM

(EMA-S3-015-2012) Advanced chemical solution deposition methods of complex electronic oxide films (Invited)

T. Schneller*, RWTH Aachen, Germany

Complex electronic oxide films offer a unique potential for applications in microelectronics, microsystems, and alternative energy de-

vices. Thus there is an increasing interest in dielectric, ferroelectric, piezoelectric, and conducting ceramic films. Among the chemical deposition techniques for such oxides, chemical solution deposition (CSD) features high flexibility with regard to composition, materials, and substrates while maintaining cost efficiency. Besides the thermal processing conditions the precursor chemistry has a significant influence on the final film quality. The increased scientific knowledge obtained in recent years opened up further interesting application areas such as deposition on oxygen sensitive base metals for capacitors and coated superconductors or low temperature fabrication of proton conducting films for solid oxide fuel cells. This presentation will review the established aspects of CSD for high-permittivity, ferroelectric, and other complex electronic oxide films. Attention is given to precursors, solution chemistry, and process development with focus on the structural evolution of the precursor solution into the crystalline state and the impact of precursor chemistry and film fabrication conditions on the transformation process. Moreover a novel approach based on dispersions of microemulsion derived nanoparticles complements the traditional precursor methods.

2:00 PM

(EMA-S3-016-2012) Orientation Control in Pb(Zr_{0.52}Ti_{0.48})O₃ Thin Films for Use in Multilayer Actuators

L. M. Sanchez*, D. Potrepka, Army Research Laboratory, USA; G. Fox, Fox Materials Consulting LLC, USA; I. Takeuchi, University of Maryland, USA; R. G. Polcawich, Army Research Laboratory, USA

Using (111) oriented Pt as the bottom electrode, (001) textured CSD PZT (52/48) thin films were processed using a PbTiO₃ seed layer and a 2-Methoxyethanol based solution. Leveraging the texture optimization on single 500 nm thick PZT thin films, the focus of this research was to analyze orientation control of the PZT films in multiple Pt/PZT/Pt layers for use in multilayer actuators (MLA). On the first sample, the PbTiO₃ seed layer was only used on the first layer of PZT. Accordingly, a highly (001)/(100) textured film is observed in the first Pt/PZT/Pt layer. However, this orientation declines by 6.9% and 10.3% in subsequent layers. In addition, both (110) and (111) orientations develop in the PZT layers. In the second sample, the PbTiO₃ seed layer was used on top of each Pt layer. Orientation declines by 6.8% between layers 1 and 2, however no further decrease in orientation is observed in the other layers. The (110) portion is less prominent in the sample with the Pt seed layer. The measurements on these films are encouraging for achieving high piezoelectric coefficient MLAs for use in tactical radios and mm-scale robotics. This presentation will cover the development of textured PZT in multilayers and will report on dielectric, ferroelectric, and piezoelectric response of multilayer PZT thin film capacitors and actuators.

2:15 PM

(EMA-S3-017-2012) Microstructural Evolution of Flux-Grown Barium Titanate Thin Films

M. J. Burch*, A. Moballeghe, D. T. Harris, J. Maria, E. C. Dickey, North Carolina State University, USA

The role of the BaO·B₂O₃ (BBO) fluxing agent on the microstructural evolution of pulsed-laser deposited (PLD) BaTiO₃ thin films was studied. Transmission electron microscopy (TEM) of both ex-situ and in-situ annealed samples was utilized to study the boron distribution in the films and the BaTiO₃ microstructure as a function of time and temperature. To facilitate these studies, thin films were directly deposited on TEM grids. A heating TEM holder was used to anneal the samples in order to observe the dynamics of crystallization and grain growth during annealing. The as-deposited films were found by diffraction to be highly disordered with no indication of long range order. The 5% BBO samples annealed at 900 °C were highly crystalline with grain size varying from 0.1 to 0.5 μm, whereas the thin films with no fluxing agent present had a grain size less than 0.1 μm and a higher porosity. The improved microstructure of the flux grown BaTiO₃ films lead to enhanced dielectric properties.

2:30 PM

(EMA-S3-018-2012) Synthesis and Characterization of $\text{Pb}(\text{Zr}_x\text{Ti}_{1-x})\text{O}_3$ Thin Films on Copper Foils by RF Magnetron Sputtering

J. Walenza-Slabe, A. D. Mason, B. J. Gibbons*, Oregon State University, USA

Thin films of $\text{Pb}(\text{Zr}_x\text{Ti}_{1-x})\text{O}_3$ (PZT) deposited and *ex situ* crystallized on copper foils and copper coated polymer substrates have expanded the opportunities for flexible, low-cost piezoelectric devices. Previous research has focused primarily on chemical solution routes for the PZT thin films. In this research morphotropic phase boundary composition PZT was deposited directly onto copper foils using rf-magnetron sputtering with controlled atmosphere *ex situ* annealing. Film quality was observed to benefit from a low temperature, low oxygen partial pressure heat treatment preceding the final crystallization step. Best results were achieved when the films were comprised of several thinner layers deposited, heat-treated, and crystallized in repeating fashion. Typical films 500 nm thick had a remnant polarization and coercive field of around 20 $\mu\text{C}/\text{cm}^2$ and 75 kV/cm, respectively. The dielectric constant and loss of these were approximately 800 and 6% at 200 Hz, respectively. Ongoing work will be presented on the piezoelectric response of these devices.

3:15 PM

(EMA-S3-019-2012) Piezoelectric MEMS on Alternative Substrates (Invited)

D. Wilke, S. Bharadwaja, S. Trolier-McKinstry*, Penn State, USA; P. Reid, D. Schwartz, Harvard Smithsonian, USA

The integration of thin film piezoelectric materials into microelectromechanical systems (MEMS) offers many distinct advantages for actuation and sensing applications. While Si substrates offer a useful platform for many applications, there are others, requiring large areas, flexibility, or a wider range of elastic moduli, where Si may not be possible. This paper will discuss incorporation of high piezoelectric coefficient PZT ($\text{PbZr}_{1-x}\text{Ti}_x\text{O}_3$) – based films onto glass and polymeric substrates. The Gen-X system is proposing 10,000 m^2 of actuable optics in order to achieve 0.1 arc second resolution. It is demonstrated that sputter deposition of PZT films and maximum process temperatures of 550 °C on space-qualified glass substrates enable high quality piezoelectrics with $|e_{31,f}|$ coefficients $> 5 \text{ C}/\text{m}^2$. Secondly, for energy harvesting applications, compliant polymer substrates enable both lower resonant frequencies for the same dimensions of the MEMS device as well as the opportunity for much higher harvested powers. It is demonstrated that laser annealing can be used to crystallize PZT films on polyimide substrates. The resulting films have remnant polarizations of $\sim 20 \mu\text{C}/\text{cm}^2$, and permittivity values > 800 .

3:45 PM

(EMA-S3-020-2012) Epitaxial-Like Polycrystalline PZT Superlattices Processed by Chemical Solution Deposition

Y. Bastani*, N. Bassiri-Gharb, Georgia Institute of Technology, USA

Leveraging the thermodynamic drive for spontaneous Zr/Ti gradient formation during crystallization of sol-gel processed PZT films, superlattice-like (SL) thin films with compositional gradient through the thickness, and centered at the morphotropic phase boundary were deposited on Pt/Ti/SiO₂/Si substrates. SL films, with stacking periodicity ranging from 12 to 60 nm were obtained. X-Ray Diffraction (XRD) patterns showed pure perovskite phase and preferential (100) orientation (Lotgering factor $>95\%$), and high order satellite peaks, indicating high quality of the superlattice structure. XRD structural refinement along with XPS depth profile chemical analysis, revealed the SL crystal structure to switch between rhombohedral and tetragonal (with in-plane polarization) phases in each deposited layer, leading to 20% higher dielectric permittivity compared with compositional gradient-free films of similar thickness. Dielectric nonlinear analysis showed also a higher extrinsic contribution to the dielectric response in SL films than in conventionally

processed films. This is possibly due to enhanced reorientation of electrical dipoles, and higher extrinsic contributions due to the motion of the “artificially-created” phase boundaries in SL films. Dependence of the dielectric response of the SL films on the stacking periodicity and the extent of the compositional gradient will be also discussed.

4:00 PM

(EMA-S3-021-2012) Effect of pre-crystallization aging on microstructure and properties of solution derived PZT thin films

K. Nittala*, University of Florida, USA; K. E. Meyer, Sandia National Laboratories, USA; S. Mhin, University of Florida, USA; J. F. Ihlefeld, G. L. Brennecke, Sandia National Laboratories, USA; J. L. Jones, University of Florida, USA

Solution deposition is routinely used to fabricate thin films of lead zirconate titanate (PZT). We observed significant microstructural differences between films crystallized at different times after pyrolysis. To understand the effect of pre-crystallization aging on the “gel” obtained after pyrolysis, aging studies were undertaken. Specifically, the effects of pyrolysis temperature (300 °C and 400 °C) and the relative humidity level during aging on the final films properties after crystallization were evaluated. Polarization-field measurements indicated that the electrical properties of films pyrolyzed at 300 °C deteriorated significantly with aging. Moreover, porosity was observed in the bulk of the film for samples aged in high humidity conditions. Films pyrolyzed at 400 °C were less affected. Aged gels with higher remnant organic content (lower pyrolysis temperature) underwent significant weight loss at temperatures corresponding to evaporation of water during thermogravimetric characterization. No distinct chemical modification could be detected from FT-IR measurements of the aged samples. Hence, the aging effect observed in the films appears to be due to absorption of water by the gel state. Sandia is operated by Sandia Corporation, a Lockheed Martin Company, for the U. S. DOE’s National Nuclear Security Administration under contract DE-AC04-94AL85000.

4:15 PM

(EMA-S3-022-2012) Chemically homogeneous ferroelectric thin films with enhanced electromechanical responses

J. Ihlefeld*, Sandia National Laboratories, USA; C. T. Shelton, North Carolina State University, USA; G. L. Brennecke, Sandia National Laboratories, USA; P. G. Lam, North Carolina State University, USA; P. G. Kotula, B. B. McKenzie, M. J. Rye, J. A. Ohlhausen, K. E. Meyer, Sandia National Laboratories, USA; B. J. Gibbons, Oregon State University, USA; J. Maria, North Carolina State University, USA

Through selection of an adhesion layer that forms a low energy interface with platinum for SiO₂/Si substrates, improved dielectric and ferroelectric responses of solution deposited BaTiO₃ and $\text{Pb}(\text{Zr,Ti})\text{O}_3$ (PZT) thin films has been observed. PZT films deposited on substrates with ZnO adhesion layers have 35% and 21% percent enhancements over traditional titanium adhesion layers in remanent polarization and permittivity, respectively, with values of 32 $\mu\text{C cm}^{-1}$ and 1950 measured. A 300% increase in room temperature permittivity of BaTiO₃ is measured on ZnO-buffered substrates compared to titanium-buffered, with values approaching 1400 measured. Chemical mapping via scanning transmission electron microscopy and energy dispersive spectroscopy and secondary ion mass spectroscopy revealed nearly completely homogeneous films deposited on the ZnO-buffered platinumized silicon substrates while films on traditional substrates possessed titanium and zirconium concentration gradients. The improvements in electromechanical response have been ascribed to significantly improved chemical homogeneity in the oxide films by eliminating titanium diffusion through the platinum films. Sandia is a multiprogram laboratory operated by Sandia Corporation, a Lockheed Martin Company, for the United States Department of Energy’s National Nuclear Security Administration under contract DE-AC04-94AL85000.

S6: Technologies for Sustainability and Green Materials Processing

Technologies for Sustainability and Green Materials Processing

Room: Coral B

Session Chair: Paul Clem, Sandia National Laboratories

1:30 PM

(EMA-S6-001-2012) Carbonate Ceramics: A Disruptive Technology for CO₂ Utilization (Invited)

R. Riman*, Q. Li, S. Gupta, M. A. Bitteto, Rutgers University, USA; V. Atakan, Solidia Technologies, USA

not available

2:00 PM

(EMA-S6-002-2012) Microwave processing of soapstone under supercritical carbon dioxide atmosphere

A. Dias*, UFOP, Brazil

Nowadays, carbon sequestration has attracted much attention in a large number of scientific areas. Rising carbon dioxide concentrations due to anthropogenic emissions are scientifically proven to be the main cause for it. One way to reduce carbon dioxide emissions is to capture CO₂ from large point sources like power plants and to store it permanently, either underground or as mineral carbonates. Mineral carbonation is the reaction of gaseous CO₂ with naturally occurring magnesium and calcium silicates such as soapstone. In this paper, a novel method to synthesize magnesium carbonates via reaction of a supercritical CO₂ with magnesium-silicate minerals under microwave radiation at 150C is presented. The reaction rate is rapid, with carbonate deposition in about 30 min. The full characterization of the products from the microwave reactions has been performed to investigate its potential role as a "CO₂-sequestering medium". We investigated the carbonates synthesized using SEM/TEM, XRD, FTIR and Raman spectroscopies. The obtained products make our method a promising complementary solution to other methods for CO₂ sequestration. The likelihood of using the resulting the obtained phases and the by-products of the process in a large number of applications makes our processing route an even more attractive solution.

2:15 PM

(EMA-S6-003-2012) NaY-Zeolite for CO₂ Capture Applications

W. Wong-Ng*, NIST, USA; J. A. Kaduk, Illinois Institute of Technology, USA; J. Burrell, Q. Huang, L. Espinal, T. Yildirim, NIST, USA

As coal-burning power plants are an important part of energy production for the foreseeable future, reduction of CO₂ emissions from these plants using efficient and low cost sorbents is important for global sustainability. Current examples of state-of-the-art solid sorbent materials include zeolites and metal-organic-framework (MOFs). Porous zeolites are a class of molecular sieve materials known to be effective sorbents for industrial applications. Crucial factors for understanding the efficiency of porous sorbent materials include the framework and pore structure, and the chemical and physical reactivity of CO₂ within the pores. This talk will discuss the results of characterization of NaY-zeolite using neutron diffraction techniques in the presence of different partial pressures of CO₂ and at temperatures between room temperature and 4K.

2:30 PM

(EMA-S6-004-2012) Greener Synthesis of Functional Oxide Nanoparticle Inks

D. Ito*, S. Yokoyama, B. A. Weintraub, K. Masuko, J. E. Hutchison, University of Oregon, USA

Oxide nanoparticle inks have potential for a variety of next generation applications including transparent electrodes, photocatalytic

water splitting, energy storage, catalysts, and sensors. Greener syntheses of nanoparticle inks that are scaleable and low-cost are important for practical commercialization of those inks. Impurity doping of oxide nanoparticles is an effective approach to enhancing their specific functions, however, it is difficult to obtain uniform impurity doping. In this presentation, we will discuss a greener synthesis of oxide nanoparticle inks that has a yield over 90%. We use only oleyl alcohol and oleic acid, non-toxic chemicals, as solvents, reagents, and surfactants during a one-step synthesis. This greener approach offers precise control of doping concentration. We will describe the synthesis method and results for tin doped indium oxide and antimony doped tin oxide with different doping concentration. We also demonstrate a self-assembled deposition of nanoparticle films by using a simple painting process using nanoparticle ink.

3:15 PM

(EMA-S6-005-2012) Sunshine to petrol: a metal oxide-based thermochemical route to solar fuels (Invited)

E. N. Coker*, J. E. Miller, Sandia National Laboratories, USA

Converting carbon dioxide and water to hydrocarbons is an attractive option for storing solar energy and, coupled with appropriate CO₂ capture technology, for recycling carbon and impacting atmospheric CO₂ concentrations. For any process, high solar-to-fuel efficiency is necessary for large scale viability and favorable economics. Thermochemical approaches for solar-to-fuel conversion are potentially highly efficient as they avoid the inherent limitations of photosynthesis and also sidestep the solar-to-electric conversion necessary to drive electrolytic reactions. Solar-driven two-step metal-oxide-based thermochemical cycles for producing the components of syngas, CO and H₂, from CO₂ and H₂O are the basis of this project; multi-cycle production of both H₂ and CO has been demonstrated over several iron- and cerium-based compositions fabricated into monolithic pieces both in the laboratory and at the National Solar Thermal Test Facility. These compositions are being developed for deployment in a unique and continuous solar-driven reactor prototype, the counter-rotating-ring receiver reactor recuperator (CR5). To aid in the design of highly efficient materials for H₂ and CO production, this work aims to identify the metal oxide phases present during thermochemical cycling and how they change as a function of temperature and gas composition.

3:45 PM

(EMA-S6-006-2012) Food additives in ceramic processing: a review

C. M. Costa, B. Walber, M. B. Quadri, D. Hotza*, UFSC, Brazil

Food additives are biodegradable, environmental friendly, readily available and affordable raw materials. Their use in ceramic processing has been mentioned in the literature for decades. In this work a descriptive approach from the point of view of food engineering concepts applied to the ceramic shaping is presented. Polysaccharides might be used as binders and plasticizers in ceramic suspensions and pastes. Oils and greases may enhance viscosity and facilitate demolding. Cellulose-based raw material might be used as templates for biomorphic ceramics. Albumine is mentioned as aid for making cellular ceramics. Alginates were cited as dispersants. Raw materials, compositions, forming and degradation steps are reviewed. The advantages and drawbacks of those substances are discussed.

4:00 PM

(EMA-S6-007-2012) Tape Casting with Non-VOC Solvents and Food Grade Additives

B. Wendt, B. P. Gorman*, Colorado School of Mines, USA

While tape casting has been widely adopted in the electronic ceramics industry as a reliable method for forming thin device structures, the use of high VOC solvents is a significant drawback. Similarly, the use

of high cost thermoplastics and other additives also significantly increases the cost of forming. In this work, the use of non-VOC solvents and all food grade, low cost additives is successfully demonstrated for tape casting. By adjusting the chemistry of the additives and a curing agent, a variety of tape thicknesses (typically between 50 μm and 1 mm) can be achieved with solidification times around 5 seconds. It is expected that these chemistries can be utilized in a wide variety of applications.

Author Index

* Denotes Presenter

A	
Aaron, D.	47
Aguilar, J.L.	31
Aksel, E.	37
Aksel, E.*	29
Allu, S.	26, 42
Alpas, A.	43
Amani, M.*	28
Amin, A.	21
An, K.	25, 40
Ansari, G.F.	50
Ansell, T.*	39
Apblett, C.	40
Araujo, E.B.*	30
Atakan, V.	52
Atallah, H.A.	37
Au, M.	26
Azough, F.	44
Azucena, C.	44
B	
Bachrach, R.	36
Badot, J.	43
Banavara Seshadri, S.	37
Banavara Seshadri, S.*	49
Bassiri-Gharb, N.	34, 51
Bassiri-Gharb, N.*	45
Bastani, Y.*	51
Bdikin, I.	30
Bell, A.	33
Bell, N.	38
Berger, M.	28
Bernal, A.	45
Bhalla, A.S.	34
Bharadwaja, S.	51
Bhattacharya, S.*	43
Bi, Z.	34
Biegalski, M.	41
Biegalski, M.D.*	41
Bilheux, H.*	42
Binder, J.R.	44
Bitteto, M.A.	52
Blendell, J.E.	24, 25, 33
Borisevich, A.	41
Borodin, O.A.	22
Borton, P.	27
Bowman, K.J.	24, 25
Braun, P.	30
Braun, P.V.	36
Brennecka, G.L.	33, 51
Brevnov, D.	36
Brewster, E.L.	41
Bruns, M.	44
Bugga, R.*	42
Burch, M.	39
Burch, M.J.*	50
Burke, J.	38
Burke, J.L.	41
Burruss, J.	52
Bux, S.*	27
C	
Cahill, D.	30
Cahill, D.*	22
Caillat, T.*	27
Cann, D.	23, 39
Cann, D.P.	38
Cha, Y.	38
Chan, P.	28, 29
Chang, Y.	29
Check, M.	27
Chen, A.*	34
Chen, J.	21
Chen, K.	36
Chen, L.	36
Cheng, C.	27
Cho, J.	30
Cho, J.*	30
Choi, J.	38
Chon, M.	25
Christen, H.M.	41
Ciftiyurek, E.	48
Cirigliano, N.	35
Clem, P.*	37
Clonts, L.G.	40
Coker, E.N.*	52
Collazo, R.	41
Collins-MacIntyre, L.	24
Costa, C.M.	52
Counce, R.	47
Cresce, A.	27
Crowne, F.	23, 37, 45
D	
Dai, S.*	38
Damjanovic, D.	21, 40, 49
Davies, J.	24
Depla, D.*	40
Desmarais, J.	33
Dhanjal, D.K.*	45
Dias, A.*	52
Dickey, E.C.	39, 50
Diercker, D.R.	49
Dittmer, R.	24
Do, Y.	39
Dong, W.	21
Doshida, Y.	24, 25
Dubrunfaut, O.	43
Dudis, D.*	27
Dudney, N.	26, 42
Dudney, N.J.	35
Dudney, N.J.*	22
Dunn, B.*	35
Duquette, D.	40
Durygin, A.	23
Dwivedi, A.*	40
Dynys, F.	27, 28
E	
Ehara, Y.*	45
Ehmke, M.*	24
Einisch, H.	47
Espinal, L.	52
F	
Fancher, C.*	25
Finkel, P.*	21
Fleurial, J.	27
Forrester, J.	37
Forrester, J.S.	25, 29
Forrester, J.S.*	29
Fox, G.	50
Fralick, G.C.	28
Freer, R.*	44
Fu, L.	26
Fukata, K.*	49
Funakubo, H.	45
Funakubo, H.*	47
G	
Gaddy, B.	41
Gai, Z.	41
Garcia, J.E.	24
García, R.	33
Garino, T.	38
Gascoin, F.	28
Gesswein, H.	44
Ghassemi, H.	26
Ghosh, D.*	29, 34
Gibbons, B.J.	33, 51
Gibbons, B.J.*	51
Gorman, B.P.*	49, 52
Gorzowski, E.*	21
Goswami, A.*	32
Gothard, N.	27
Grantab, R.	26
Gregory, O.J.	28
Guduru, P.R.*	25
Guilmeau, E.	28
Guo, R.	34
Gupta, S.	52
Gutierrez, S.	23
Guyomard, D.	43
H	
Ha, S.	28
Hadjikhani, A.	23
Hagen, M.	25
HaiBo, X.*	45
Hailemariam, A.	41
Hakimeh, G.	27
Hamad, E.K.*	37
Hamby, D.	42
Han, H.	29, 34
Haridasan, V.	47
Harris, D.T.	50
Harris, D.T.*	39
Harris, S.J.	43
Hasegawa, T.	47
Hatano, K.	25
Haugan, T.	32, 38
Haugan, T.J.*	41
Hausselt, J.	44
Hébert, S.	28
Hector, L.G.	43
Heeg, T.	33
Heitmann, A.A.	40
Heo, M.H.	31
Herbert, E.G.	27
Hernandez-Sanchez, B.A.	38
Ho, J.	27
Hoke, B.*	23
Holc, J.	39
Hong, K.	22
Hopkins, P.*	22
Hotza, D.*	31, 52
Huang, Q.	23, 52
Huey, B.D.*	33
Hunte, F.	34
Hutchison, J.E.	52
Hwang, H.K.	31

I

Idrobo, J.C.*26
 Ihlefeld, J.40
 Ihlefeld, J.*51
 Ihlefeld, J.F.33, 51
 Iijima, T.45
 Im, D.31
 In-Tae, S.45
 Irving, D.41
 Ishikaw, M.47
 Ito, D.*52

J

Jahantigh, F.*32
 Jakoby, R.44
 Jančar, B.36
 Jang, M.34
 Jankovic, S.49
 Jee, S.31
 Jee, S.*48
 Jeon, C.31, 36, 37
 Jeon, Y.*33
 Jia, Q.34
 Jing, Y.33
 Jo, W.24
 Jones, J.37
 Jones, J.L.25, 29, 34, 40, 49, 51
 Jones, J.L.*21
 Jones, W.23
 Jow, T.R.*22
 Jung, J.*30
 Jur, J.S.*46

K

Kaduk, J.A.23, 52
 Kakimoto, K.25, 49
 Kakimoto, K.*24
 Kalnaus, S.22
 Kaneko, R.24
 Kang, C.39
 Kang, I.38
 Kang, K.*35
 Karbasi, A.*23
 Karimi, S.33
 Kawai, A.*25
 Kemp, E.27
 Kholkin, A.L.30
 Kim, B.30, 38
 Kim, B.*34
 Kim, D.48
 Kim, E.37
 Kim, E.*30, 31, 36
 Kim, K.Y.31
 Kim, T.31
 Kim, Y.41
 Kirchhofer, R.49
 Kobayashi, K.*24
 Kocic, L.49
 Kohler, C.*44
 Kosec, M.39
 Kotula, P.G.51
 Kowalski, B.*32
 Kulkarni, A.30
 Kumar, B.*47
 Kumar, S.*24
 Kundaliya, D.*42
 Kunej, S.47
 Kung, H.*33
 Kurosawa, M.47
 Kutnjak, Z.*39

L

Lam, P.*44
 Lam, P.G.39, 51
 Lamas, J.40
 Lauter, V.41
 Lawton, J.47
 Lebeau, J.41
 Lee, G.W.31
 Lee, J.26, 28, 30
 Lee, K.38
 Lee, S.30
 Lee, S.*31
 Leech, S.33
 Lestriez, B.*43
 Lettman, B.29
 Levasseur, S.43
 Li, B.24
 Li, Q.52
 Lima, E.C.30
 Liu, D.42
 Liu, G.23, 39
 Liu, H.30
 Llano, C.25
 Llano, C.*37
 Lopatin, S.*36
 Losego, M.30
 Lu, F.28, 29
 Lu, N.*46
 Lu, P.38, 43
 Lucht, B.*22
 Luo, T.23
 Lynch, C.S.21

M

Ma, C.25, 42
 Mackey, J.*27
 MacManus-Driscoll, J.L.34
 Mahajan, S.K.*50
 Maier, J.26
 Maierhafer, D.40
 Maignan, A.*28
 Maiti, T.*34
 Malič, B.39
 Maria, J.39, 41, 42, 44, 50, 51
 Martha, S.26
 Martha, S.K.*35
 Martin, J.23
 Masó, N.39
 Mason, A.D.51
 Masuko, K.52
 Masumdar, E.U.*46
 Matias, V.*41
 McKenzie, B.B.51
 McMaster, M.48
 Mehta, A.41
 Mench, M.47
 Messing, G.L.29
 Meyer, K.E.51
 Mhin, S.51
 Miller, J.E.52
 Mion, T.23, 37
 Mion, T.*37, 45
 Mi-Ri, J.45
 Mishra, K.42
 Mita, S.41
 Mitic, V.*28, 49
 Mizuno, Y.24
 Moballegh, A.50
 Moore, D.L.38
 Moore, M.47
 Morales, J.*37

Morita, T.47
 Muchenik, T.I.*21
 Mukherjee, P.26, 42
 Mukhopadhyay, A.42
 Nadimpalli, S.25

N

Nahm, S.34
 Nahm, S.*38
 Nakajima, M.45
 Nakarmi, M.L.48
 Nanda, J.26, 35, 42
 Nazri, G.*48
 Nedin, J.28, 49
 Neuefeind, J.25
 Nikkel, J.39
 Nino, J.32
 Nino, J.C.29, 34
 Nittala, K.*51

O

Ochoa, D.A.24
 Oder, T.*48
 Ogawa, H.49
 Ohlhausen, J.A.51
 Oikawa, T.45
 Oldham, C.J.46
 Oliveira, A.A.31
 Osman, R.39

P

Paisley, E.*41
 Pamungkas, M.A.*38
 Pan, M.21
 Pannala, S.42
 Pannala, S.*26
 Pantelides, S.T.26
 Papandrew, A.47
 Parizzi, A.A.40
 Park, K.*31
 Parsons, G.N.46
 Patterson, E.*23
 Paunovic, V.28, 49
 Pavlovic, V.49
 Pennycook, S.J.26
 Perre, E.35
 Pierce, B.*32
 Pierce, B.T.41
 Pirc, R.39
 Polcawich, R.G.50
 Polcawich, R.G.*21
 Porter, W.D.35
 Potrepka, D.21, 23, 37, 45, 50
 Prakash, O.30
 Pramanick, A.25
 Pramanick, A.*40
 Prater, J.T.*44
 Prewitt, A.D.49
 Pulskamp, J.21
 Purenovic, J.28, 49

Q

Qi, Y.43
 Qin, L.*36
 Qu, W.40
 Quadri, M.B.52

